MARMARA UNIVERSITY

INSTITUTE FOR GRADUATE STUDIES IN PURE AND APPLIED SCIENCES

TREATMENT OF HIGH LOADING DAIRY INDUSTRY WASTEWATER BY ANAEROBIC DYNAMIC MEMBRANE BIOREACTOR

MÜGE PAÇAL

Ph.D. THESIS

Department of Environmental Engineering

Thesis Supervisor

Assoc.Prof. Dr. Neslihan SEMERCİ

ISTANBUL, 2021

ACKNOWLEGMENT

The title of this thesis is Treatment of High Loading Dairy Industry Wastewater by Anaerobic Dynamic Membrane Bioreactor. I would like to express my gratefulness to my thesis supervisor Assoc.Prof. Dr Neslihan Semeri for her endless support. I wish to express my special thanks to Prof.Dr.Barış Çallı for his grate support that made this thesis possible. I gratefully acknowledge for the financial support from The Scientific and Technological Research Council of Turkey (TUBITAK) (114Y812) and Marmara University Scientific Research Project Coordination Unit (FEN-C-DRP-120417-0182).

I wish to express my thanks to Recep Önder Sürmeli, Zeynep Yücesoy, Hatice Yeşil for their help and support.

I would like to thank my parents for their patience, support and love.

March, 2021 **Müge PAÇAL**

TABLE OF CONTENTS

ACKNOWLEGMENT i

TABLE OF CONTENTS ii

ÖZET vi

ABSTRACT vii

CLAIM FOR ORIGINALITY viii

SYMBOLS ix

ABBREVIATIONS xi

LIST OF FIGURES xiii

LIST OF TABLES xvi

1. INTRODUCTION 1

1.1. Dairy Industry 1

1.1.1. The characteristics of dairy wastewaters 2

1.1.2. Methods for dairy wastewater treatment 3

1.2. Introduction to Dynamic Membrane (DM) 6

1.2.1. Historical development of DM 7

1.2.2. The classification of DM formation and support materials 7

1.2.2.1. The classification of DM formation 7

1.2.2.2. Support materials 8

1.2.3. The structure of self-forming DM 8

1.2.4. DM formation and operation 9

1.2.5. Filtration system 10

1.2.6. DM module and AnDMBR configuration 11

1.2.7. Comparision of AnDMBR with AnMBR 16

1.2.8. Factors affecting DM formation 16

1.2.8.1. Properties of support layer 16

1.2.8.2. The properties of sludge 17
1.2.8.3. Operation conditions of DM 18
1.2.8.4. The characteristics of wastewater in AnDMBR applications 23
1.2.9. Cleaning strategies 23
1.2.10. Membrane fouling 24
1.2.11. The relationship between particles and membrane blocking mechanisms 26
1.3. Scope of The Thesis Study 28
2. MATERIALS AND METHODOLOGY 31
2.1. Investigation of Treatment Performance of Synthetic Wastewater and Cheese Whey in UASB and AnDMBR 31
2.1.1. Experimental set-up 31
2.1.2. Experimental plan 35
2.1.3. Wastewater characteristics and seed sludge 38
2.2. Investigation of The Effect of Pore Sizes on The DM Formation Time, and Cleaning Frequency 39
2.2.1. Experimental set-up 39
2.2.2. Experimental plan 41
2.2.3. Critical flux experiment 42
2.2.4. Wastewater characteristics and seed sludge 43
2.3. The Effect of CFV on a Well-Formed DM Operation and The Characteristics of Well-Formed DM 44
2.3.1. Experimental set-up 44
2.3.2. Experimental plan 45
2.3.3. Wastewater characteristics and seed sludge 46
2.4. Modelling of DM Development 46

2.5. Performance of DM Treatment in Long-Term Operation and Analyzing Characteristics of DM for Dairy Wastewater 47
2.5.1. Experimental set-up 47
2.5.2. Experimental plan 48
2.5.3. Wastewater characteristics and seed sludge 50
2.6. Analytical Methods 50
2.7. Morphological Analysis 51
2.7.1. PSD analysis 51
2.7.2. SEM-EDX analysis 51
2.7.3. FTIR analysis 51
2.7.4. ICP-MS analysis 52
2.7.5. XRD analysis 52
3. RESULTS AND DISCUSSION 53
3.1. Investigation of Treatment Performance of Synthetic Wastewater and Cheese Whey in UASB and AnDMBR 53
3.1.1. Evaluating treatment performance by DM 53
3.1.2. Filtration performance 62
3.1.3. Biogas generation 66
3.2. Investigation of The Effect of Pore Sizes on DM Formation Time, and Cleaning Frequency 68
3.2.1. Critical flux 68
3.2.2. Filtration and treatment performance of DM 69
3.2.3. DM resistance 83
3.3. The Effect of CFV on a Well-Formed DM Operation and The Characteristics of Well-Formed DM 86
3.3.1. The effect of CFV on a well-formed DM operation 86
3.3.2. The characteristics of well-formed DM 91

3.4. Blocking Mechanisms 92
3.4.1. Blocking mechanism for 10 μm 93
3.4.2. Blocking mechanism for 20 μm pore size 98
3.4.3. Blocking mechanism for 40 μm pore size 100
3.4.4. Blocking mechanism for 70 μm pore size 103
3.4.5. Blocking mechanism for 40 μm pore size operated under CFV 107
3.5. Performance of DM Treatment in Long-Term Operation and Analyzing Characteristics of DM for Dairy Wastewater 109
3.5.1. Effect of CFV on DM formation 110
3.5.2. DM formation and the stable operation phase 114
3.5.3. Membrane resistance 115
3.5.4. System treatment performance 117
3.5.5. Morphological and chemical characteristics of the DM layer 123
3.5.5.1. PSD analysis of DM layer 123
3.5.5.2. SEM-EDX analysis of DM layer 124
3.5.5.3. FTIR analysis of DM layer 126
3.5.5.4. XRD analysis of DM layer 128
3.5.5.5. ICP-MS analysis of DM layer 128
4.CONCLUSION 130
REFERENCES 133
APPENDIX A 152
APPENDIX B 153
APPENDIX C 154
APPENDIX D 155
APPENDIX E 156
BACKGROUND 157

ÖZET

YÜKSEK ORGANİK YÜKLÜ SÜT ENDÜSTRİSİ ATIKSUYUNUN ANAEROBİK DİNAMİK MEMBRAN BİOREAKTÖR İLE ARITIMI

Bu çalışmada süt ürünleri atık sularının arıtımında Dinamik Membran (DM) teknolojisi uygulanmıştır. Çalışmanın ilk aşamasında, yüksek organik yüklü sentetik süt ürünleri ve peynir altı suyu atık suyu arıtımı için laboratuvar ölçekli bir anaerobik dinamik membran biyoreaktör (AnDMBR) geliştirilmiştir. 344 gün boyunca organik madde ve askı katı madde (AKM) giderim verimleri incelenmiştir. Sentetik atık su arıtımı sırasında, sırasıyla 70 ve 10 µm gözenek çaplarına sahip destek filtre bezlerinin entegre edildiği AnDMBR de %78-%96 ve %66-%92 aralığında KOİ giderim verimleri elde edilmiş ve sistem 2.34-5.02 kg/m^3.gün aralığındaki organik yüklerle işletilmiştir.

Yukarı akışlı çamur battaniyesi reaktörünün çıkışına yerleştirilen bir harici filtrasyon ünitesinde farklı gözenek çaplarına sahip destek malzemeleri kullanılarak farklı işletme koşullarında DM oluşum süresi ve katı madde giderim verimlerindeki değişim incelenmiştir. Sonuçlar destek malzemeleri ilk defa işletmeye alındığında, gözenek boyutları azaldıkça DM oluşum süresi kısaldığını ve filtrasyon verimlerinin ise arttığını göstermiştir. Ayrıca, DM oluşturulduktan sonra destek malzemesi orijinal özelliklerini kaybetmiş ve filtrasyon özelliklerinin gözenek çapından bağımsız hale gelmiştir. Aynı sistemde membran yüzeyine çapraz akış hızı (CFV) uygulamalarının DM kalınlığını azalttığı ve DM oluşma süresini arttığı gözlenmiştir.

Çalışmanın son aşamasında, CFV kontrollü AnDMBR reaktörü 92 gün boyunca çalıştırılmış ve çıkış suyu AKM değerleri 27 mg/L'lere indirilmiştir. DM tabakasının analizi hem inorganik hem de organik malzemelerin sıkı/yoğun bir kek tabakasının oluşumuna katkıda bulunduğunu göstermiştir.

Anahtar Kelimeler: Süt Endüstrisi Atıksuyu, Dinamik Membran, filtrasyon, naylon ağ, por ebadı

20.03.2021 **Müge Paçal**

ABSTRACT

TREATMENT OF HIGH LOADING DAIRY INDUSTRY WASTEWATER BY ANAEROBIC DYNAMIC MEMBRANE BIOREACTOR

DM technology was applied for treatment of dairy wastewater. In first phase of study, a laboratory-scale anaerobic dynamic membrane bioreactor (AnDMBR) was developed for the treatment of synthetic dairy with high organic loading and cheese whey wastewater. Removal efficiencies of organic matter and suspended solid (SS) were investigated for 344 days. During synthetic wastewater treatment, 78-96% and 66-92% of COD removal efficiencies were obtained in AnDMBR integrated with filter having 70 and 10 µm pore sizes, respectively, and the system was operated in range of 2.34-5.02 kg/m^3day of organic loading rate.

Changes in DM formation time and solid removal efficiency were investigated at different operational conditions using support materials having different pore sizes in an external filtration unit being situated at the outlet of up flow sludge blanket reactor. Results showed that when support layer was used for the first time, as pore sizes of support layer decreased, DM formation time became shorter and filtration efficiency increased. Additionally, once DM was formed, the support layer lost its original properties and its filtration characteristics became independent of pore size. In the same system, it was observed that applications of cross flow velocity (CFV) on the surface of membrane, decreased thickness of DM and increased DM formation time.

In last phase of study, AnDMBR, controlled by CFV, was operated for 92 days and SS value in effluent was decreased to 27 mg/L. Analysis of DM layer showed that both inorganic and organic materials contributed to formation of a compact/dense cake layer.

Keywords: Dairy Wastewater, Dynamic Membrane, filtration, nylon mesh, pore size

20.03.2021 **Müge Paçal**

CLAIM FOR ORIGINALITY

It is known that dairy industry is one of the most important industry among food processing industry. A significant amount of milk and milk products have been consuming in the worldwide. With the increase in population, the consumption amount and demand of milk and milk products are increasing day by day. The dairy industry have high pollution potential due to occurrence of waste as a result of dairy processing. There have been many reported studies about treatment of dairy wastewater by conventional methods and membranes under aerobic and anaerobic conditions. However, there can be encountered with some difficulties during dairy wastewater treatment related to high organic content and lipid dairy effluent (high organic content, lipids). A good treatment has been accomplished by use of up flow sludge blanket reactor to some extent. However, the difficulties encountered during operation of the reactor and the high operating costs cause for search new treatment methods.

Dynamic Membrane Technology can be alternative method for dairy wastewater treatment with its innovative approach. The treatment and operation problem can be overcome by integrating dynamic membrane into system. Differently from reported studies, under anaerobic conditions, dynamic membrane was applied for dairy wastewater treatment and evaluated for the first time.

March 2021 **Assoc.Prof. Dr Neslihan SEMERCİ** **Müge PAÇAL**

SYMBOLS

α_c : Specific cake resistance
c_b : Concentration of sludge
A : Membrane surface area
Ca : Calcium element
Ca^{+2} : Calcium ion
$CaCO_3$: Calcium carbonate
CH_4 : Methane
cm : Centimeter
Co : Cobalt element
CO_2 : Carbon dioxide
CO_3^{-2} : Carbonate ion
COO- : Carboxylate salts
d_f : Particle diameter
$d_{particle}$: Particle size
d_{pore} : Pore size
Fe : Iron element
Fe^{+2} : Ferrous ion
H_2S : Hydrogen sulfide
J : Flux
K : Potassium element
Kg : Kilogram
L : Liter
m^2 : Meter square
m^3 : Meter cube
mg : Milligram
Mg : Magnesium element
Mg^{+2} : Magnesium ion
Mn : Manganese element

Na	: Sodium element
NH_4-N	: Ammonium nitrogen
Ni	: Nickel element
NTU	: Nephelometric turbidity unit
º	: Degree
ºC	: Degree celsius
O	: Oxygen element
OH^-	: Hydroxide ion
PAC	: Poly aluminum chloride
pH	: Activity of hydrogen ion
P	: Phosphorus element
PO_4^{-3}	: Phosphate ion
PO_4-P	: Phosphate phosphorus
R	: Membrane resistance
R_c	: Reversible filtration resistance due to cake formation
R_m	: Hydraulic resistance of virgin support layer
R_p	: Irreversible filtration resistance due to the gel layer formation
Rpm	: Revolutions per minute
S	: Sulfur element
SO_4^{-2}	: Sulfate ion
t	: Time
T	: Temperature
V	: Cumulative volume of permeate
$ZrOCl_2$	: Zirconyl chloride
%	: Percentage
µ	: Dynamic viscosity
µm	: Micrometer

ABBREVIATIONS

AFBR	: Anaerobic fluidized bed reactor
AnDMBR	: Anaerobic dynamic membrane bioreactor
AnMBR	: Anaerobic membrane bioreactor
AnSBR	: Anaerobic sequencing batch reactor
ASDFA	: Anaerobic semicontinuous digester with flocculant addition
AUFFR	: Anaerobic up flow fixed film reactor
CFV	: Cross flow velocity
COD	: Chemical oxygen demand
CP	: Contact process
CSTR	: Continuous stirred tank reactor
DM	: Dynamic membrane
DNA	: Deoxyribonucleic acid
DUHR	: Down flow up flow hybrid reactor
EDX	: Energy dispersive X-ray analysis
EGSB	: Expanded granular sludge bed
EPS	: Extracellular polymeric substances
FBR	: Fluidized bed reactor
FTIR	: Fourier-Transform infrared spectroscopy
HRT	: Hydraulic retention time
Hybrid AnBR	: Hybrid anaerobic biological reactor
ICP-MS	: Inductively coupled plasma mass spectrometry
Mag	: Magnitude
MBR	: Membrane bioreactor
MF	: Microfiltration
MLSS	: Mixed liquid suspended solid
MR	: Membrane reactor
OLR	: Organic loading rate
P/C	: Protein/Carbon
PSD	: Particle size distribution

SEM	: Scanning electron microscope
SEM-EDX	: Scanning electron microscopy (SEM) with energy dispersive X-ray analysis
SMP	: Soluble microbial products
SRT	: Solid retention time
SS	: Suspended solid
t/V	: Time/Volume
TMP	: Trans membrane pressure
TSMAMD	: Two-stage mixed anaerobic membrane digester
TSUAD	: Two-stage unmixed anaerobic digester
UAF	: Up flow anerobic filter process
UASB	: Up flow anaerobic sludge blanket
UF	: Ultra filtration
v/v	: Volume to volume ratio
VFA	: Volatile fatty acids
XRD	: X-ray powder diffraction

LIST OF FIGURES

Figure 1.1. The structure of self forming Dynamic Membrane..... 9
Figure 1.2 Filtration modes Cross Flow filtration (a,b) and Dead-End filtration (c) 10
Figure 1.3 Schematic view of flat sheet membrane (a) (Ersahin et al., 2013), and tubular membrane (b)..... 12
Figure 1.4 The membrane configurations: Side-stream (External) (a), Submerged (Internal)(b) and Submerged (External) (c) (Dvorâk et al., 2016) 13
Figure 1.5 Schematic view of particles exposed to different forces during filtration under CFV (Kisielius, 2012)..... 19
Figure 1.6 Schematic view of critical flux determination (Le- Clech et al., 2003)..... 22
Figure 1.7 Diagram for the inorganic fouling formation on membrane surface (Meng et al., 2009) 25
Figure 1.8 Schematic view of membrane blocking mechanisms 27
Figure 2.1 Schematic diagram of UASB reactor system used in this study..... 33
Figure 2.2 AnDMBR system..... 34
Figure 2.3 The diagram of experimental set-up 40
Figure 2.4 The schema of experimental set-up..... 45
Figure 2.5 Schematic view of AnDMBR system used in the study 48
Figure 3.1 COD (a), VFA (b), Suspended solids (c) in the effluent during the operation 56
Figure 3.2 Settling zone of AnDMBR (10 µm) (a) and Dynamic Membrane (10µm), taken out of the reactor in the end of phase 4 (b). 61
Figure 3.3 Particle size distribution of the solid in the settling zone of AnDMBR..... 61
Figure 3.4 The Fluxes in AnDMBR, 70 µm (a, Phase 2) and 10 µm (b, Phase 4) during operation with synthetic wastewater..... 64
Figure 3.5 Membrane flux (a) and TMP (b) variations and the AnDMBR (10µm) during the treatment of diluted cheese whey (Phase 6)..... 65
Figure 3.6 Biogas production and CH_4 concentration in the effluent of UASB and AnDMBR..... 67
Figure 3.7 The methane (CH_4) yield during the operation..... 67
Figure 3.8 Critical flux determination for support material with 10 µm pore size 68

Figure 3.9 Change of Flux and TMP (a), Turbidity (b) and Membrane Resistance (c) versus time at support material with 10 μm pore size 71
Figure 3.10 Change of Flux and TMP (a), Turbidity (b) and Membrane Resistance (c) versus time at support material with 20 μm pore size 74
Figure 3.11 Change of Flux and TMP (a), Turbidity (b) and Membrane Resistance (c) versus time at support material with 40 μm pore size 76
Figure 3.12 Change of Flux (a), TMP (b), Turbidity (c) and Membrane Resistance (d) versus time at support material with 70 μm pore size 79
Figure 3.13 The variation in CFV and TMP (a) Turbidity (b) and during the operation 87
Figure 3.14 The variation in Flux (a) and Membrane Resistance (b) during the operation 89
Figure 3.15 SEM Photo of DM Layer (Mag=1.00KX) (a) EDX analysis of the DM layer (40 μm) (b)..... 91
Figure 3.16 FTIR spectrum of DM layer..... 92
Figure 3.17 Flux decline rate (10 μm) for membrane fouling mechanisms in Run-1 and Run-2 94
Figure 3.18 Flux decline rate (10 μm) for membrane fouling mechanisms in Run-3 97
Figure 3.19 Flux decline rate (20 μm) for membrane fouling mechanisms in Run-1 and Run-2 99
Figure 3.20 Flux decline rate (40 μm) for membrane fouling mechanisms in Run-1 and Run-2 101
Figure 3.21 Flux decline rate (40 μm) for membrane fouling mechanisms in Run-3 .. 102
Figure 3.22 Flux Decline Rate (70 μm) for membrane Fouling Mechanisms in Run-1 and Run-2 104
Figure 3.23 Flux decline rate (70 μm) for membrane fouling mechanisms in Run-3 .. 105
Figure 3.24 Flux decline rate for membrane fouling mechanisms in Run-1 during operation with 40 μm pore size 107
Figure 3.25 Flux decline rate for membrane fouling mechanisms in Run-2 during operation with 40 μm pore size 108
Figure 3.26 Flux (a), CFV (b) and TMP (b) determined during the AnDMBR operation 111
Figure 3.27 Turbidity during the AnDMBR operation..... 115

Figure 3.28 Membrane resistance during the AnDMBR operation..... 116
Figure 3.29 COD in the settling zone of the reactor (a) and COD in membrane effluent (b) during the AnDMBR operation 118
Figure 3.30 Suspended solid concentration in the settling zone of the reactor (a) and Suspended solid concentration in the membrane effluent (b) during the AnDMBR operation 120
Figure 3.31 Biogas and CH_4 concentration (a) and CH_4 yield (b) in the AnDMBR effluent 122
Figure 3.32 PSD of the settling zone of the reactor (a) and DM layer (b) 123
Figure 3.33 SEM Photos with EDX analysis (20 μm): Virgin support material (a), Gel layer (b) DM layer in the end of system operation (c, d, e, f)..... 124
Figure 3.34 EDX analysis of the DM layer(a,b,c,d)..... 126
Figure 3.35 FTIR spectrum of DM layer..... 127

LIST OF TABLES

Table 1.1 COD and BOD values reported for Dairy products 2
Table 1.2 Some reported studies about treatment of Dairy Wastewater 5
Table 1.3 The Several Configurations of the AnDMBR that have used in reported studies 11
Table 1.4 Some reported AnDMBR studies 14
Table 1.5 Definition of blocking mechanisms (Liu et al., 2009) 28
Table 2.1 The methodology of the study 32
Table 2.2 Operation timeline with UASB and AnDMBR 36
Table 2.3 The feeding UASB with synthetic wastewater and diluted cheese whey 37
Table 2.4 The feeding AnDMBR with synthetic wastewater and diluted cheese whey 37
Table 2.5 The characterization of synthetic wastewater and cheese whey 38
Table 2.6 Characteristics of the submerged membrane module 41
Table 2.7 Applied mesh pore sizes and operating conditions in all tested runs 42
Table 2.8 The membrane flux, corresponding to different speed of pump during critical flux operation 43
Table 2.9 The characteristics of UASB effluent water used in critical flux 43
Table 2.10 The characteristics of UASB effluent used in filtration experiment 43
Table 2.11 The characteristics of UASB effluent used in filtration under CFV 46
Table 2.12 Membrane filtration models and blocking mechanisms 46
Table 2.13 Characteristics of wastewater 50
Table 3.1 The feeding UASB with synthetic wastewater and diluted cheese whey 55
Table 3.2 The feeding AnDMBR with synthetic wastewater and diluted cheese whey 55
Table 3.3 DM formation time for run-1, TMP and Flux after DM formation for run-1,2 and 3 72
Table 3.4 The turbidity removal with different pore size 82
Table 3.5 The membrane resistance, calculated during the operation with 10, 20, 40 and 70 μm pore size 84
Table 3.6 The membrane resistance of 40 μm pore size; Total resistance, Pore blocking, Cake resistance and Virgin layer 85

1. INTRODUCTION

1.1. Dairy Industry

Huge amount of dairy products are consumed around the world. Its demand has been rising year by year in parallel with standard of living and population increase (Karadağ et al., 2015a). The total milk production of Turkey has exhibited a significant increase over the past few years as a result of the higher annual milk yield per cow and increased amount of milking animal holdings (Kırdar and Karaca, 2017).

The main constituents of milk are fat, proteins, water lactose (milk sugar), and minerals (salts). Majorly, water (more than 80 %) occupies milk, and milk includes solid compounds, lactose, protein, fat, and minerals such as Sodium (Na), Magnesium (Mg), Calcium (Ca) (Joshiba et al., 2019). The main products are bottled pasteurized milk, yogurt, cheese, ice cream, cream, and butter (Britz et al., 2006). Cheese whey, which is green-yellowish liquids, is by-products of dairy effluents. Cheese whey is considered as the most important polluted waste that is produced during dairy processing owing to its high organic load and extreme volume (Carvalho et al.,2013). Cheese whey occurs as a result of sedimentation and elimination of milk casein in processing of dairy product (Prazeres et al., 2012). Chemical Oxygen Demand (COD) content of different dairy products in terms of milligram per liter is presented in Table 1.1.

A large amount of water is consumed by dairy industries in order to manufacture dairy products. Thus, dairy industry produces important amount of wastewater among other industries . In the preparation of dairy products, a large amount of clean water is used in the processes such as heating, sterilization, cooling, pasteurization, cleaning (Joshiba et al., 2019). In addition to this, all steps that take part in dairy chain, consisting of production, processing, handling, and packaging operations generate wastes in different quantity and quality (Britz et al., 2006).

Table 1.1 COD and BOD values reported for Dairy products

Product	COD, mg/L	BOD, mg/L	References
Whole milk	183,000	114,000	Kessler, 1981
	190,000	111,000	Odlum, 1990
Evaporated Milk	378,000	271,000	Kessler, 1981
Whey	65,000	42,000	Kessler, 1981
Skim Milk	147,000	90,000	Kessler, 1981
	120,000	85,000	Odlum, 1990
Butter Milk	61,000	134,000	Kessler, 1981
	75,000	110,000	Odlum, 1990
Cream	400,000	750,000	Kessler, 1981
Ice cream	292,000		Wendorff, 2001

1.1.1. The characteristics of dairy wastewaters

Dairy wastewater is produced from quality control laboratory analyses, cleaning of milk containers and milking equipment, from by-product of dairy process, manufacturing whey, cheese, and ice-cream (Karadağ et al., 2015b). The production of dairy wastewater is occurred in discontinuous way. Therefore, flow rates of dairy effluents vary importantly (Demirel et al.,2005). High seasonal variations in production of dairy wastewater can happen frequently. These seasonal variations have an important effect on volume of milk taken for processing of dairy product. This is low in winter months whereas high in summer (Demirel et al., 2005). The type of product being processed has an effect on the characteristics of dairy effluents depending upon employed the operation methods and the system type (Vidal et al., 2000). In addition to this, the applied cleaning strategy in dairy industry has an effect on dairy wastewater characteristics, and causes in highly variable pH in dairy effluents (Demirel et al., 2005).

The dairy wastewater includes lower toxic chemical substances than other industrial plant effluent (Joshiba et al., 2019). Generally, dairy wastes include organic matter, suspended solid, high amount of nitrogen and phosphorus, and oil and greases. In addition to this, they include trace elements due to cleaning of milk boiler (Ahmad et al., 2019). Major components of dairy effluents are lactose lipids, mineral salts, soluble proteins and detergents. In addition to this, heavy metals with low concentrations have been reported

in dairy wastewater from control laboratories in dairy plants. Dairy wastewater generally includes high COD content and is characterized by its comparatively elevated temperature (30-40ºC) (Karadağ et al., 2015b). Due to high COD contents, wastewaters of dairy industry are high in strength (COD content: up to to 80 g /L) (Karadağ et al., 2015b) and unstable in nature (Demirel et al., 2005). In addition to high organic content, dairy wastewater includes important amount of nutrients, stemming from milk and milk products. Phosphorus, and nitrogen are important nutrients found in dairy effluents. Phosphorus is encountered in dairy wastewaters in inorganic forms; polyphosphate ($P_2O_7^{-4}$) and orthophosphate (PO_4^{-3}) and organic forms. Nitrogen derives from milk proteins in dairy wastewaters. Nitrogen is present in various forms; inorganic nitrogen such as nitrate (NO_3^-), Nitrite (NO_2^-) and Ammonium (NH_4^+) and organic nitrogen (nucleic acids, proteins, urea) (Demirel et al., 2005). In addition to this, elements detected in dairy effluents such as Cobalt (Co), Nickel (Ni) and Manganese (Mn), stemming from processing of dairy products. The heavy metals were detected in dairy effluent in low concentration that did not affect biological treatment (Demirel et al., 2005).

1.1.2. Methods for dairy wastewater treatment

Conventional treatment methods is applied to treat dairy effluents. Dairy wastewater is treated by using biological and physical-chemical treatment methods. Biological treatment processes are preferred due to high cost of reagents, inefficient COD removal in physical-chemical treatment processes (Vidal et al., 2000). Among these treatment processes, treatment in ponds, activated sludge plants, and anerobic treatment are used for treatment of dairy wastewater (Demirel et al., 2005). However, many problems have been stated in the treatment of dairy wastewater by conventional methods. These are low sludge settleability, difficulties in removal of nitrogen and phosphorus and encountered problems in the removal of fat, oil, dyes, low resistance to shock loads, and high production of scum (Machado et al., 2002).

It is known that anaerobic treatment has superiority over aerobic treatment in terms of production of low sludge, low energy requirement, operation at higher organic loading rate, biogas production and low nutrient requirement (Lin et al., 2013). COD concentrations of dairy effluents vary importantly (Demirel et al., 2005). The high organic

content and warm temperature of dairy effluent enables them ideal for anaerobic treatment (Elangovan and Sekar, 2012).

There have been various studies for dairy wastewater treatment (Table 1.2). Up flow anaerobic sludge blanket (UASB) reactors have been used for treatment of dairy wastewater (Demirel et al., 2005). The success of UASB is related to properties of sludge that is used in these systems. The dense sludge bed forms at the bottom of reactor, where all biological processes happen (Seghezzo et al., 1998). Bacterial growth and accumulation of incoming suspended solids form this sludge bed. The aggregation of bacteria can normally aggregate in sludge granules and flocs. The dense aggregates have good properties of settling in reactor that they are not prone to washout from the system. As a result, the retention of active granular sludge and, also active flocculent sludge, provide good performance in wastewater treatment at high loading rates within UASB reactor (Seghezzo et al., 1998). UASB can overcome high suspended solids loads and shock loads (Xu et al., 2003; Seghezzo, 1998; Leitao et al., 2006; Di Berardino, 2019). The influent flow and produced biogas under anaerobic conditions enable good contact between biomass and wastewater in UASB systems (Seghezzo et al., 1998). Although UASB provides good removal performance, it can be encountered with some difficulties during dairy wastewater treatment. Dairy effluents include a very important amount of lipids. The accumulation of these lipids causes undesired sludge floatation problems that could result escape of biomass in UASB system (Karadağ et al., 2015b; Karthikeyan and Kandasamy, 2009).

The integration of a membrane into bioreactor, a membrane coupled reactor, can decrease solid losses from the reactor. Anaerobic Membrane Bioreactor (AnMBR) can obtain very high solid-liquid separation efficiency and allows independent control of the Sludge Retention Time (SRT) and Hydraulic Retention Time (HRT). In addition, with the integration of a membrane into bioreactor, a membrane coupled reactor, the particulate organic substrate stays longer in the system and can be hydrolyzed eventually and be degraded at long SRTs (Zhang et al., 2010).

Table 1.2 Some reported studies about treatment of Dairy Wastewater

Waste Type	Type of Reactor	HRT day	OLR kgCOD/m^3day	Temperature (°C)	Removal (%)	Methane Yield $m^3CH_4/gCOD_{removed}$	References
Diluted Whey Permeate	AnMBR	5-13	2-6	37	>90	0.28	Dereli et al., 2019
Whey (%75 cheese whey) and liquid dairy manure	UASB	2.2	19.4		94.7 (COD)		Rico et al.,2015
Whey (%60 cheese whey) and liquid dairy manure	UASB	1.3	28.7		95.1(COD)		Rico et al.,2015
Whey Permeate	CSTR	31	3.1	37	86	-	Dereli et al., 2015
Cheese Whey	AnSBR	8.3-25	1.5-4.6	55	87	0.29-0.32	Fernandez et al., 2015
High strength milk permeate	Anarobic moving bed biofilm	6.8-14	0.5-6.2	20-25ºC	84 (COD)		Wang et al.,2009
Whey	AF	1-5	1-4	35	72-90.2	0.089-0.28	Gannoun et al.,2008
Dairy wastewater	UASB	36-48 hours	7.9-45.42	36ºC	98 (COD)		Najafpour et al.,2008
Dairy	Hybrid UASB	0.25	8-20	-	65-93	0.25-0.31	Banu et al.,2008
Whey	AF	10-15	2.2-3.3	37	90	-	Zayed and Winter, 2000
Dairy	AF	0.83-12.5	0.5-6.5	32-34	-	0.32-0.34	Ince,1998
Dairy	Hybrid UASB	1.9	0.97-2.82	35	91-97	0.27-0.359	Strydom et al.,1997
Cheese Whey	UASB	5	0.9-7.6	33	>90	-	Yan et al.,1990
Cheese Whey	ASDFA	-	16.1	-	99	-	Barford et al.,1986

In other words, membrane integration into reactor provides the complete substrate and biomass retention in the system. Thus, due to larger contact time between microorganisms and substrate, membrane integration into reactor produces high quality effluent in terms of total suspended solid (TSS) and COD (Ribero-Pi et al., 2020). AnMBR seems to be convenient for treatment of various wastewaters such as food industrial wastewater. In addition to complete suspended solid retention, advantages of AnMBR compared to conventional treatment, include small footprint, total biomass retention, high effluent quality, and rapid start-up (less than 2 weeks) (Lin et al., 2013). On the other hand, there have been still obstacles in AnMBR applications, such as low membrane flux, high cost of membrane modules, rapid membrane fouling and complicated cleaning methods operation (Ersahin et al., 2012).

1.2. Introduction to Dynamic Membrane (DM)

Dynamic Membrane (DM) could be favourable technique to solve the problems happened during treatment by Membrane Bioreactor (MBR) systems (Ersahin et al., 2012). The formation of membrane fouling is an important disadvantage for conventional membrane during operation. The application of DM can turn this disadvantage into advantage. In the promising approach of DM filtration, membrane fouling is utilized for creating a low-cost, self-forming, and reformed membrane layer (Ersahin et al., 2012; Alibardi et al., 2014; Zhang et al., 2014a).

DM layers consist of an “underlying gel layer” and “cake layer”. An underlying gel layer forms through the attachment and deposition of the solutes and colloids on the support layer (fabric filter, nylon/dacron mesh) and strict tightly to the filter surface (Ersahin et al., 2012). Thus, allowing the use of cheap support material instead of conventional membranes enables an important cost reduction in the system. Using cheaper support materials instead of conventional membranes allow higher flux rates under lower transmembrane pressure. The large particles, which have attached loosely over gel layer, mostly constitute the cake layer. One of the significant advantages working with DM is that solid retainment which obtained by secondary membrane (cake layer). Moreover, DM can be regenerated by physical cleaning methods (brushing, air-water backwash) instead of using chemical reagents (Ersahin et al., 2012).

1.2.1. Historical development of DM

The application of DM was started with applying Zirconyl chloride-DM ($ZrOCl_2$-DM) to reject salts in reverse osmosis (Marckinkowsky et al., 1966). Then, the following DM studies, the researchers focused on retainment of salt by reverse osmosis (Freilich and Tanny, 1978; Tanny and Johnson, 1978; Igawa et al., 1977). In the beginning of 1980s, the applications of DM in Ultrafiltration (UF) processes was started for the treatment of industrial wastewater such as dye, food industry (Gaddis et al., 1979; Kishihara et al., 1984; Groves et al., 1983; Jiraratananon et al., 1997). Although high retention was obtained in this process, low permeability, high-cost support material hindered usage of this technology (Ersahin et al., 2012). DM application by Microfiltration (MF) processes has been applied since 1990s particularly for wastewaters. However, high capital costs in membranes (microfiltration and ultrafiltration) low permeability and energy requirement became problem in MBR technology. Replacing these membranes (microfiltration and ultrafiltration) with low-cost support material, having macro porous, seemed more encouraging technology in the mid-1990s (Ersahin et al., 2012). The self-forming DM system was applied for aerobic treatment in mid-1990s for the first time (Al-Malack et al., 1998; Yamagiva et al., 1994). Moreover, many researchers reported satisfactory removal efficiencies by DM systems under anaerobic conditions (Seo et al., 2002; Kiso et al., 2000). DM applications in anaerobic systems began in 1994 (Pillay et al., 1994). The applications of self-forming DM in anaerobic systems have been increasing since 2007 (Hu et al., 2018a; Ersahin et al., 2012).

1.2.2. The classification of DM formation and support materials

1.2.2.1. The classification of DM formation

DM can be categorized into two types depending on formation methods. These are self-forming DM and pre-coated DMs (Ersahin et al., 2012). Self-forming DM is produced by substances in filtered liquor (suspended solids e.g.). There is no need for external material. Pre-coated DMs are generated by passing a solution, including specific components (Poly aluminum chloride e.g.) on the surface of the porous material (Ersahin et al., 2012). Thus, the main disadvantage of pre-coated DMs over self-forming DM is the requirement of an

external material. Due to convenient and economical properties, self-forming DM has mostly been taken attention (Zhang et al., 2014a).

1.2.2.2.Support materials

The low-cost support materials (woven, non-woven fabrics and meshes e.g.) have been used in DM applications (Mahat et al., 2018). These low cost support materials have large pore sizes that are mostly between 20 and 100 micrometer (μm). Thus, working with large pore size allows working with a higher flux at a very lower pressure (Mahat et al., 2018). Till this time, woven (Ersahin et al., 2016a,b; Alibardi et al., 2014; Ersahin et al., 2014), non-woven (Meng et al., 2013; An et al., 2009; Chang et al., 2001) and meshes (Yang et al., 2020; Hu et al., 2018b; Quek et al., 2017; Salerno et al., 2017; Park et al., 2017) have been used as support material for separating solid from liquid in both anaerobic and aerobic conditions.

Mesh filter is created by connected strands of fiber, metal, ductile material. Woven fabrics is a yarn made of single or multi extruded synthetic fibers. Non-woven fabric is a yarn made web of man-made filaments and web of natural filaments (Ersahin et al., 2012). The flat structure of mesh may cause insufficient sludge accumulation (Kiso et al., 2005) whereas filtration resistance of meshes is low (Satyawali and Balakrishnan, 2008). Kiso et al., 2005 reported that despite the thickness of the non-woven fabric, sludge particles were retained in the pores among the fiber matrix. These blocked pores made the removal of deposited sludge from fabric difficult in long term operation.

1.2.3. The structure of self-forming DM

DM layer has a significant effect on retainment of particulate matter in Dynamic Membrane Bioreactors (DMBRs) (Chu and Li, 2006). According to Zhang et al., 2014a, DM was formed by retention of soluble and colloidal particles that are “Extracellular polymeric substances” (EPS) and its soluble form “Soluble Microbial Products” (SMP), and sludge particles during filtration operation. It is known that EPS are produced by microbes. It consists of high amount of carbohydrates and proteins. In addition to this, DNA and humic substances are found in EPS (Liu and Fang, 2002).

As mentioned above, the biomass layer of DM could be divided into two sub-layers namely; “gel layer” and “cake layer” (Figure 1.1). Mainly the gel-like matter (EPS and SMP) forms gel layer. The gel layer sticks tightly to the filter surface. It is difficult to remove gel layer from support layer by physical cleaning methods (Ersahin et al., 2012).

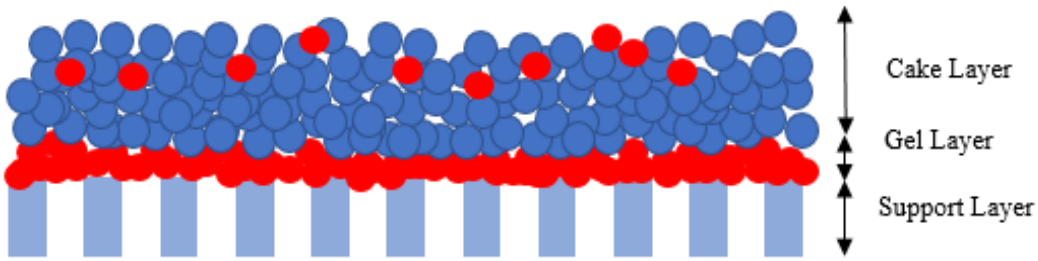


Figure 1.1. The structure of self-forming Dynamic Membrane

According to the reported studies, the gel layer has an important effect on rejection capability of fine particles in DMBRs (Ersahin et al., 2012). The cake layer was mainly consisted of many microbes and sludge flocs which were attached loosely to the membrane (Fan and Huang, 2002). The cake layer acted as barrier by retaining most of coarse flocs, and could improve effluent quality. It could protect both gel layer and support layer from the direct interaction of larger particles (Cao et al., 2010). Moreover, organic carbon conversion in the cake layer may happen due to microbial activity through the cake layer during permeation (Ersahin et al., 2012). Table 1.4 presents the reported self-forming DM studies.

1.2.4. DM formation and operation

According to Chu et al., 2008, DM operation includes three stages. These are DM layer formation, filtration, and backwash. In DM formation stage, fine particles cannot be retained by support layer due to large pore size. Thus, this causes poor permeate quality in the effluent. Therefore, the effluent water needs to recirculated into the system till high effluent quality is obtained. At filtration stage, the formation of DM is completed, and the effluent quality reaches to conventional membrane effluent quality. In last stage, backwash, which is one of the cleaning strategies, is applied due to decrease in flux as a result of fouling (Mahat et al., 2018). In addition to this, in DM studies, the flux, suspended solid (SS) and turbidity were used as an indicator of DM formation during operation (Li et al.,

2017). The time when turbidity, suspended solid (SS) or flux become stable, indicates DM formation time (Li et al., 2017).

1.2.5. Filtration system

The filtration system has an significant role in decreasing of fouling (Mahat et al., 2018). The membranes can be operated in two ways namely; "dead-end filtration" and "cross-flow filtration" (Figure 1.2). In dead-end filtration systems, the feed flow is forced through the membrane by pressure. There is only one influent and effluent stream. The filtered particles are accumulated on the membrane surface (Calabro and Basile, 2011). As particles accumulate on the filter, membrane permeability decreases owing to clogging. In the following step, removal of accumulated particle is needed (Calabro and Basile, 2011). Moreover, this system is found to be insufficient to overcome fouling in long-term filtration (Mahat et al., 2018). The filtration systems can be helpful technique for filtration of concentrating compounds (Calabro and Basile, 2011). Li et al., 2018 reported quick DM formation in dead-end filtration application. In that study, one physical cleaning was done and particles were removed from mesh with high effort.

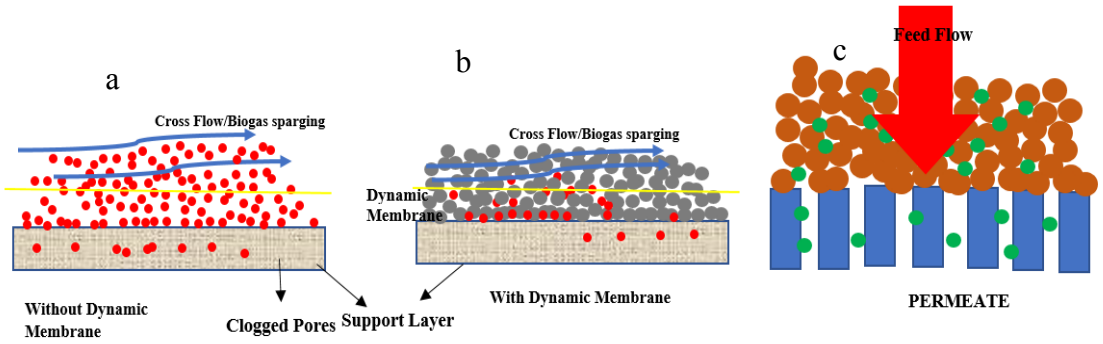


Figure1.2 Filtration modes Cross Flow filtration (a,b) and Dead-End filtration (c)

Cross-flow filtration system is a pressure-driven separation process. In this filtration system, the permeate flow is vertical to the feed flow (Song and Elimelech, 1995). In cross-flow filtration system, the feed is circulated along the membrane with a pump, and the permeate is withdrawn by transmembrane pressure, created with a pump (Jaffrin, 2011). Moreover, cross-flow filtration aims to increase the stability of flux and it intends to retain particles by using shear forces on the surface of the membrane by a flow of feed

along the membrane (Bruggen, 2018). According to reported studies, cross flow filtration mode have been mostly applied during Anaerobic Dynamic Membrane Bioreactor (AnDMBR) operations (Hu et al., 2018a; Hu et al., 2018b; Yang et al., 2020; Berkessa et al., 2020; Jia et al., 2020; Saleem et al., 2018; Wang et al., 2018).

1.2.6. DM module and AnDMBR configuration

The various kinds of bioreactors can be used in AnDMBR studies such as Continous Stirred Tank Reactor (CSTR), UASB, Expanded Granular Sludge Bed (EGSB), Fluidized Bed Reactor (FBR). The membranes can be integrated into various type of anaerobic bioreactor to produce several AnMBRs (Hu et al., 2018a). Until this time, the DM module has been integrated into only CSTRs and UASBs to form AnDMBRs (Table 1.3). Most of the AnDMBR studies have used the CSTR, whereas there are limited studies that UASB has been used as a reactor (Hu et al.,2018a; Siddiqui et al., 2021). In most of AnMBR studies, CSTR is used as reactor type owing to easy construction and operation. However, there is limitation during operation with membrane-coupled CSTR systems. These systems usually are operated at a lower biomass concentration than the anaerobic reactors (high rate) in order to fouling control (Chen et al., 2016). Thus, lower organic loading rate is applied to the system (Chen et al., 2016).

Table 1.3 The Several Configurations of the AnDMBR that have used in reported studies

Reactor Type	Module Type	Membrane Configuration
UASB	Flat-sheet	Submerged (Internal) Submerged (External)
CSTR	Tubular	Side-Stream

Membrane coupled UASB systems have benefits such as improved methane (CH_4) production and less fouling problems (Chen et al., 2016). Compared to CSTR-coupled membrane systems, UASB-coupled membrane systems can be operated with higher membrane fluxes (Quek et al., 2017; Hu et al., 2018a). In addition to this, many researchers have attempted to integrate membrane into UASB in AnMBR systems in order to benefit from its advantages such as less fouling and improved CH_4 production due to application of higher organic loading rate (Chen et al., 2016). There are three types

of membrane module, which could be used for DM applications. These are flat-sheet (Figure 1.3a), hollow fiber and tubular type (Figure 1.3b) (Hu et al., 2018a). Mostly, flat-sheet module type has been used in AnDMBR systems (Table 1.4).

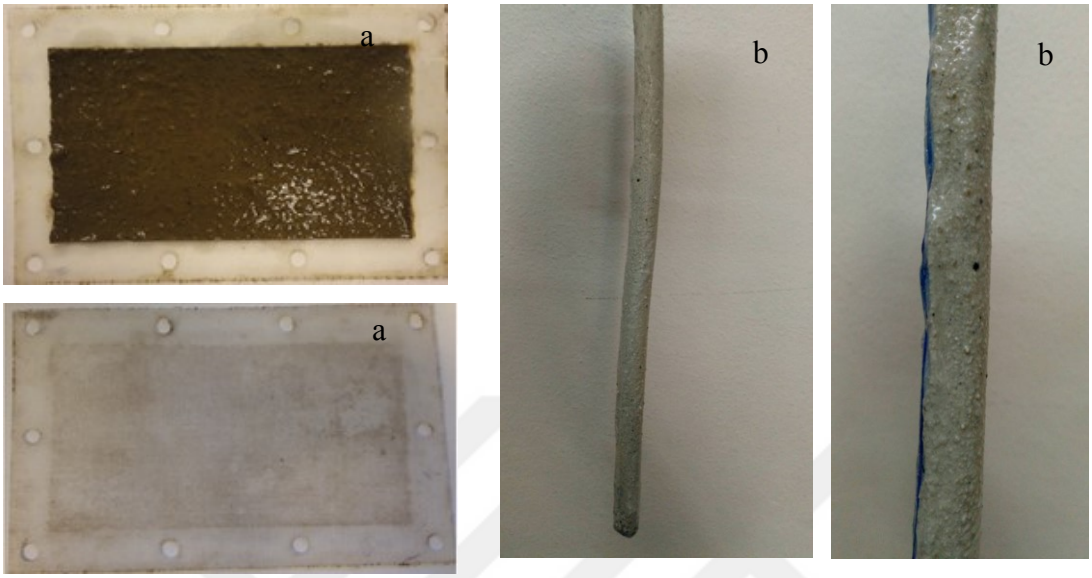


Figure 1.3 Schematic view of flat sheet membrane (a) (Ersahin et al., 2013), and tubular membrane (b)

Ersahin et al., 2012 reported that the sludge layer formed on tubular module was thicker than that flat sheet module. Moreover, Xiong et al., 2014 compared DM formation on tubular and flat sheet mode. The researchers found that cake layer on tubular mode more uniform than the flat membrane modules that produced good effluent for the stable operation of DM. Moreover, there has been no known hollow-fiber module type used in AnDMBR systems. This is likely due to low intensity of DM in hollow fiber module and the complicated fabrication procedures (Hu et al.,2018a).

There are three type membrane configurations, used in AnDMBR operation (Figure1.4). The membrane module is directly placed inside the reactor (internal), or outside the reactor (external) in submerged configuration. In submerged MBR, the membrane module (externally or internally) is operated under vacuum at the effluent side. In addition to this, the submerged membrane is also operated by gravity. In side-stream MBR, the membrane module is placed outside the bioreactor, and operated under pressure at feed side of the system (Hu et al. ,2018a). According to reported studies, membrane cost and gas sparging rate (fouling control) in side-stream AnDMBR were three times higher than they are in submerged AnDMBR (Jeison and van Lier, 2008). Additionally, the energy

requirement per permeate flow volume for pumped side-stream membrane was much higher than the energy requirement for submerged membrane in AnMBRs (Martin-Garcia et al., 2011). Due to low investment cost (less footprint) and low energy consumption per permeate flow, the submerged configuration is preferred (Ersahin et al., 2017).

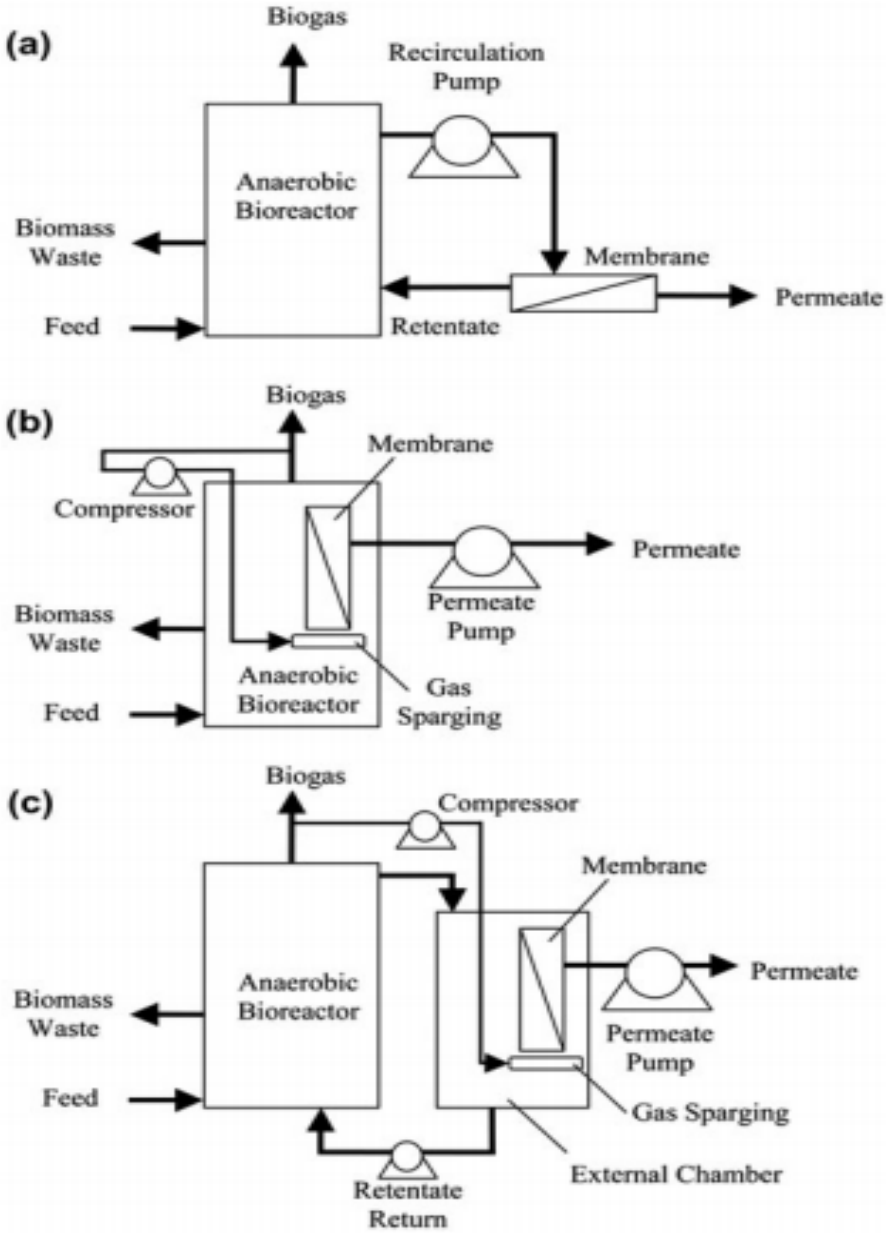


Figure 1.4 The membrane configurations: Side-stream (External) (a), Submerged (Internal)(b) and Submerged (External) (c) (Dvorâk et al., 2016)

Table 1.4 Some reported AnDMBR studies

Operation mode	Membrane configuration	Volume (L)/ temperature (ºC)	Effective Filtration (m^2)	Pore Size (µm)	Support Material	Flux (L/m^2h)	OLR (kg m^3/d)	TMP (mbar)	Waste Water Type	MLSS (gSS/L)	COD removal (%)	References
Submerged	Flat sheet	3/50	0.0188	30	Non-woven	3	-	-.	Synthetic	7.2	-	Jeison et al.,2008
Side-stream	Flat sheet	3/30	0.0292	15	Mesh	0.5-3	-.	-.	Synthetic	25.6	-	Jeison et al., 2008
Submerged	Flat sheet	3/30	0.0188	20	Mesh	0.5-3	-	-	Synthetic	17.5	-	Jeison et al.,2008
Submerged	Cylindrical	15/n.a.	n.a.	30-100-140	Woven nylon mesh	44	3.75 (gVS/Ld)	-	Synthetic municipal waste	-	-	Walker et al., 2009
Submerged/	Tubular	12.9/15-20	0.98	0.64	Non-woven fabric	5	2.36	< 400	Municipal	-	70	An et al., 2009
Submerged	Flat sheet	45/Ambient	n.a.	61	Dacron mesh	65	-	<250	Municipal	-	70	Zhang et al., 2011
Submerged	Flat Sheet	48/37	n.a.	40	Dacron mesh	6	4.87	< 500	Landfill leachate	-	94	Xie et al., 2014
Side-stream	Flat Sheet	0.7+0.05/35	0.004	200	Nylon mesh	1.0-7.2	0.7-5	< 250	Synthetic	10-25	62	Alibardi et al., 2014
Submerged	Flat Sheet	6.8/35.7	0.018	10	Monofilament woven fabric	2.6	2	<800 mbar	Synthetic	5-6.5	64-94	Ersahin et al., 2014
Submerged	Tubular	14/35	0.0314	10	Silk	1.0-2.0	-	130 mbar	Waste sludge	15-20		Liu et al.,2016
Side-stream	Flat Sheet	0.7+0.06/20-24	0.004	200	Nylon mesh	1.4-28	0.16-3.3	< 200 mbar	Synthetic	2-12	>89	Alibardi et al., 2016
Side-stream	Flat sheet	7.4/35.5	0.014	10	Monofilament woven fabric	2.2	2-3.6	< 450 mbar	Synthetic	6.4	>99	Ersahin et al.,2016a
Submerged	Flat sheet	7.4/35.5	0.014	10	Monofilament woven fabric	2.2	2	< 600 mbar	Synthetic	20.2	>99	Ersahin et al.,2016b
Submerged	Flat Sheet	7.4/35.7	0.014	10	Monofilament woven fabric	2.2	2	<700 mbar	Synthetic	6.45 g/L	99.5	Ersahin et al., 2017
Side-stream	Flat Sheet	7.4/35.5	0.014	10	Monofilament woven fabric	2.2	2	<400 mbar	Synthetic	6.4 g/L	99.1	Ersahin et al.,2017

Table 1.4 Some reported AnDMBR studies (Continued)

Operation mode	Membrane Configuration	Volume (L)/ temperature (ºC)	Effective Filtration (m^2)	Pore Size (µm)	Support Material	Flux (L/m^2h)	OLR (kg m^3/d)	TMP (mbar)	Waste Water Type	MLSS (gSS/L)	COD removal (%)	References
Submerged	Flat Sheet	25/37	0.04	50	Nylon mesh	2-11.2	-	10 cm water level	Food waste	20-40 g/L	27.4	Tang et al.,2017
External	Flat Sheet	6.9/25-30	0.005	50	PET mesh	30-60-100	1.5-3	< 400 mbar	Municipal	-	64-71	Quek et al.,2017
Submerged	Flat Sheet	3.5/22-25	0.02	75	Nylon mesh	22.5	0.88-1.55-3.01	< 300 mbar	Municipal	5.6 g/L		Hu et al.,2018b
Side-Stream	Flat Sheet	0.8L/34±1ºC	0.00165-0.0033-0.0066	21-52	Monofilament nylon mesh	5-6.2	-	<400 mbar	Synthetic	14 g/L	-	Saleem et al.,2018
Submerged	Flat Sheet	15 L/25±2ºC	0.04	30	Polyester non-woven fabrics	10-30	-	-	Synthetic Municipal	3.5 ±0.5 g/L	89.4	Sun et al.,2018
Hollow	Cylindrical	14 L/25ºC	0.04	150	Polyamide nylon mesh	50-100-150	-	-	Synthetic	3 g/L	80	Wang et al.,2018
External	Tubular	10L/ Ambient Temperature		26-38-54-61-74	Nylon mesh	0.5-4 $m^3/m^2/d$	-	<700 mbar	Synthetic	4-10	-	Siddiqui et al., 2019
Submerged	Flat	3.6/20-25ºC	0.02	75	Nylon mesh	22.5-45-90-180	0.82-1.63-3.01-6.8	< 400 mbar	Real Domestic	72.4	74.4-77.3-70.6%	Yang et al., 2020
External (Submerged)	Flat	10L/ 37±1ºC	0.01	100	ABS Filament	14-28	1-5	< 400mbar	Synthetic	10.8	> 93 %	Berkessa et al., 2020
Submerged	Flat	6.8 L/ 35 ºC	0.018	200	Carbonmesh polyester mesh	4.125	1.115	>400 mbar	Artificial	26	Up to 98%	Jia et al., 2020
Side-stream	Flat	10/37	0.01	100	Acrylonitrile Butadiene styrene Filament h	14-28		350	Textile	10.8	98.5	Waktole et al., 2020
Submerged	Flat	4/35	0.01	20	Nylon mesh	8		450	Textile	10	91-93	Yurtsever et al., 2021

1.2.7. Comparision of AnDMBR with AnMBR

In AnDMBRs, the solid-liquid separation is done by DM itself. Particularly, dynamic membrane uses cake layer as filtration device (Mahat et al., 2018). However, the treatment performance of AnDMBR is comparable or slightly lower than of AnMBR (Hu et al., 2018a). The reason was the support layer has less retention capability of solutes and colloids during DM formation stage. According to reported studies, suspended solid concentration in AnDMBR effluent was less than 20 mg/L (Yang et al., 2020; Ersahin et al., 2014, 2016a,b). This value is much lower than the value, obtained by the conventional bioreactor operated under anaerobic condition (Hu et al., 2018a) and can be used for some purposes such as pretreatment and irrigation. However, this could affect retention of biomass to some extent due to escape of small particles. This negative impact could be overcome by improving both rapid and stable formation of DM and extending SRT in the system (Hu et al., 2018a). As mentioned before, lower filtration resistance and higher membrane flux can be obtained by the usage of cheap and coarse-pore support layer in AnDMBR systems. Besides, as mentioned in previous section (Section 1.1.3), there is no difference between AnDMBR and AnMBR for other properties such as biogas production, temperature sensitivity, organic loading rate, footprint, sludge production, alkalinity requirement, start-up time (less than 2 weeks) (Hu et al., 2018a).

1.2.8. Factors affecting DM formation

There are some factors that affect DM formation in the reactor. These are properties of support layer, sludge characteristics, operation conditions of DM such as cross flow velocity, organic loading rate (OLR) and HRT, Transmembrane Pressure (TMP)-Flux, Critical Flux, Membrane Resistance, and the characteristics of wastewater.

1.2.8.1. Properties of support layer

DM forms on the support material, thus to select a convenient support material is very important in order to retain particles and form DM layer on its surface. In addition to this, the support material should strong enough to resist required pressure and should be very cheap. The pore size of DM layer has an effect on both permeate flux and DM formation rate. Thus, pore size of support layer and particle size should be considered together for

best separation performance. Due to the fact that support material pore size is larger than conventional membranes, the effluent quality will be lower at the beginning of operation (Ersahin et al., 2012).

Jeison et al., 2008 reported cake layer formation was impossible on support material with large pore sizes (larger than 60-70 μm). In addition to this, they added that mesh with small pore size (between 1 and 10 μm) led to a quick increase in resistance of cake layer. However, there have been lots of reported studies that DM was formed on larger pore sizes (more than 60μm) (Zhang et al., 2010; Zhang et al., 2011; Ma et al., 2013; Alibardi et al., 2016; Hu et al., 2018b; Yang et al., 2020). The mesh should have convenient pore size that provide both long-term operation and retainment of sludge floc in the system (Siddiqui et al., 2019).

1.2.8.2. The properties of sludge

The effect of sludge properties (flocculability, settleability, dewaterability and EPS) on DM formation have been investigated by several researchers (Ersahin et al., 2016b; Zhang et al., 2014b; Yu et al., 2019; Hu et al., 2020). Organic substances (such as EPS and SMP) is widely accepted as main factor for formation of membrane fouling (Zhang et al., 2011). Ersahin et al., 2016b reported that high amount of EPS in DM layer contributed to the formation of a strict cake layer and efficient retention of soluble COD. Yu et al., 2019 studied about the effect of sludge properties on DM formation. They reported that normal sludge (concerning EPS, flocculability, settleability and dewaterability) exhibited a more satisfactory DM formation performance than sludge, having poor properties. Hu et al., 2020 added a chemical substance (zero valent iron) in AnDMBR system in order to investigate its effect on sludge properties and treatment performance. Zero valent iron can change sludge properties by serving as a coagulant, thus it can improve flocculating capability and particle size. In addition to this, they can improve inorganic fouling in DM layer (Hu et al., 2020). These researchers reported that addition of zero valent iron resulted in dense cake layer and also added that adequate amount of zero valent iron improved treatment performance. It can be inferred that sludge properties are important factors affecting the performance of the DM system. Another researcher reported that the granular sludge improved removal of COD to a certain extent in the AnDMBR (Zhang et al., 2014b). The reason of this result was acidogenic and methanogenic bacteria could

effectively showed their cooperation within the granular sludge. Organic degradation by co-metabolism process improved microbial activity. Moreover, because granular sludge had good settling properties, a stable sludge layer could be maintained at the bottom of the reactor. By this way, both bio-adsorption and biodegradation effects could improve treatment efficiency. According to the reported studies, a long SRT resulted decline in the production of EPS and SMP (Masse et al., 2006; Ahmed et al., 2007). Siddiqui et al., 2019 reported that humic acid was found as dominant compound in EPS. In that study, humic acid attached rapidly to the support material and kept stable. Furthermore, polysaccharide was found to be main material that formed DM. Moreover, Quek et al., 2017 stated that the protein/carbohydrate ratio was very important in DM formation. The protein attached to membrane surface easily due to hydrophobic characteristics, and caused to membrane fouling. Thus, higher Protein/Carbon (P/C) in bound of EPS could help formation and stabilization of DM. The microbial properties of sludge have been investigated by researchers in AnDMBR systems. Ersahin et al., 2016b found that different microbes in bulk sludge and DM layer due to different microenvironments such as hydrogen pressure, organic bioavailability, pH gradient. The similar results were observed by Quek et al., 2017 and they added that adaptation to different environments in bulk sludge and DM layer resulted in presence of different microbes. Moreover, they stated that the analyzing of microbial community would provide a chance to search the effect of microenvironments on abundance of microbes. By this way, microbial species, which improve production of CH_4 and removal of particles, developed the system (Quek et al., 2017).

1.2.8.3.Operation conditions of DM

Cross flow velocity (CFV)

DM layer should be controlled to prevent very thick layer that cause significant decrease in membrane permeability and increase in TMP. It is very important to control cake layer thickness to obtain longer and sustainable operation for effective DM layer control. Control of DM layer development related with membrane configuration similar to conventional membranes. Mostly, gas addition (biogas recirculation/aeration) is used in submerged module configuration whereas the liquid CFV is applied to the external modules (Alibardi et al., 2014). Gas addition has lower energy consumption than CFV

(Judd, 2006). Thus, submerged MBRs have been applied extensively. However, the application of gas addition in submerged MBRs can prevent their continuous operations and the preservation of anaerobic conditions in AnMBRS. Thus, CFV application on external configuration could be more convenient for AnMBRs (Ho and Sung, 2009).

In conventional membranes, CFV is applied to prevent membrane fouling. On the other hand, the membrane permeability and thickness of cake layer can be controlled by CFV in DM systems. By applying CFV, stable DM layer can be provided, high increase in TMP can be prevented and need for frequent membrane cleaning are eliminated (Alibardi et al., 2014). CFV simply creates a shear force that cause back transport of accumulated solids that detach the loosely (particles have greater size than pore size) and slow down formation of cake layer (Chang et al., 2002). On the other hand, shear force is ineffective for smaller colloids that result blocking inside the pores of filter (Wang et al., 2020). It also breaks up the large particles generating fine colloids and microbial cells which results in formation of dense cake layer on membrane (Chang et al., 2002). The mechanisms of back transport in a CFV system contains inertial lift, shear-induced diffusion, and Brownian diffusion (Figure 1.5). These forces that generated by CFV tend to raise with CFV and particle size except for Brownian diffusion, which generally occurs when the particle diameter (d_f) is less than 0.1 μm (Kim et al., 2004).

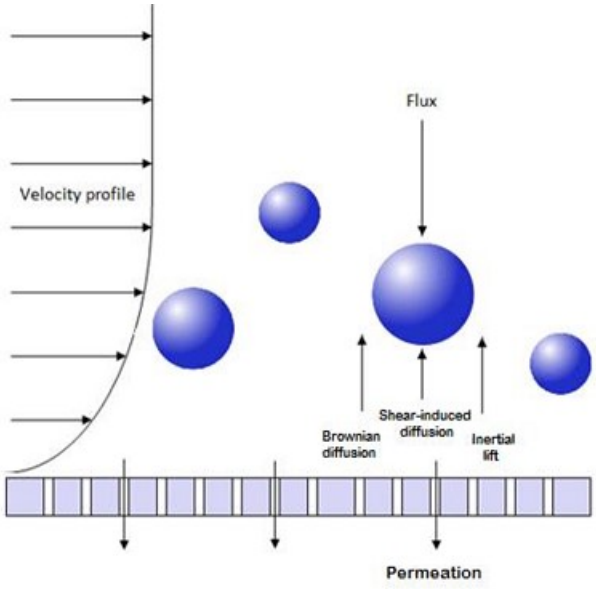


Figure 1.5 Schematic view of particles exposed to different forces during filtration under CFV (Kisielius, 2012)

There is an inverse relationship between Brownian diffusion force and particle size (Belfort et al., 1994). Brownian diffusion also occurs in the absence of shear velocity (cross flow velocity). The shear-induced force generally happens when the particle diameter between 1 μm and 10 μm, including colloids like macromolecules, cell debris, microbes (Buffle and Leppard, 1995). The inertial lift generally happens when particles higher than 10 μm. In addition to this, there is a direct proportion between temperature and back transport velocity of particles. As the size of particle and applied CFV increase, the back transport velocity of the particles increases (Belfort et al., 1994). Thus, tangential shear, created by CFV can hinder accumulation of large particles more effectively than small particle (Choo and Lee, 1998). Accordingly, it can be inferred that higher CFV lose its back transport effect on colloids.

OLR and HRT

HRT is one of the factor that affect DM treatment performance. Alibardi et al., 2016 operated AnDMBR under varied HRT and OLR. They reported that low HRT (less than 0.5 day) induced deterioration of cake layer resulting solid escape into the effluent. In addition to this, growth rate of biomass could not be proceeded sufficiently with low HRT. They also reported that as HRT decreased (less than 0.5 day), removal of COD declined (less than 80 %) and decrease in HRT resulted in CH_4 loss from the system. Yang et al., 2020 studied with various HRT and OLR during municipal wastewater treatment by AnDMBR (75μm). HRT decreased (from 8h to 1h), and OLR increased (from 0.82 to 6.8 kg/m^3day) in that study. They stated that increase in OLR could induce substrate inhibition of anaerobic microorganisms. In addition to this, they added that operation with short HRT could cause incomplete organic degradation. However, other factors (such as pore size) should be considered such that large pore size can result escape of more solid from the system and this can affect system performance. Moreover, Hu et al., 2018a reported that AnDMBR could be operated with high OLR because high biomass could be kept in the system. In addition to this, there have been reported ADMBRs/ AnDMBRs studies that more than 95 % COD removal was obtained with high concentration of OLR more than 10 kg COD/m^3d (Mahat et al., 2018).

TMP-FLUX

Transmembrane pressure and membrane flux are the best indicators of membrane fouling (Abdelrasoul et al., 2013). TMP is important operating parameter that indicates of DM formation and filtration performance, and it is necessary for a longer and sustainable operation (Hu et al., 2018a). According to Alibardi et al., 2014, TMP profile is described by three stage. These are DM formation stage, rapid fouling stage and consolidated stage.

During formation stage of DM, TMP is almost negligible. Accumulation of particles and biofilm growth on support layer do not sufficiently affect TMP. After a while, due to rapid fouling sharp increase in TMP happens. The reason of this rapid fouling is accumulation of solids and sustained biofilm growth over cake layer, that has already accumulated on support layer and lead to complete blocking of pores of support layer. In consolidated stage, this layer becomes more compacted and thicker, resulting in stable TMP. Moreover, the correlation between TMP and the thickness of DM in long-term operation was mentioned by Pootschi et al., 2015. Xiong et al., 2014 reported higher pressure resulted in denser DM formation and this resulted in lower turbidity in effluent.

DM formation is also indicated by decrease in flux (Hu et al., 2016). Moreover, Sun et al., 2018 reported that flux variation under constant pressure during AnDMBR operation.

The variation of flux includes two stages; DM formation, the operation with sustainable flux. During DM formation stage fast decrease in initial flux happens. After DM formation, flux proceeded to decrease with very slow decreasing rate (sustainable flux).

In addition to this, the effect of applied flux on DM formation was detected. Alavi Moghaddam et al., 2002, applied high flux during DM operation and observed that high flux caused deterioration in the effluent quality due to suction of particles which pass through the large pores of the filter. However, dense and compact DM layer was created by applying high flux in the beginning of operation (Saleem et al., 2016).

Critical flux

Critical flux has been applied to estimate and avoid fouling. It is described as decline in flux with time does not happen, whereas above this flux, fouling occurs in DMs

(Satyawali and Balakrishan, 2008). The critical flux is detected in order to determine operational flux in order to provide longer filtration time (Li et al., 2017).

Flux-step methods (Le Clech et al., 2003) are applied to detect critical flux (Figure 1.6). However, Alibardi et al., 2014 and Ersahin et al., 2013 reported that critical flux was not exact indicator and only parameter for long-term filterability of DM. Chu et al., 2014 stated that operation conditions, properties of membrane could have effect on critical flux. There are some studies that have reported CFV values (Li et al., 2017).

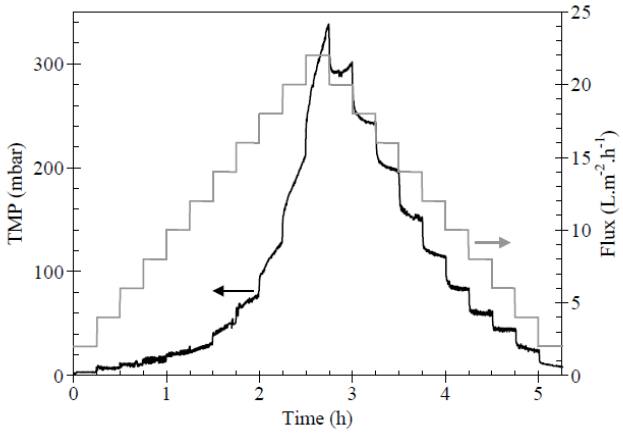


Figure 1.6 Schematic view of critical flux determination (Le- Clech et al., 2003)

Membrane resistance

Membrane resistance is an important indicator of DM filter capability (Xiong et al., 2016). Membrane resistance is generally governed by cake layer formation both in Aerobic Dynamic Membrane Bioreactor (ADMR) and AnDMBR (Ersahin et al., 2012). In DM operation, total resistance is the sum of cake layer, gel layer and virgin layer. Ersahin et al., 2012 reported that cake layer had an important effect in filtration resistance. Moreover, mostly cake layer resistance forms total resistance. During DM operation, as cake layer formation continues, this causes additional increase in membrane resistance. The excess cake layer is regarded as DM fouling. DM fouling declines permeate flux and shortens DM operation time. Thus, it is important to control cake layers in order to operate at a lower membrane resistance (Xiong et al., 2016).

1.2.8.4.The characteristics of wastewater in AnDMBR applications

Mostly, industrial wastewater and real-simulated municipal wastewater has been used as feed in AnDMBR operations. The various wastewaters have various characteristics such as biodegradability, toxicity, and composition (Hu et al., 2018a). During industrial wastewater treatment with AnDMBR, it can be encountered with some difficulties such as toxicity, high biodegradability, and high toxicity (Dereli et al., 2012). Moreover, biodegradability of municipal wastewater is high and it has low toxicity. During municipal wastewater treatment with AnDMBR, high filtration performance, low fouling potential and good treatment of wastewater can be obtained (Mc Carty et al., 2011).

1.2.9. Cleaning strategies

When DM layer is formed, high-quality permeate in the effluent can be obtained. The high-quality effluent obtained by DM can be comparable with conventional membranes (Mahat et al. ,2018). However, flux decreases due to membrane fouling. Thus, application of cleaning methods is needed to obtain longer and sustainable operation for effective DM layer control, accomplishing separation and reformation of DM. There have been reported studies about application of DM cleaning strategies (Hu et al., 2018a). The methods of physical cleaning are backwashing, biogas sparging, mixed liquor recycling, membrane relaxation, brushing; liquid cross-flow, vibration. There is a reported study that applied chemical cleaning for reformation of DM (Hu et al., 2018a). However, there have been lots of reported studies that applied physical cleaning method during DM operation. The recirculation of sludge was done in order to create shear force (CFV) on DM surface to control fouling (Yang et al., 2020). The combination of biogas sparging and backwashing was applied for reformation of DM (Jia et al., 2020). In another study, cycling of mixed-liquor was done in order to create CFV on DM surface in order to control fouling (Alibardi et al., 2016). Both sustainable and longer operation were achieved by using these cleaning methods due to govern DM fouling efficiently and accomplish separation of DM layer and regeneration of DM layer (Hu et al., 2018a). All these results show that it is applicable to perform combined or individual cleaning strategy (biogas recycling, sludge recirculation, e.g.) to control DM fouling in AnDMBR systems. It is found that physical cleaning method is enough to regenerate DM layer and

permeability of DM layer. It should be noted that the efficiency of physical cleaning under anaerobic condition is similar to cleaning performance obtained under aerobic conditions (Hu et al., 2018a). There have been limited researchers about application of chemical cleaning for regeneration of DM (An et al., 2009). Due to no usage of additional chemicals, easy operating and control method, physical cleaning could be desired cleaning strategy in DM applications (Hu et al., 2018a).

1.2.10. Membrane fouling

As mentioned above, membrane fouling is a disadvantage for conventional membranes whereas, it is an advantage for dynamic membrane operation. As mentioned before, DM includes gel and cake layer. The cake layer, that formed by loosely attached foulants refers to reversible fouling. The gel layer, caused by strongly attached foulants refers to irreversible fouling. The physical cleaning methods can not remove the irreversible fouling easily (Meng et al., 2009).

Membrane fouling can be categorized as inorganic fouling, organic fouling, and biofouling (Meng et al., 2009). Biofouling corresponds to accumulation, metabolism and growth of bacteria cells and flocs on the membranes. It could begin with the accumulation of individual cell and cell clusters on the surface of membrane. The bacteria cells multiply and produce a biocake. SMP and EPS excreted by bacteria has an important effect on formation of biological foulants and cake layer (Flemming et al., 1997; Ramesh et al., 2007; Liao et al., 2004).

Organic fouling corresponds to the accumulation of biopolymers such as polysaccharides and proteins on the membrane (Meng et al., 2009). Generally, membrane fouling mostly consists of organic fouling, and biofouling rather than inorganic fouling even though all of them happen at the same time during membrane filtration of particles. The inorganic fouling can happen by two manners. These are biological and chemical precipitation.

Concentration polarization is continuous transport of feed to the surface which contribute to the accumulation of very little particles over the surface of membrane (Sadr and Saroj, 2015). The feed wastewater can include anions and cations. Thus, due to originating from feed wastewater, a large amount of anions and cations such as Hydroxide ion (OH^-), Sulfate ion (SO_4^{-2}), Phosphate ion (PO_4^{-3}), Carbonate ion (CO_3^-), Aluminium ion (Al^{+3}),

Magnesium ion (Mg^{+2}), Calcium ion (Ca^{+2}), Ferrous ion (Fe^{+2}) e.g. and other cations/anions is existing in MBR. Concentration polarization contributes to retainment of salts in high concentration on the surface of membrane. When concentration of chemical species surpass the saturation concentrations as a result of concentration polarization, chemical precipitation happens. Carbonates are one of significant salts, that take part in inorganic fouling. In addition, biological precipitation contributes to inorganic fouling. Proteins, polysaccharides (biopolymers) involve ionizable groups (OH^-, Carboxylate salts (COO^-), CO_3^{-2}, SO_4^{-2} and PO_4^{-3} e.g.) (Figure 1.7) (Meng et al., 2009).

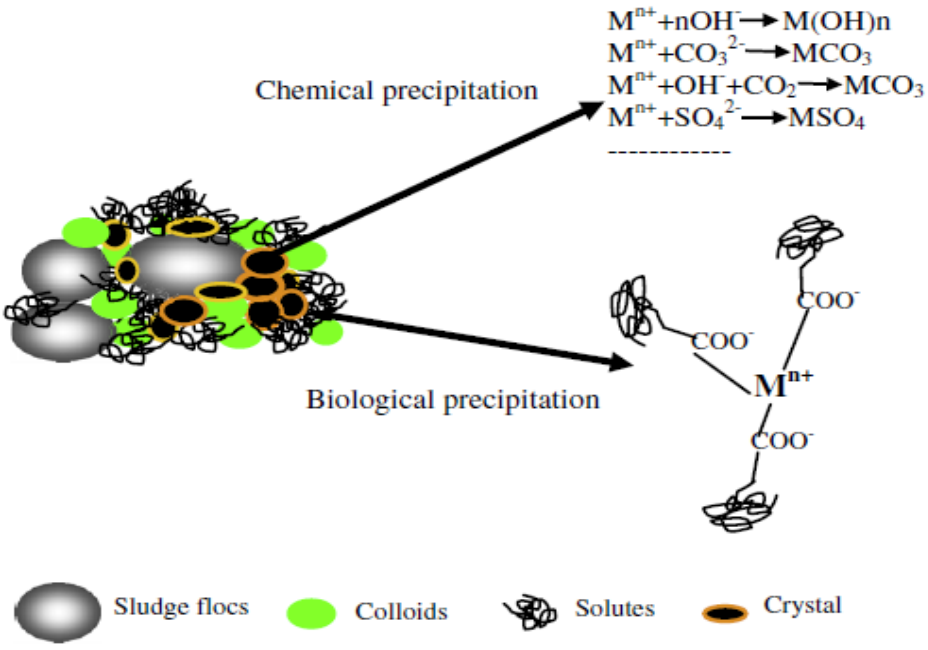


Figure 1.7 Diagram for the inorganic fouling formation on membrane surface (Meng et al., 2009)

Metal ions can capture these negative ions. Moreover, acidic functional groups and calcium can produce complexes and develop a gel layer or thicker cake layer, which could cause more decline in flux. During filtration, metal ions move through the membrane, they are captured by the bio-cake layer over the membrane by way of charge neutralization and complexing. This speed up membrane fouling. Metal ions has an important effect on formation of the fouling layer, that can bridge biopolymers (protein, polysaccharides etc.) and accumulated cells and produce a dense cake layer (Meng et al.,

2009). The organic and inorganic components of DM have been analyzed and reported in some studies. For instance, Ersahin et al., 2016b reported organic components (such as polysaccharides, proteins e.g.), microbial communities and inorganic components (such as Mg, Ca) in DM layer and added that these compounds affected structure of DM layer and thus treatment performance of the system.

1.2.11. The relationship between particles and membrane blocking mechanisms

Membrane fouling is an encountered problem in conventional membrane applications that result decrease in flux or increase in TMP. As mentioned before, DM is quite different from conventional membranes such that gel/cake layer, which is a part of membrane fouling, behave as a filter in DM applications (Mahat et al., 2018). An excess growth of dense and thick fouling layer prevents a long-term operation of DM owing to extreme loss of membrane permeability (Saleem et al., 2017). Mathematical modelling is an appropriate tool that has been carried out for analyzing fouling in conventional membranes (Hermia, 1982). Additionally, the classic filtration laws (four models) have been also applied in DM to evaluate the fouling variation over time by indicating as standard blocking, complete blocking, intermediate blocking, and cake filtration model (Lin et al., 2009; Gong et al., 2014; Saleem et al., 2017). However, modelling study of DM has not been discussed deeply (Mahat et al., 2018). DM formation is a complex process consisting of many both microbiological mechanisms and physicochemical (pore blocking, internal deposition, and cake formation) (Liu et al., 2009). According to Liu et al., 2009, DM formation mechanism was divided into 4 stages. These were formation of substrate formation, separation layer, fouling layer, and filtration cake. The formation of these four stages were testified by classic filtration laws model (blocking mechanisms) (Liu et al., 2009). In addition to this, Saleem et al., 2017, applied these mathematical models to detect blocking mechanisms, formed in DM. They found that only cake layer filtration described DM formation. As mentioned before, the reported studies are limited so more studying is needed to understand blocking mechanisms that happen in DM. The schematic view of membrane blocking mechanisms are presented in Figure 1.8.

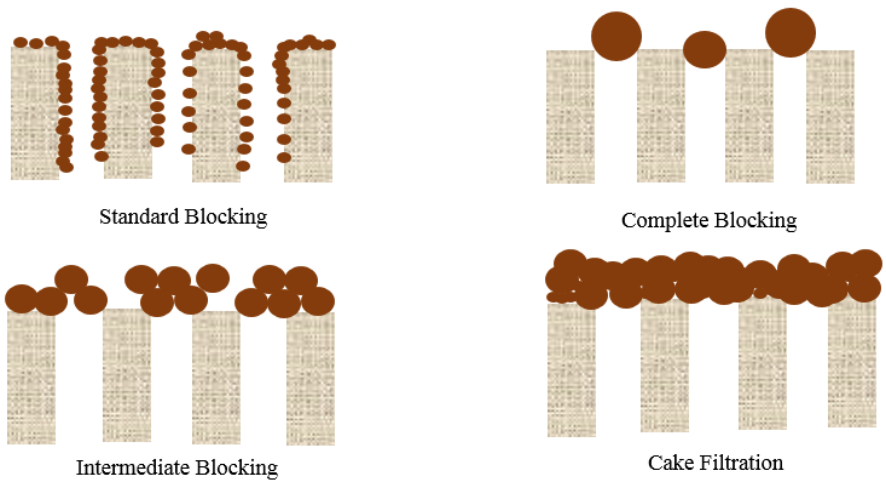


Figure 1.8 Schematic view of membrane blocking mechanisms

Intermediate blocking, complete blocking, standard blocking and cake filtration models have been developed to express flux behaviors for dead-end filtration under constant filtration pressure in conventional membranes (Hermia,1982). Complete pore blocking mechanism happens when each particle reaching the membrane blocks a pore without accumulating on each other. Standard blocking model happens when particles deposit within the pores of membrane. Intermediate blocking happens when particles accumulate on other particles that have already blocked some pores of membrane and block some pores of membrane. Cake filtration model happens when depositing particles do not block pores; particles deposited on membrane surface due to having bigger particle size than pore size of membrane or because the membrane pores are already covered by other particles (Bowen et al.,1995). All models indicate that flux decline happens depending on the ratio of pore diameter to particle size (support layer) (Table 1.5) (Ye et al., 2005). The blocking mechanism is determined by the proportion of the particle size ($d_{particle}$) to membrane pore size (d_{pore}) (Wang et al., 2020). The particle size has an important effect on membrane fouling. When $d_{particle}$ is less than d_{pore}, the particles can be deposited onto pore walls or surface of membrane, or the particle moves through the membrane. When $d_{particle}$ is equal d_{pore}, the particles block internally/externally pores of membrane or form gel/cake layer over the surface of membrane. When $d_{particle}$ is higher than d_{pore}, the particles typically block pore of membrane or forms gel/cake layer over the surface of membrane (Wang et al., 2020).

Table 1.5 Definition of blocking mechanisms (Liu et al., 2009)

Blocking Mechanism	Definition of Blocking Mechanism
Standard Blocking	Particles smaller than the membrane pore size deposit onto the pore walls and this reduces the pore size of membrane
Complete Blocking	Pore Blockage by particles without laying over other Particles
Intermediate Blocking	Pore Blocking by particles with laying over other particles
Cake Filtration	Particles larger than the membrane pore size deposit over the surface of membrane

1.3. Scope of The Thesis Study

The dairy industry is one of the important food industry. Milk and milk products include vital nutrients which is essential for human life. They have also economic value (Karadağ et al., 2015b). Dairy wastewater is produced due to activities occurring in dairy plants (Karadağ et al., 2015b). Dairy wastewater has high organic content (Joshiba et al. ,2019). The researchers have been employed UASB as a reactor for dairy wastewater treatment (Demirel et al., 2005). As mentioned before, some problems could be encountered during dairy wastewater due to its high lipid content (Karadağ et al., 2015b). Membrane integration into system can solve this problem. On the other hand, it increases capital and operational costs. In addition to this, low membrane flux and rapid fouling are another problems that are encountered in membrane applications. DM technology could overcome these problems (Ersahin et al.., 2012). Fouling is a disadvantage for conventional membrane while advantage for DM systems. In DM applications, cake layer act as a filtration device (secondary membrane) due to capability of particle rejection (Hu et al., 2018a). DM, formed on coarse-pore support material, can be operated with higher flux than conventional membranes (Ersahin et al., 2012).

In this study, considering these advantages, DM technology for dairy wastewater treatment was applied to investigate its applicability and treatment capability. There are factors that have effects on the treatment performance of DM such as properties of support material (pore size e.g.) and operational conditions (CFV, e.g.) (Hu et al., 2018a).

Properties of support material is an important factor due its effect on formation of DM, flux, and filtration performance (Ersahin et al., 2012). CFV is another important factor to control DM layer for sustainable operation by changing it in order to prevent sudden membrane fouling on support layer and enable cake layer formation on support layer. All in all, in first phase of the study (Section 3.1), the treatment performance of self-formed DM with selected pore size for dairy wastewater was investigated. During the operation, DM layer thickness was controlled by the CFV created by the internal recycle process. At the beginning of the study, synthetic milk wastewater was used as feed, and then real cheese whey was used as feed. To the best of our knowledge, this is the first study focusing on the treatment of cheese whey with an AnDMBR.

The support material, where DM forms, should have a convenient pore size for productive and sustainable DM operation. The usage of large pore size can provide both low cost and filtration resistance of membrane module (Alibardi et al., 2016). Larger pore size provided higher flux and lower solid retainment than smaller pore size in AnDMBR studies (Hu et al., 2018a). Salerno et al., 2017 found that larger pore size caused slower cake formation and clogging of support layer while smaller pore size obtained stable and low turbidity values. Sahinkaya et al., 2017 reported larger pore size provided stable operation whereas small pore size resulted in rapid fouling and frequent physical requirement. All things considered together, in second phase of the study, firstly, the influence of various pore sizes on DM formation, flux and filtration performance was investigated. In the second part of this phase, the same pore size (40 μm) as in previous study (Section 3.2) was selected to investigate and compare the effect of CFV on the DM formation and filtration operation. Modelling of DM was done with the data gathered from previous parts of second phase of the study (Section 3.2 and Section 3.3). The purpose of this last step of the second phase (Section 3.4) was to clarify the mechanisms responsible for external DM formation under various conditions.

As a result of filtration experiments, it was decided to use small pore size (20 μm) for DM formation and effective solid retainment from the beginning of the operation, and apply CFV for long-term operation. In this section (Section 3.5), filtration time was prolonged to gain experience with long-term operation and observe the problem that could arise during operation. The effect of CFV on submerged DM in a UASB reactor has not been discussed comprehensively until this study. An effective internal

recirculation was applied to make solids in suspended and to create efficient CFV on support layer. By doing this, the interaction between solids and membrane was enhanced and the application of CFV became more effective on DM formation and operation. More solid filterability and effective applicability of CFV created condition for forming strict and dense DM layer that could enable higher COD removal efficiencies. Dune et al., 2020 reported that increasing cross flow by increasing the recirculation rate could be beneficial, although at some point, it could have negative effect on both performance and stability of AnDMBR. In this study, DM layer formation was controlled by way of the combination of increasing and decreasing (the increase followed by the decrease) of CFV. The goal of this procedure was to provide removal of large particles that cause sudden membrane fouling on support layer and attachment/deposition of small particles for formation of compact DM layer. The objective of this study was to assess the effectiveness of CFV in controlling the DM formation with an extended operation time. Thus, by operating system continuously with CFV, the anaerobic condition could be prolonged without renewal of DM. This could affect treatment performance and biogas production positively. The feed and sludge have important effect on DM formation and system performance. Thus, a detailed characterization of DM layer including inorganic and organic components, and its morphology was determined and discussed.

2. MATERIALS AND METHODOLOGY

Experimental set-up, experimental procedures and analytical methods are given in this chapter. A lab-scale UASB reactor was employed in the experiments. In certain periods of the study, a dynamic membrane module was integrated into the UASB reactor to operate the system as AnDMBR. Experimental study consisted of three phases; In the first phase, treatment performance of synthetic wastewater and cheese whey was investigated in both UASB and AnDMBR with different pore sizes. In the second phase of the study, the effect of pore sizes on the dynamic membrane formation time, cleaning frequency, characteristics and content of the dynamic membrane layer were investigated. Also, the effect of CFV on DM formation and fouling mechanisms were modelled by using the data gathered during dynamic membrane formation period. In the third phase of the study, dairy wastewater treatment performance was investigated in AnDMBR with a longer duration than the first phase with the application of variable cross flow velocities during the dynamic membrane formation and DM stability period. The methodology of the study is presented in Table 2.1.

2.1. Investigation of Treatment Performance of Synthetic Wastewater and Cheese Whey in UASB and AnDMBR

In this phase, treatment efficiency and filtration capability of AnDMBR for dairy wastewater treatment were investigated. The operation lasted 344 days. Synthetic wastewater and diluted cheese whey were used as feed for 287 and 57 days, respectively. The study began with control experiments, in which operation was carried out with UASB. Two different pore size nylon meshes (70 and 10 μm pore size) were used as support material.

2.1.1. Experimental set-up

The experimental setup used in this part of the study is shown in Figure 2.1. UASB reactor had height of 50 cm and diameter of 12 cm. The total volume of UASB reactor was 5.65 Liter (L) with a working volume of 4.52 L.

Table 2.1 The methodology of the study

First Phase: Treatment of synthetic wastewater and cheese whey by the anaerobic dynamic membrane bioreactor	Second Phase: Evaluation of Dynamic Membrane Formation with Different Pore sizes, CFV Effect on Well-Developed and The Characteristics of Well-formed DM Mathematical Modeling of Dynamic Membrane	Third Phase:Performance and Characteristics of Dynamic Membranes for Dairy Wastewater Treatment Under Anaerobic Conditions
• Start-up of UASB reactor for system stabilization OLR: 1.34 ± 0.1kg/m^{3}day Feed: Synthetic Milk Wastewater • AnDMBR (70 µm pore size nylon polyester mesh integrated into system) OLR: 2.6 ± 1.1 kg/m^{3}day Feed: Synthetic Milk Wastewater • UASB (Control Experiment) OLR: 4.0 ± 1.19 kg/m^{3}day Feed: Synthetic Milk Wastewater • AnDMBR (10 µm pore size nylon polyester mesh integrated into system) Two period with physical cleaning Period 1: OLR: 4.4 ± 1.3 kg/m^{3}day Physical Cleaning Period 2 OLR: 5.0 ± 1.0 kg/m^{3}day Feed: Synthetic Milk Wastewater • UASB (Control Experiment) OLR: 3.6 ± 1.6 kg/m^{3}day Feed: Synthetic Milk Wastewater • AnDMBR (10 µm pore size nylon polyester mesh integrated into system) OLR: 3.71 ± 2.69 kg/m^{3}day Feed: Cheese Whey Wastewater • UASB (Control Experiment) OLR: 3.95 ± 2.44 kg/m^{3}day Feed: Cheese Whey Wastewater	First Part a)The Experiment of Critical Flux for 10 µm pore size. Feed: UASB effluent b) Filtration Experiments for 10 µm , 20µm, 40 µm and 70 µm nylon polyester mesh. Three run was done for each pore sizes. Physical cleaning was done after each run. Physical cleaning was done two times for each pore sizes. Feed: UASB effluent Second Part a) Filtration Operation with 40 µm pore size nylon polyester mesh under Cross Flow Velocity. CFV experiments were done. Two run was done. Physical cleaning was done between runs. Feed: UASB Effluent b) The components of Dynamic membrane was investigated by SEM-EDEX, FTIR. Third Part a) Mathematical Modelling Hermia's Equations were used to detect membrane fouling mechanism of Dynamic Membrane.	• AnDMBR (20 µm pore size nylon polyester mesh integrated into system) OLR: 8.1 ± 1.5 kg/m^{3}day Feed: Synthetic Milk Wastewater The combination of Cross Flow Velocity and backwash was done to control cake layer thickness. Filtration operation was done continuously in 92 days. • DM layer characteristics were determined by PSD, SEM-EDX, FTIR, XRD, ICP-MS.

The working volume of UASB reactor consisted of a sludge zone where granular sludge was located and wastewater was degraded, and a settling zone, where particles were suspended. The settling zone played as a separation zone between suspended particles and upflowing water. There was 1.13 L volume above the working volume which was used to collect biogas in an aluminum balloon. Totally, there were six ports for pipe connections in the reactor. One port (port 1) was used for feeding the system. Another two ports, which were in same level with port 1, was inactive. Two ports (port 2 and port 4) were used for internal recycle. Two port, which was at the top of the reactor, one of them was used for collecting of gas (port 3) and another was inactive.

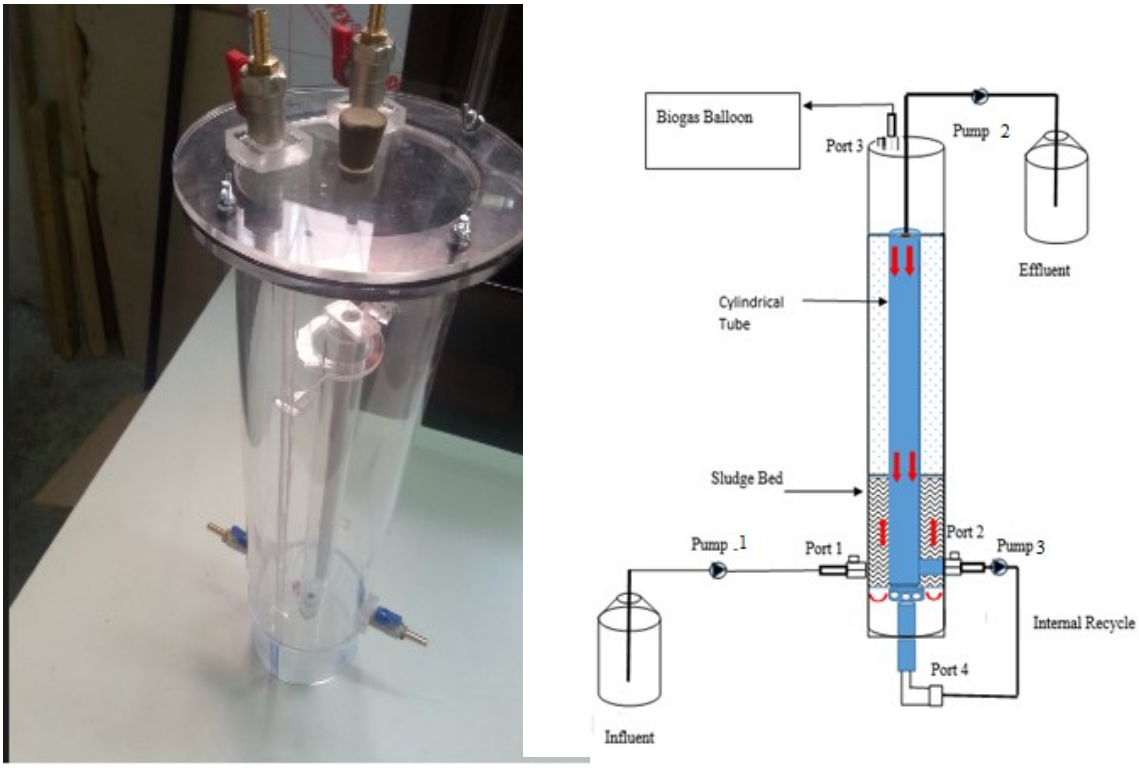


Figure 2.1 Schematic diagram of UASB reactor system used in this study

A peristaltic pump (Watson Marlow 323) was employed to feed wastewater into the UASB and to collect the effluent from the reactor. The wastewater entered into the system from port 1 (pump 1), which was very close to the bottom of the reactor. A sealed cover was placed to the top of the reactor to prevent entrance of air to the reactor. The treated water was removed from the reactor with the outlet pipe (pump 2). During dynamic

membrane operation periods, filtration modules were mounted in a cylindrical Plexiglas tube located to the middle of the reactor. The diameter and length of cylindrical tube was 3 cm and 40 cm, respectively. Internal recirculation was obtained by taking reactor content from the bottom of the cylindrical tube and giving back to the bottom of the reactor with a peristaltic pump (pump 3). By this was, CFV was also created, and particulates were kept in suspension.

The schematic drawing of AnDMBR is presented in Figure 2.2 The AnDMBR system consisted of a 4.52-L UASB reactor and two submerged tubular membrane modules made of commercially available nylon polyester mesh (Beyaztaş, Karaköy) with openings of 70 (phase 2) and 10 µm (phase 4 and 6).

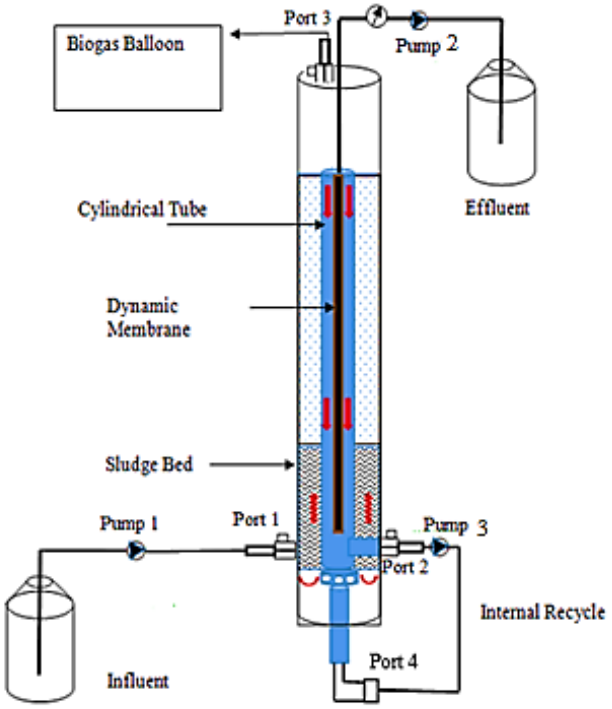


Figure 2.2 AnDMBR system

The membrane modules were located in the cylindrical zone during different periods of the study. The effective filtration area for the membrane module was 0.003 meter square (m^2). A peristaltic pump (pump1)(Watson Marlow 323) was employed to feed wastewater into the AnDMBR and another peristaltic pump (pump 2) was used to collect the permeate

from the reactor. A different peristaltic pump (pump 3) was used to create a CFV on the membrane surface.

The effluent pressure was measured using a 0~-1 bar Mini Dial Vacuum Pressure Gauge Manometer (Aterna, Turkey) placed in the effluent line. TMP was calculated by Equation 2.1.

$$\text{Transmembrane Pressure (TMP)} = \bar{P} - P_E \quad (2.1)$$

where;

$\bar{P}$ = The averaged hydraulic head at the mid-point of the membrane module

P_E = The effluent pressure

The measurement of influent and effluent pHs was done daily with a probe (Hach, pH/ISE meter, United States). The temperature of the reactor was maintained at 35°C with an aquarium heater (EHEIM GmbH&Co.KG, Germany).

Daily effluent of the reactor was measured by the use of a bench scale.

The membrane flux J (L/m^2h) was calculated according to Equation 2.2.

$$J = L/At \quad (2.2)$$

Where; L denotes the volume of permeate liquid per unit membrane area (A), and t refers to filtration time.

Total filtration resistance is a function of TMP, flux, and viscosity of the water. The filtration resistance was calculated using the following Equation (2.3).

$$R = TMP/\mu \times J \quad (2.3)$$

where R is the permeation resistance, TMP is the transmembrane pressure drop, μ is the dynamic viscosity and J is the membrane flux of the AnDMBR module.

2.1.2. Experimental plan

This study consisted of seven phases. During the operation, COD loading rate was increased in each phase (Table 2.1). Biogas was measured to detect biogas production capability of the system. At the beginning, synthetic wastewater was used as feed. The filtration operation was done by AnDMBR, and the control experiments was done by UASB. The polyester nylon mesh with 70 μm pore size was integrated into the system (Phase-2). The polyester nylon mesh with 10 μm pore size was used as filter in Phase-4 and Phase-6 (Table 2.2). In the last two phases, cheese whey was used as a feed.

COD, SS, VSS, oil-grease, alkalinity, ammonium nitrogen (NH_4-N), and Phosphate phosphorus (PO_4-P) were determined for the characterization of wastewaters. COD, Volatile Fatty Acids (VFA), SS, Volatile Suspended Solid (VSS), was determined to detect removal efficiency of the system. pH and alkalinity was measured daily to control the operation. The control treatment consisted of the operation performed with a UASB reactor in the 1st, 3rd, 5th, and 7th phases whereas; the 2nd, 4th, and 6th phases were run with the AnDMBR in (Table 2.2).

Table 2.2 Operation timeline with UASB and AnDMBR

Phase 1	Phase 2	Phase 3	Phase 4		Phase 5	Phase 6	Phase 7
			Physical Cleaning				
			First Period	Second Period			
UASB	AnDMBR (70 µm)	UASB	AnDMBR (10 µm)	AnDMBR (10 µm)	UASB	AnDMBR (10 µm)	UASB
Feed:Synthetic Wastewater	Feed: Synthetic Wastewater	Feed: Synthetic Wastewater	Feed: Synthetic Wastewater	Feed: Synthetic Wastewater	Feed: Synthetic Wastewater	Feed: Diluted Cheese Whey	Feed: Diluted Cheese Whey
COD Loading Rate: 1.34 ±0.19 $kgm^{-3}d^{-1}$	COD Loading Rate : 2.6±1.1 $kgm^{-3}d^{-1}$	COD Loading Rate: 4.0±1.19 $kgm^{-3}d^{-1}$	COD Loading Rate: 4.4±1.3 $kgm^{-3}d^{-1}$	COD Loading Rate: 4.4±1.3 $kgm^{-3}d^{-1}$	COD Loading Rate: 3.6 ±1.6 $kgm^{-3}d^{-1}$	CODLoading Rate:3.7±2.69 $kgm^{-3}d^{-1}$	COD Loading Rate: 3.95 ±2.44 $kgm^{-3}d^{-1}$
Operation days: 0-80	Operation days: 81-207	Operation days: 208-225	Operation days: 226-239	Operation days: 226-239	Operation days: 268-287	Operation days:288-315	Operation days:316-344

Table 2.3 (UASB) and Table 2.4 (AnDMBR) are presented influent and COD loading rate for all phases. HRT was set between 12 – 15 hours (0.5 - 0.625 days) during the experiments. The average pH value was 8.08 ± 0.52. CFV was used to control DM layer formation. During the operation of the 10-µm pore size AnDMBR, the membrane module was taken out at the end of the first period of phase 4 and cleaned with tap water physically with the help of an another pump and was then placed into the cylindrical tube. At the end of the operation, particle size distribution (PSD) analysis of settling zone was done.

Table 2.3 The feeding UASB with synthetic wastewater and diluted cheese whey

Stage	Days	Operation Conditions	Wastewater Type	Influent COD mg/L	COD Loading Rate, kg/m^{3}d
Phase 1	0-80	UASB	Synthetic Wastewater	1509 ± 118	1.34 ± 0.19
Phase 3	208–225	UASB	Synthetic wastewater	6025 ± 264	4.0 ± 1.19
Phase 5	268-287	UASB	Synthetic Wastewater	5864 ± 767	3.6 ± 1.6
Phase 7	316-344	UASB	Diluted CheeseWhey	11560 ± 1200	3.95 ± 2.44

Table 2.4 The feeding AnDMBR with synthetic wastewater and diluted cheese whey

Stage	Days	Operation Conditions	Wastewater Type	Influent COD mg/ L	COD Loading Rate, kg/m^{3}d
Phase 2	81-207	AnDMBR (70 µm)	Synthetic Wastewater	3309 ±1429	2.6 ± 1.1
Phase 4					
First Period (prior to physical cleaning)	226-239	AnDMBR (10 µm)	Synthetic Wastewater	5989 ± 234	4.4 ± 1.3
Second Period (after physical cleaning)	240-267	AnDMBR (10 µm)	Synthetic Wastewater	6035 ± 876	5.0 ± 1.0
Phase 6	288-315	AnDMBR (10 µm)	Diluted Cheese Whey	7699 ±2185	3.71 ± 2.69

2.1.3. Wastewater characteristics and seed sludge

The reactor was inoculated with anaerobic granular sludge produced under mesophilic conditions from an anaerobic tank at the Cartoon Industrial Wastewater Treatment Plant, İstanbul, Turkey. The granular sludge concentration was 49.6 g/L. During phases 1, 2, 3, 4 and 5, synthetic commercial wastewater was used as substrate, and was prepared by diluting commercial milk powder (Pınar, Turkey) with tap water. The characteristics of synthetic wastewater for 2 g/L are presented in Table 2.5. The milk powder (2 g/L) consisted on 1.04 g/ L carbohydrate, 0.025 g/L Ca^{+2}, and 0.72 g/L protein. During reactor operation with synthetic wastewater, the concentration of milk powder was increased stepwise, in the order of 1.5, 2, 2.5, 3, 4, 5, 6 and 7.5 grams of milk powder diluted in 1 L of tap water. Alkalinity was added to provide the target pH value of 7.5 for anaerobic treatment.

The concentrated whey permeate was attained from a dairy product manufacturer, Çayirova Dairy Product Company, in Turkey. Starting from day 288, diluted cheese whey was introduced as feed. Cheese whey was diluted with tap water in the following proportions volume/volume (v/v): 1/10, 1/8, 1/6, and 1/4. Alkalinity was added to adjust pH to the target value of 7.5. Both the high-strength synthetic wastewater and cheese whey wastewater characteristics are shown in Table 2.5.

Table 2.5 The characterization of synthetic wastewater and cheese whey

Parameter	Synthetic wastewater for concentration of 2 g/L	Cheese whey
COD, mg/L	2200	53000
PO_4-P, mg/L	3.42	825
NH_4-N, mg/L	8	75
SS, mg/L	605	7970
VSS, mg/L	510	5270
Alkalinity, mg $CaCO_3$/L	1430	1366
pH	6.96	6.8
Oils and Grease, mg/L	75	10000

2.2. Investigation of the Effect of Pore Sizes on The DM Formation Time, and Cleaning Frequency

At the beginning of second phase, critical flux was determined. Then, in following operational time, the imposed flux was kept higher than critical flux. By doing this, all pore size (10,20, 40 and 70 μm pore sizes) could be evaluated in terms of cake layer formation and filtration performance in shorter operational time. 10,20, 40 and 70 μm tubular polyester nylon mesh were used, respectively for filtration operation. Filtration performance was evaluated by flux, TMP, and membrane resistance. In contrast to the first phase, filtration operation prolonged after DM formation for a while. Different from previous phases, turbidity was used additionally to monitor DM formation. At the end of each run for 40 and 70 μm pore size COD was measured to detect treatment capability of filters.

2.2.1. Experimental set-up

The experimental setup used in second part of the second phase is presented in Figure 2.3. The system was operated semi-continuously. The filtration operation was done about 9-10 hours in a day. A peristaltic pump (pump 1) (Watson Marlow 323) was employed to feed the synthetic milk wastewater into the UASB. Another peristaltic pump (pump 2) was used to collect the permeate from the reactor. The effluent of the bioreactor collected in a tank and used as filtration operation. The collected UASB effluent was fed into the cylindrical tube (1 L) using laboratory peristaltic pump (pump 3) (Labor Technik, Dusseldorf). As seen in Figure 2.3, the filtration was done in cylindrical tube, where the membrane module was located in. Mixing was carried out with a magnetic stirrer in order to keep solids in suspension. The aim was to enhance the contact between particulates and surface of nylon mesh. The filtrated water collected with a pump (pump 4) in a tank, where was set on a volumetric weighing scale. Experiments were carried out at room temperature (20°C).

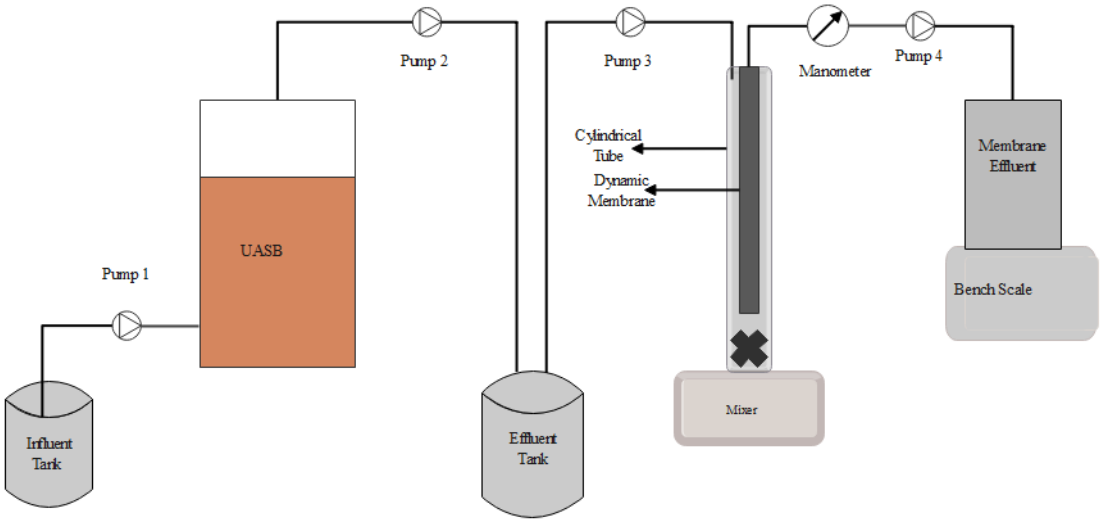


Figure 2.3 The diagram of experimental set-up

Characteristics of the support layers used in these experiments are presented in Table 2.6. The supporting membrane was of a polyester nylon mesh with tubular configuration. The effective area of the membrane module was 0.014 m^2. Pressure was determined via 0~-1 bar Mini Dial Vacuum Pressure Gauge Manometer (Aterna, Turkey) placed in the effluent line. During whole operation, HRT was 33±6 hours and the temperature of the reactor was maintained at 28°C with an aquarium heater (EHEIM GmbH&Co.KG, Germany) in UASB.

TMP was calculated according to the procedure reported by Le Clech et al.,2003. Filtration capability of membrane modules were evaluated with membrane resistance parameter. The membrane resistance, which is the sum of cake layer, gel layer and the intrinsic membrane resistance, was calculated according to Equation 2.4.

$$R_t = R_m + R_P + R_c \quad (2.4)$$

Where R_m is the hydraulic resistance of virgin support layer, R_p is the irreversible filtration resistance due to the gel layer formation, and R_c is the reversible filtration resistance due to cake formation.

R_t was calculated by using flux and TMP obtained during dynamic membrane filtration.

R_m was calculated by using the flux of tap water on virgin support layer and corresponding TMP.

After the cake layer was removed from the support layer by spatula, the filtration of tap water on gel layer (including support layer) was done. As a result of filtration, the flux and TMP was used to calculate the resistance (R_m+R_p). R_p was calculated by subtracting R_m from R_m+R_p.

R_c was calculated by subtracting R_t from the sum of R_m and R_p. (Equation 2.4).

Table 2.6 Characteristics of the submerged membrane module

Category	Module
Membrane Module Type	Tubular
Material	Polyester
Pore Size, μm	10-20-40-70
Effective Filter Area, m^2	0.014

2.2.2. Experimental plan

The effect of support material pore size on the filtration behaviors were assessed during start-up and stabilized stages of DM. The various range of support materials (10, 20, 40 and 70 μm) were used in filtration operation. Prior to filtration experiments, critical flux to shorten the DM formation time. By doing this, the effect of pore size on DM formation was evaluated efficiently by comparing filtration results with each other. The critical flux was only determined for 10 μm to assess convenient operational flux for all studied pore sizes. When TMP increased higher than 800 mbar, filtration continued for a while. The membrane module was taken away in that case and cleaned with tap mater to remove cake layer on nylon mesh. After physical cleaning, membrane module was put into cylindrical tube. The filtration were repeated three times and physical cleaning was carried out at the end of each filtration period. In other words, in totals, 3 runs were carried out for each pore sizes. Initial fluxes together with test time are presented in Table 2.7 for all studied pore sizes and number of run phase.

Table 2.7 Applied mesh pore sizes and operating conditions in all tested runs

Runs	Mesh Pore Size, µm	Initial Flux, L/m^2h	Test Time, Hours
Run-1	10	98	3.28
Run-2	10	84	2.83
Run-3	10	85	5.05
Run-1	20	97	9.26
Run-2	20	73	11.66
Run-3	20	91	10.083
Run-1	40	95	68.43
Run-2	40	89	64.03
Run-3	40	55	14.8
Run-1	70	93	95.86
Run-2	70	91	21.83
Run-3	70	96	14.23

Turbidity in UASB and membrane effluents measured during the operation of filtration. Turbidity was measured to detect dynamic membrane formation. At the end of filtration operation with 40 and 70 µm pore sizes, COD concentration were measured in the membrane effluent for all runs. SS in the membrane effluent was measured during the filtration operation with 10, 20 and 70 µm pore sizes only for first run. TMP was measured to detect solid accumulation on support material. The membrane resistance was calculated to determine filtration capacity of the filters. Moreover, COD, SS were also detected in UASB effluent from time to time.

2.2.3. Critical flux experiment

The critical flux is defined as a flux in which below a decrease in membrane permeability with time does not happen and above which fouling is observed (Field et al.1995). Critical flux can be determined by flux-run method (Figure 2.4). In this experiment, the critical flux was determined by applying the method reported by Le Clech et al., 2003. It is called flux-run method and flux was increased at every 15 minutes by increasing the speed of peristaltic pump. In the study of Le Clech et al., 2003, flux increased in 2 L/m^2h increments at the end of each 15 minutes. In our experiment, the laboratory peristaltic pump used (Labor Technik, Dusseldorf) had less sensitive RPM range. Thus, flux was increased as presented in Table 2.8 at the end of each 15 minutes.

Table 2.8 The membrane flux, corresponding to different speed of pump during critical flux operation

Rpm	Flux, L/m^{2}h
10	11
20	22
30	40
40	60
50	73
60	82
70	92
80	95

The membrane flux was incrementally increased, and the pressure change was followed with help of a manometer. Under the experimental conditions, the water level above the membrane module was kept at a constant level, and TMP presumed to vary only depending on alterations in permeate pressure because of fouling.

2.2.4. Wastewater characteristics and seed sludge

The effluent of UASB that was used for critical flux experiment is presented in Table 2.9 During filtration operation, the characteristics of UASB effluent is presented in Table 2.10

Table 2.9 The characteristics of UASB effluent water used in critical flux

Parameters	Value
COD, mg/L	650
SS, mg/L	280
pH	8.16

Table 2.10 The characteristics of UASB effluent used in filtration experiment

Parameters	Value
COD, mg/L	1817±728
SS, mg/L	1477±660.8
Turbidity, NTU	818±246
pH	7.73

2.3. The Effect of CFV on a Well-Formed DM Operation and The Characteristics of Well-Formed DM

In the second part of Phase 2, effect of CFV on DM formation was investigated. Besides, the organic and inorganic components of DM were also investigated.

2.3.1. Experimental set-up

After the effect of pore size on DM formation was investigated (first part of second phase), the effect of CFV on DM formation and operation were investigated. CFV (between 9 m/h and 77.52 m /h) is an important parameter to control cake layer thickness. In previous section, DM was formed in shorter time under high flux. In this part, filtration operation was done by controlling cake layer formation to improve filtration time. 40 µm pore size was selected for filtration operation. Filtration performance was evaluated by flux, TMP, and membrane resistance. In contrast to first phase, after DM formation, filtration operation prolonged for a while. In addition to this, turbidity was used to indicate DM formation.

A submerged polyester nylon mesh with 40 µm pore size was used for filtration operation. The system was operated semi-continuously. The filtration operation was done about 9-10 hours in a day. UASB was operated under the same conditions as first part of second phase (Dynamic Membrane Characteristics of Different Pore Sizes). The effluent of the bioreactor collected in a tank and UASB effluent was feed for filtration operation and the collected reactor effluent was pumped (pump 3) into the cylindrical tube that the membrane module was set in (Figure 2.4). Then filtered water was taken by a laboratory peristaltic pump (pump 4) (Labor Technik, Dusseldorf) and the filtered water collected in a tank, where located on volumetric weighing scale. The filtration was done at temperature of about 20 ºC. Pressure was measured by 0~-1 bar Mini Dial Vacuum Pressure Gauge Manometer (Aterna, Turkey) placed in the effluent line. CFV was used to control cake layer on support layer. It was created by taking retentate from the of the cylindrical tube and returning it to the bottom of the cylindrical tube using another peristaltic pump (Watson Marlow 323) (pump 5). During filtration operation, flux decreased and TMP increased as a result of cake formation. When TMP increased higher than 800 mbar and filtration continued for a while. Then the membrane module was taken

out and physical cleaning was done with help of tap water to remove fouling layer on support material. In the second run, membrane module was put into the system and filtration operation continued.

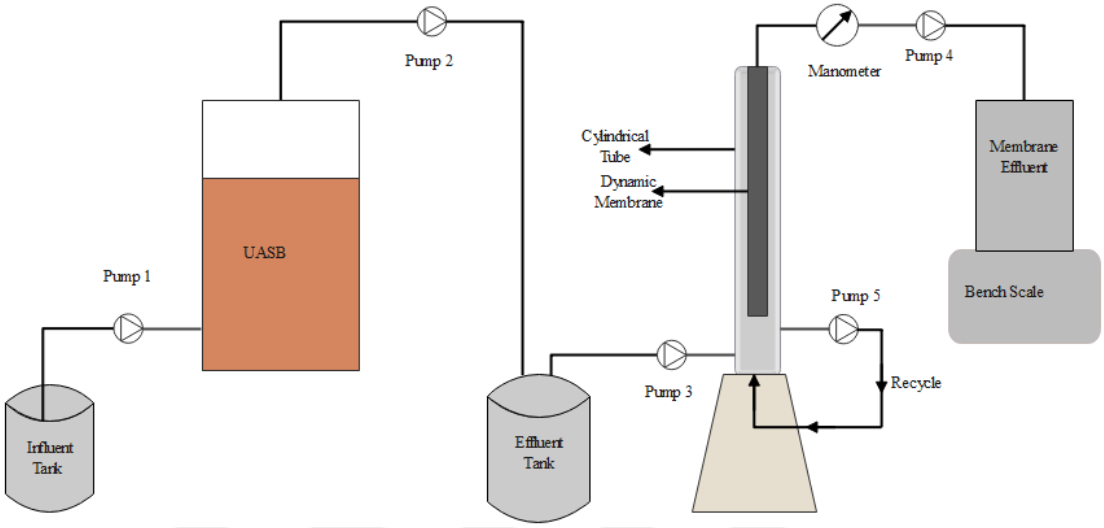


Figure 2.4 The schema of experimental set-up

2.3.2. Experimental plan

In this section (second part of second phase), the effect of CFV on DM formation at room temperate was investigated. UASB system was not changed and only filtration part was changed (Figure 2.5). In this part, filtration was done under cross flow velocity and polyester nylon mesh with 40 µm pore size was used as filter. After filtration was done for all pore sizes (10, 20, 40 and 70 µm), the filtration experiments were conducted at CFV with the support material with 40 µm pore size. CFV was applied to control cake layer thickness in DM systems. CFV was operated in the range of 77.52 m /h and 9 m /h. Operation conditions (UASB part) were not changed. A new experimental setup was prepared for filtration part. CFV was modified to provide removal of large particles that cause sudden membrane fouling on support layer, and attachment/deposition of small particles (colloids, solutes) on pore of support layer for compact cake layer. CFV was raised up to 77.52 m /h to prevent membrane fouling, and reduced to 9 m /h to avoid disrupting the cake layer. Two runs were done and the physical cleaning was done only once. Turbidity in UASB effluent and membrane effluent measured during the operation. After filtration operation, the components of DM were investigated by Scanning

Electron Microscopy with Energy Dispersive X-Ray Analysis (SEM-EDX), and Fourier-Transform Infrared Spectroscopy (FTIR) analysis. Scanning Electron Microscopy (SEM) images showed that the cake layer on the surface of the nylon mesh with 40 µm pore size. Energy Dispersive X-Ray (EDX) detected chemical components in cake layer. FTIR analysis determined organic components in cake layer.

2.3.3. Wastewater characteristics and seed sludge

This study was second part of second phase. During filtration operation under CFV, the characteristics of UASB effluent is presented in Table 2.11.

Table 2.11 The characteristics of UASB effluent used in filtration under CFV

Parameters	Values
COD, mg/L	1431±593
SS, mg/L	1254±547
Turbidity, NTU	759±186
pH	7.5

2.4. Modelling of DM Development

According to Hermia's model (Hermia, 1982), dominant fouling mechanism can be estimated by using permeate volume (V) and time (t) obtained in membrane the membrane process. The data obtained during filtration operation with 10, 20, 40 and 70 µm pore size (First part of second phase), were used for modelling of DM development. Mathematical equations for filtration models are presented in Table 2.12.

Table 2.12 Membrane filtration models and blocking mechanisms

Filtration Model	Mathematical Equations
Standard Blocking	$t/V = at + b$
Complete Blocking	$-\ln(J/J_0) = at + b$
Intermediate Blocking	$1/J = at + b$
Cake Filtration	$t/V = aV + b$

If the curve of time/Volume (t/V) versus t is linear, the main mechanism is standard blocking. If the curve of t/V versus t is linear, the main mechanism is standard blocking. If the curve of -ln(J/Jo) versus t is linear, the main mechanism is complete blocking. If

the curve of 1/J versus t is linear, the main mechanism is intermediate blocking. If the curve of t/V versus V is linear, the main mechanism is cake layer formation.

where V is the cumulative volume of permeate at time t;

J is the flux;

J_0 is the initial flux; and

a and b are the model parameters.

The linear coefficients, a and b, of the cake filtration model can be related to physical quantities by Equation 2.5 and 2.6.

$$a = \mu c_b \alpha_c / 2A^2 TMP \quad (2.5)$$

$$b = \mu R_m / TMP\ A \quad (2.6)$$

where μ is the dynamic viscosity, α_c is the specific cake resistance, R_m is the hydraulic resistance of the virgin support layer, TMP is the trans-membrane pressure, A is the membrane surface area, c_b is the concentration of sludge (Liu et al., 2009).

2.5. Performance of DM Treatment in Long-Term Operation and Analyzing Characteristics of DM for Dairy Wastewater

2.5.1. Experimental set-up

The experimental set up used in the third phase is presented in Figure 2.5. AnDMBR in Experiment 2.5 was modified by adding Port5 in order to .remain the water level in the reactor constant. AnDMBR system consisted of an UASB reactor that had a working volume of 3.8L and a submerged tubular membrane module. The working volume was decreased by adding pebble stone to the bottom of reactor and creating dead zone. In this phase, 20 μm pore size tubular polyester nylon mesh was integrated into the system for dairy wastewater treatment. In the first phase (Treatment of Dairy Wastewater by AnDMBR and Development of DM on Selected Pore Size), effective DM was not formed on support layer with 70 μm pore size. In first part of second phase (Dynamic Membrane Characteristics of Different Pore Sizes). DM formation time on 20 μm pore size was a little higher than 10 μm pore size. Thus, due to not to sudden DM formation, 20 μm pore size tubular nylon mesh was selected as a filter. The support layer with a pore size of 20 μm, was located in the cylindrical zone. The effective filtration area for the module was

0.012 m^2. A peristaltic pump (pump 1) (Watson Marlow 323) was utilized to feed wastewater into reactor and another peristaltic pump (pump 2) was used to collect membrane-filtered effluent from AnDMBR. Another peristaltic pump (pump 3) was used both to recycle retentate from the membrane compartment to the reactor and to create CFV on the membrane surface.

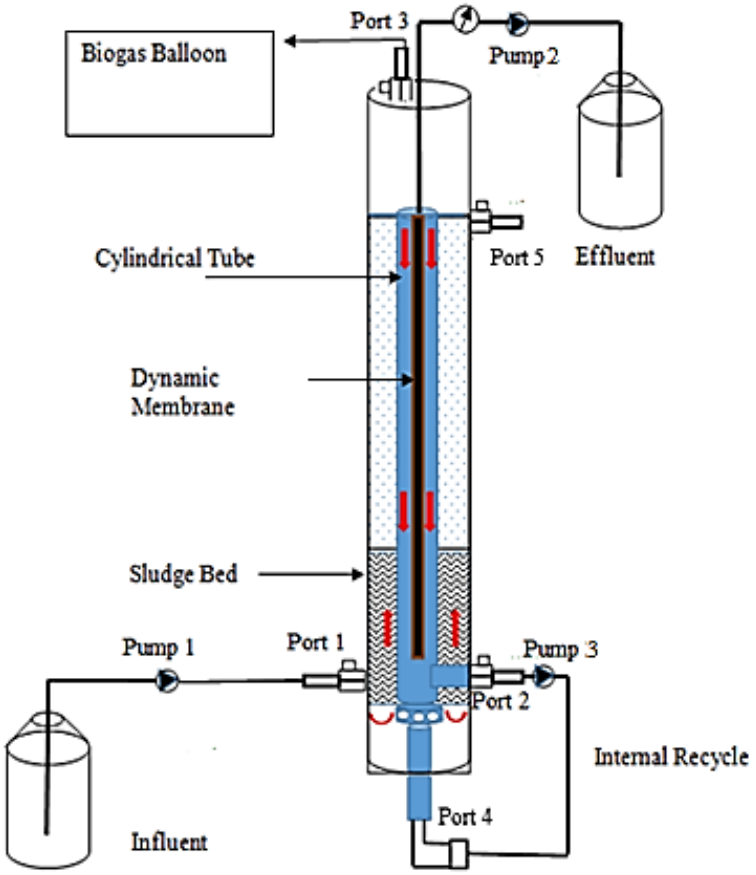


Figure 2.5 Schematic view of AnDMBR system used in the study

Pressure was measured by 0~-1 bar Mini Dial Vacuum Pressure Gauge Manometer (Aterna, Turkey) placed in the effluent line. TMP was calculated as reported via (Le Clech et al., 2003). The influent and effluent pHs measured by probe daily (Hach, pH/ISE meter, United States).

2.5.2. Experimental plan

The polyester nylon mesh with 20 µm pore size was integrated into the system. This phase consisted of two period; dynamic formation and stable operation period. Biogas was

measured to detect biogas production capability of the system. Synthetic milk wastewater was used as feed. COD, SS, VSS, oil-grease, alkalinity, NH_4-N, PO_4-P were determined for the characterization of wastewater. COD, VFA, SS, VSS, was determined to detect removal efficiency of the system. Ph and alkalinity was measured daily to control the operation. During the operation, TMP was measured daily to detect solid accumulation on support material. Turbidity was measured to detect dynamic membrane formation.

A single laboratory-scale continuously fed UASB reactor was started-up with the gradual increase of COD loading rate using dairy wastewater before AnDMBR put into operation. AnDMBR operation lasted for 92 days. Organic loading rate was kept at 8.1±1.5kg m^3/day. During periods of increased TMP, the flow that cannot be drawn through the membrane was discharged through an overflow pipe (Port 5) located at the top of the reactor. By this way, the water level in the reactor remained constant. Thus, a constant HRT of 26±2 hours was provided throughout the experimental period. By this way, retention time and membrane flux became independent from each other (Quek et al.,2017).

AnDMBR was operated at a constant temperature of 37 °C with the help of a heat jacket. The average pH values were 8.08 ± 0.52 in the effluent. Turbidity in the membrane effluent and TMP were measured daily to monitor DM development. COD and SS were measured in settling zone of reactor and membrane effluent to observe the effect of DM on treatment performance. The samples in settling zone of the reactor were taken by the help of Port 5. CFV and backwashing were used to control the dynamic cake layer thickness on the surface of the polyester nylon mesh. As seen in Figure 2.5, CFV was created by taking retentate from the bottom of the cylindrical tube and returning it to the bottom of the reactor by using another peristaltic pump (pump 3). The method followed for CFV application was in that high CFV was applied to prevent sudden TMP increase and membrane fouling. If no significant change observed in flux and then CFV was decreased to low values to stimulate the cake layer formation and eliminate unnecessary energy consumption. CFV was selected according to reported studies (Hu et al., 2018a). The applied CFV was in wide range of 5 m/h and 54.1m/h.

The selected CFV values were determined during the operation with the aim of preventing sudden increase in membrane permeability. At the beginning of operation, CFV was 26.4

m/h. The CFV was raised up to 54.1 m /h to prevent membrane fouling, and reduced to 5 m /h to avoid disrupting the cake layer. Depending on the flux, CFV was changed and kept at a constant value of 13 m/h from day 39 till the end of operation. Backwash was done once in a day by reversing the direction of the effluent flow. It lasted for 15 minutes with a flowrate of 170.4 L/h. After operation, SEM-EDX, FTIR, PSD, ICP-MS and XRD analysis was done to determine the characteristics of DM.

2.5.3. Wastewater characteristics and seed sludge

AnDMBR was inoculated with anaerobic granular sludge, which was produced under mesophilic conditions from an EGSB reactor at the Cartoon Industrial Wastewater Treatment Plant, İstanbul, Turkey. The initial concentration of the granular sludge was 50 g/ L. Dairy wastewater prepared by dissolving 10 gram of semi skimmed cow milk (Pınar, Turkey) in 1 L of tap water. Table 2.13 presents the characteristics of dairy wastewater.

Table 2.13 Characteristics of wastewater

Parameters	Value
COD, mg/L	10139 ± 766
Turbidity, NTU	10125 ± 1792
SS, mg/L	4344 ± 660
pH	6.75
NH_4^+-N, mg/L	68
PO_4-P, mg/L	7.012
Ca^{+2}, mg/L	131
Protein, mg/L	3159
Oil-grease, mg/L	1570

2.6. Analytical Methods

A variety of experimental analyses was done during the study. COD, SS, VSS, Oil and grease, NH_4^+-N, PO_4-P and alkalinity were measured according to Standard Methods (APHA, 2005). Turbidity measurements of feed and permeate samples were carried out with Hach 2100 N turbidimeter (Hach Company, range 0-1000 NTU). A gas chromatograph (Shimadzu GC-2014, Japan) equipped with a flame ionization detector (FID) was used to analyze VFA. The quantity of biogas was measured daily with help of water displacement method. In addition to this, the composition of biogas was detected

by gas chromatography (Shimadzu GC-2014ATF) equipped with a thermal conductivity detector (TCD).

2.7. Morphological Analysis

To understand the characteristics of DM, the morphological analyses were done. After the filtration operation has been ended, the membrane was taken out from the system. The entire cake layer deposited over the filter surface was removed prior to gel layer sampling. The cake layer on support layer was carefully scraped off via a sheet and put into the plastic cylindrical tube. The sample was dried in 100 ºC oven for analysis. SEM-EDX, FTIR, PSD, Inductively Coupled Plasma Mass Spectrometry (ICP-MS) and X-Ray Powder Diffraction (XRD) analysis were done. The analysis was described in the following sections.

2.7.1. PSD analysis

PSD of SS both in the cake layer and in the settling zone of AnDMBR were detected with help of a Mastersizer 2000 (Malvern Instruments, Hydro 2000 MU), an instrument, which utilizes a laser diffraction technique for measuring the sizes of particles with a detection range of 0.1-2000 μm.

2.7.2. SEM-EDX analysis

The samples were coated with aurum-platinum alloy for SEM analysis (Quorum, SC7620). The major elements of DM layer were determined by applying the EDX system (Zeiss, Evo Ma 10).

By SEM, surface morphology of membrane layer can be identified. SEM images showed that the cake layer on the surface of the nylon mesh. In addition, gel layer was observed with help of SEM. Combination of SEM and EDX was used to point out the chemical composition that exist in the surface of cake layer and gel layer.

2.7.3. FTIR analysis

An FTIR spectrometer (Jasco FT/IR-4700, Japon) was employed to characterize the major functional groups of DMs. The spectrum was calculated over the wave number ranging from 4000 to 400 cm^{-1}.

2.7.4. ICP-MS analysis

ICP-MS allows quantitative or semi-quantitative measurement of a large number of elements in solid and liquid samples. ICP-MS was conducted with an Apilent 7700 ICPMS system to analyze inorganic elements in DM.

2.7.5. XRD analysis

XRD analysis was used to analyze the structure of crystalline materials in cake layer. XRD analysis was carried out with a Shimadzu 6100 XRD using CuKα radiation and working at a power of 40 kV and 30 mA. The samples were collected in the angular range from 10º to 40º with 0.02º of step size.

3. RESULTS AND DISCUSSION

3.1. Investigation of Treatment Performance of Synthetic Wastewater and Cheese Whey in UASB and AnDMBR

In this part, treatment, and filtration capability of AnDMBR for dairy wastewater treatment was investigated. The operation took 344 days. The study began with control experiments, which operation was done only by UASB, followed by AnDMBR operations. From the beginning to day 287, the synthetic wastewater was used as feed. Then diluted cheese whey was used as feed from day 288 to the end of experiment. In the beginning system was operated only by UASB, then 70 µm tubular polyester nylon mesh pore size was integrated into the system and operated for 127 days. Due to inefficient cake layer formation with 70 µm pore size in a given time, lower pore size was selected as filter. After control experiments, operation was continued with 10 µm tubular polyester nylon mesh pore size for 43 days and synthetic milk wastewater was continued to use as feed. Then, diluted cheese whey was begun to use as feed and a new 10 µm pore size was integrated into system simultaneously. At the end of 315 days of AnDMBR operation, this experiment continued and completed with only UASB. During operation COD, SS, VFA and biogas production was done to detect treatment performance. Filtration performance was evaluated by flux, TMP, and membrane resistance. In first step, a submerged nylon mesh with 70 and 10 µm was integrated into UASB, respectively. Dairy wastewater was treated by UASB coupled submerged (internal) DM with selected pore sizes (10-70 µm).

3.1.1. Evaluating treatment performance by DM

In phase 1, the average COD removal was 82 ± 7.4 % at a COD loading rate of 1.34 ± 0.19 kg/m^{3}d (Table 3.1). When the 70-µm pore size nylon mesh membrane module was submerged into the reactor, the COD loading rate was doubled (Table 3.2). The amount of COD in the effluent in the beginning of phase 2 was close to the value of effluent COD during phase 1; and this level increased as the COD loading rate doubled (Figure 3.1a). COD removal during phase 2 was slightly higher than that in phase 1. The AnDMBR achieved COD removal values above 84 %, with a peak of 96 % on day 105 and an

average value of 89 ± 5% (Table 3.2). A membrane is expected to improve treatment performance; and a compact and stable cake layer that forms over a support material is expected to increase COD removal. However, because the cake layer formed in our study was not sufficient, the solid/liquid separation on the nylon mesh caused only a small increase in COD removal rate. In the case of domestic wastewater treatment with a shorter HRT (8 hours), Hu et al., 2018b reported a COD removal efficiency of 75% -92% in an AnDMBR with a pore size of 75 μm. Longer HRTs result in higher COD removal rates. A short HRT does not allow enough time for anaerobic bacteria, especially the methane-forming bacteria, to degrade substrate (Polprasert and Kottatep,2017), resulting in lower COD removal. In our study, the AnDMBR with the pore size of 70 μm did not improve COD removal; however, COD removal improved when HRT was increased. During phase 3, the COD loading rate of 35 % was increased, resulting in no change in the effluent COD (Figure 3.1a).

In this phase (phase 3), the COD loading rate was close to that fed to the reactor during the first period of phase 4 (Table 3.2). During this time, lipids that formed in the pipes during previous phases accumulated, resulting in slightly decreased COD removal efficiency of 75 ± 6 %. Thus, the old pipes were replaced. The effect of the AnDMBR on COD removal performance was observed in the second period of phase 4; the performance of the AnDMBR in treating synthetic wastewater was better than that of the UASB reactor during phase 3, with a higher COD loading rate of 20 %. COD removal by the AnDMBR peaked at 90 % during this period. COD removal increased during the second period, and this is probably related to an increase in solids retention by the AnDMBR, as discussed below. Sun et al.,2018 attained a similar level of COD removal efficiency (89.4 %) using a submerged membrane with a 30 μm pore size within a CSTR treating synthetic wastewater. Quek et al.,2017 attained 71 % and 64 % COD removal with shorter HRTs of 6 and 3 hours, respectively, using 28 μm pore size mesh located external to the UASB reactor; and they achieved 70 % COD removal using a 50-μm pore size mesh treating municipal wastewater. We achieved slightly higher COD removal values compared to those of Quek et al., 2017, which could be mostly due to applying the longer HRT in our study.

Table 3.1 The feeding UASB with synthetic wastewater and diluted cheese whey

Stage	Days	Operation Conditions	Wastewater Type	Influent COD mg/L	COD Loading Rate kg/m^{3}d	COD removal, %	SS_{eff} mg/L
Phase 1	0-80	UASB	Synthetic Wastewater	1509 ± 118	1.34 ± 0.19	82±7.4	228±41
Phase 3	208-225	UASB	Synthetic wastewater	6025 ± 264	4.0 ± 1.19	83 ± 2	491 ± 35
Phase 5	268-287	UASB	Synthetic Wastewater	5864 ± 767	3.6 ± 1.6	89±3	215±36
Phase 7	316-344	UASB	Diluted CheeseWhey	11560±1200	3.95 ± 2.44	70 ± 9	454 ± 223

Table 3.2 The feeding AnDMBR with synthetic wastewater and diluted cheese whey

Stage	Days	Operation Conditions	Wastewater Type	Influent COD mg/ L	COD Loading Rate kg/m^{3}d	COD removal %	SS_{eff} mg/L
Phase 2	81-207	AnDMBR (70 µm)	Synthetic Wastewater	3309 ± 1429	2.6 ± 1.1	89 ± 5	229 ± 114
Phase 4 First Period (prior to physical cleaning)	226-239	AnDMBR (10 µm)	Synthetic Wastewater	5989 ± 234	4.4 ± 1.3	75 ± 6	317 ± 71
Second Period (after physical cleaning)	240-267	AnDMBR (10 µm)	Synthetic Wastewater	6035 ± 876	5.0 ± 1.0	83 ± 7	228 ± 51
Phase 6	288-315	AnDMBR (10 µm)	Diluted Cheese Whey	7699 ± 2185	3.71 ± 2.69	86 ± 12	191 ± 58

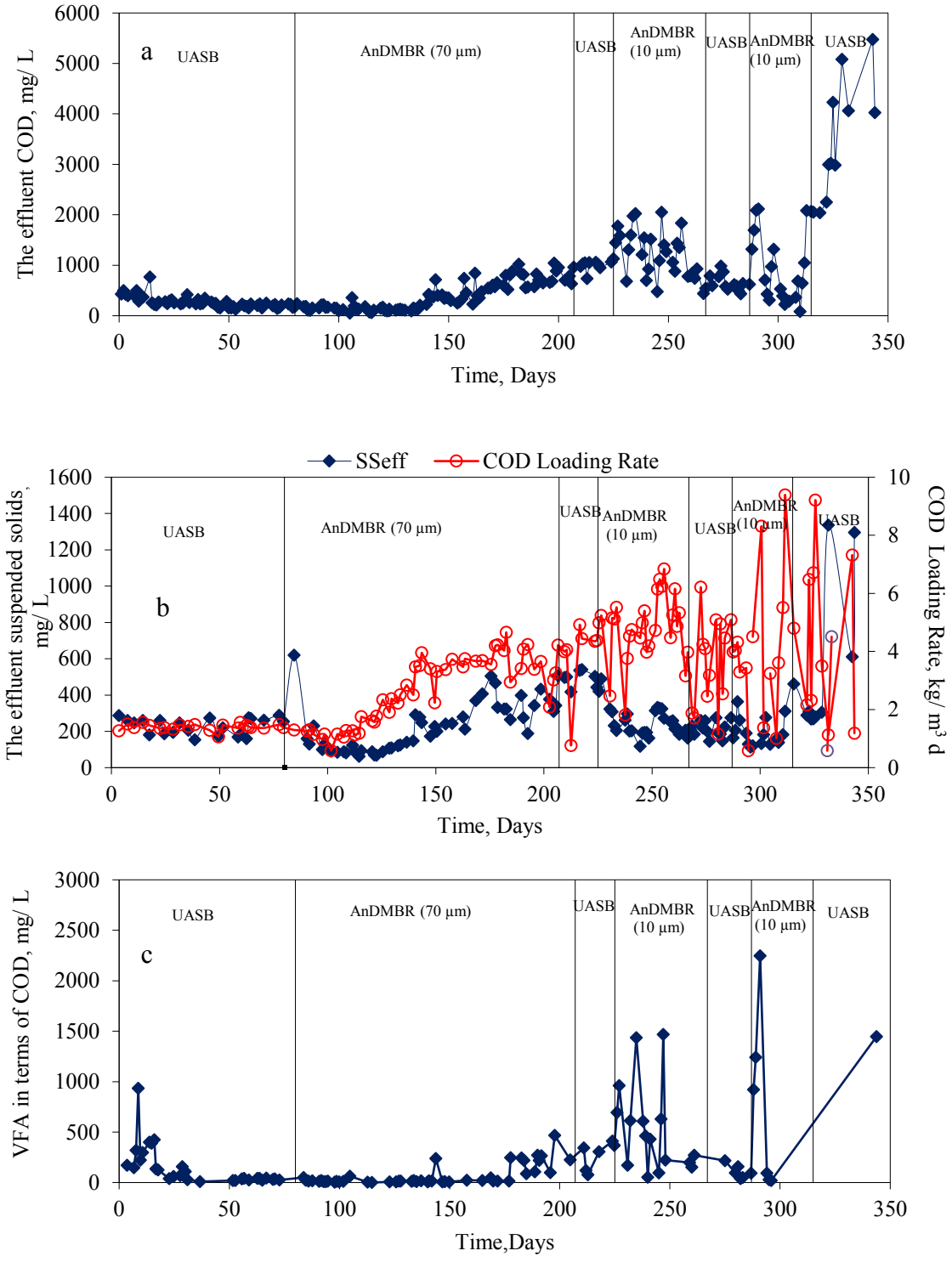


Figure 3.1 COD (a), VFA (b), Suspended solids (c) in the effluent during the operation

Ersahin et al., 2014; 2016a, b; 2017 obtained higher levels of COD removal (>99 %) using a compact and stable DM, formed on woven fabric support material (10 µm pore size) submerged in a CSTR. All of these results show that operational conditions and the

presence of an effective cake layer can affect treatment performance. During phase 5, the system was operated without a membrane, and the COD was applied at a loading rate similar to that in phase 4. Real industrial wastewater was used as feed during phase 6, and in the first days, the COD removal rate decreased from 90 % to 59 % due to insufficient alkalinity. After adding the appropriate level of alkalinity to the system, COD removal efficiency reached 98 % on day 310.

As seen in Table 3.2, there was no important distinction in COD removal efficiencies between 10 μm pore size AnDMBR treating either synthetic wastewater (phase 4) or cheese whey (phase 6), indicating that this type of AnDMBR can treat both types of wastewater. The effect of the AnDMBR on real industrial wastewater treatment was investigated by comparing the COD removal efficiencies in phases 6 and 7 (Table 3.2). After the membrane module was removed, the COD removal efficiency of 16 % decreased further in phase 7. Although the COD loading rates in phases 7 and 6 were similar, a higher COD removal efficiency of 86 ± 12 % was obtained during phase 6 (Table 3.2), thus demonstrating the effect of the AnDMBR on treatment efficiency. The treatment of cheese whey under anaerobic condition has been studied by several researchers using various types of reactors and the performances of these reactor configurations are summarized in Table 1.2. Most of the reported HRT values in Table 1.2 are longer than that used in our study; however, similar COD removal rates have been obtained throughout all these studies. The comparable COD removal we obtained using a shorter HRT could be due to the presence of the membrane module that separates solids by retaining material over its surface. A maximum COD removal efficiency of 98 % was obtained in this experiment, thus demonstrating the AnDMBR can be applied for the treatment of real industrial wastewater.

The solids retention capacity of the membrane module was determined by comparing the effluent suspended solids in the UASB reactor and the AnDMBR. During phase 1, the effluent suspended solids were 228 ± 41 mg/L at COD loading rate of 1.3 ± 0.19 kg/m^3d (Table3.1). During phases 1, 3, 5 and 7, the system was operated with the UASB reactor and an increased COD loading rate, resulting in an increase in the effluent suspended solids. On day 81 of phase 2, a 70 μm pore size nylon mesh membrane module was submerged into the reactor to determine the solids retention efficiency of the membrane unit. Initially, suspended solids in the effluent reached 620 mg/L with an average value

of 229 ± 114 mg/L (Figure 3.1b). Suspended solids removal was about 70 %, and the amount of suspended solids in the effluent did not decrease significantly in phase 2. Thus, the 70-µm pore size support material was not effective in retaining suspended solids. Jeison and van Lier, 2008 reported that it was impossible to develop a stable DM layer on support materials with pore sizes larger than 60-70 µm. However, Zhang et al.,2011 formed a thick cake layer in 20 days on a 61 µm pore size Dacron mesh located in upper part of a UASB reactor. Hu et al., 2018b formed a cake layer on nylon mesh (75 µm) in less than 40 days using a similar reactor configuration as Zhang et al.,2011. Our reactor configuration was similar to those described in these studies, however, we were not able to obtain an effective cake layer. Lin et al.,2010 reported that certain operational parameters, such as permeate flow rate and mixed liquor suspended solids, have a significant effect on cake layer formation. The fast DM formation reported by Zhang et al., 2011 can be explained by their use of a higher constant flux of 65 L/m^{2}h. Wang et al., 2018 also reported faster DM formation through higher flux. However, Hu et al., 2018b were able to achieve fast DM formation in an AnDMBR performed at a flux of 22.5 L/m^{2}h by performing sludge recycle in the bioreactor. The sludge recycle converted more sludge into suspended form, thus increasing the interaction between suspended solids and the supporting membrane. Lee et al., 2001 indicated that small solutes and colloids reduce membrane permeability, while suspended solids, especially microbial flocs, induce the formation of a dynamic membrane. Granular sludge has a tendency to settle, and in our study, no measures were taken to keep the sludge suspended. Thus, the suspended solids concentration in the cylindrical tube of the reactor was low and percolated a small amount of solids on membrane module, thus slowing down cake layer formation. In the case of a CSTR, Alibardi et al., 2014 reported cake layer formation in 30 days on an external membrane module with a pore size of 200 µm. All these results show that both reactor configuration and operational conditions have effects on cake layer formation time.

The amount of suspended solids in the effluent was 491 ± 35 mg/L during phase 3 (with UASB reactor). When the nylon mesh membrane module with 10 µm pore size was submerged into the bioreactor, the initial level of effluent suspended solids of 425 mg/L decreased to 204 mg/L on day 234 (first period of phase 4) (Figure 3.1b). The accumulation of suspended solids on the mesh surface resulted in a decline in the suspended solids in the effluent. Thus, the AnDMBR retained suspended solids during

this period, showing that the AnDMBR is superior to the UASB reactor in terms of suspended solids removal. At the end of the first period, the fouling layer on support material was physically cleaned with tap water to restore membrane permeability. In the second period of phase 4, the effluent suspended solids of 202 mg/L increased to 363 mg/L during the subsequent days (Figure 3.1b). The increase in levels of effluent suspended solids was related to the insufficient development and consolidation of the dynamic membrane in the first ten days of the operational period. By the end of this period, effluent suspended solids decreased to 163 mg/L along with the formation of a cake layer. In phase 4, 83 % (first period) and 88 % (second period) of suspended solid were removed from synthetic wastewater by the AnDMBR during treatment. This result is consistent with Quek et al., 2017 who reported 86 % – 91 % removal of suspended solids by mesh having a pore size of 28 μm coupled with a UASB reactor and 87 % removal of suspended solids by a mesh (50 μm) coupled with a UASB reactor. However, there are reports of greater than 99 % removal of suspended solids when the AnDMBR was coupled to a CSTR (Ersahin et al., 2014; 2016a). In this case, biogas recirculation kept sludge suspended, thus improving sludge accumulation on the woven fabric with pore size of 10-μm, resulting in higher suspended solids removal (Ersahin et al., 2014; 2016a). In addition, Ersahin et al., 2014 operated the DM for more than 30 days after the DM was formed. This extended time enabled more biomass retention and stable cake layer formation, resulting in high solids removal. Moreover, Quek et al., 2017 obtained highest suspended solid removal efficiency (91 %) in longer operation time using DM coupled to UASB. Saleem et al., 2018 removed more than 93 % of suspended solids using nylon meshes (52 and 21 μm pore size separately) coupled to a CSTR with an HRT of 1 day. The mixed liquor produced by the CSTR circulated along the mesh and the retentate was returned to the reactor, thus forming a cake layer within a short period of time (2 days) (Saleem et al.,2018). In our study, the cake layer formed on support layer just as the operation was ended due to rising water level in the reactor due to flux decrease as membrane permeability decreased. If the operation was allowed to proceed, a more stable and compact cake layer would have formed, leading to the accumulation of more solids on the support material. Thus, we intend to prolong the operational time in future studies to attain the best solids removal efficiency. In our study, the amount of suspended solids in the effluent in our study was comparable with the effluent suspended solids reported by

Saleem et al.,2016, who studied an AnDMBR. Casu et al., 2012 and Alibardi et al., 2014 reported that the AnDMBR was unable to completely remove suspended solids.

The solids retention capacity of the dynamic membrane unit was calculated only in the first period of phase 4. Because the reactor could not be opened frequently to maintain anaerobic conditions, a limited number of samples was collected from the reactor during this phase. At the end of period 1, the dynamic membrane was taken out of the reactor for physical cleaning. The cake layer on the support material was scraped with a spatula weighed, and the solids concentration in this cake layer was calculated (37.5 g/L). On the same day, a suspended solids sample was collected from the settling zone when the reactor outlet was the closed. The suspended solids concentration was 973 mg/L. By comparing this with the amount of suspended solids in the effluent, we calculated that the solids retention capacity of the dynamic membrane was 72 %. The decrease in effluent suspended solids via high solids retention on the DM is a clear indication of cake layer formation (Figure 3.2). However, this solids retention capacity is lower than those reported previously (Ersahin et al., 2016a; Alibardi et al., 2016), which is due to the reasons mentioned above. We have shown that a support material with a 10 µm pore size is more effective than a 70 µm pore size support material for solids retention. Ersahin et al., 2012 noted that pore size and particle size of the cake layer material should both be considered to achieve the best separation. PSD analysis of solids in the reactor is presented in Figure 3.3. The median particle size based on volume was 35 µm. Thus, the solids are within the size range that can be retained on the support material with a 10 µm pore size.

During cheese whey treatment (phase 6), the effluent suspended solids concentration reached 363 mg/Land declined to 113 mg/L as the cake layer was formed on the nylon mesh (Figure 3.1b). As a consequence, the suspended solids in the effluent decreased to 69 % of its highest value and 85 % of the suspended solids were removed by the AnDMBR during this phase. When the system was operated on a UASB only mode (phase 7), the effluent suspended solids increased to 1296 mg/L. These results show the effect of the 10 µm pore size AnDMBR on solids retention and cake layer formation during treatment of cheese whey. However, higher levels of suspended solids remained in the effluent during reactor operation with the 70 µm pore size AnDMBR, showing that the solids retention capacity of this AnDMBR was lower than that of the 10 µm pore size

AnDMBR. Thus, the performance of the cake layer in the AnDMBR with 10 µm pore size was better than that of the AnDMBR with 70 µm pore size.

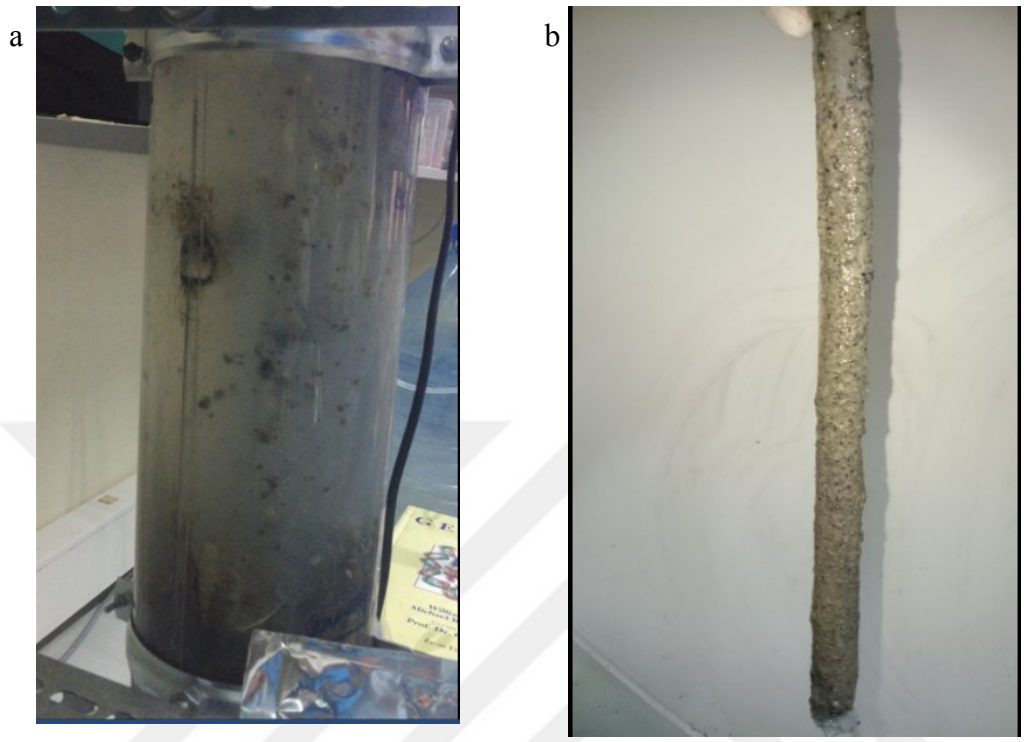


Figure 3.2 Settling zone of AnDMBR (10 µm) (a) and Dynamic Membrane (10µm), taken out of the reactor in the end of phase 4 (b).

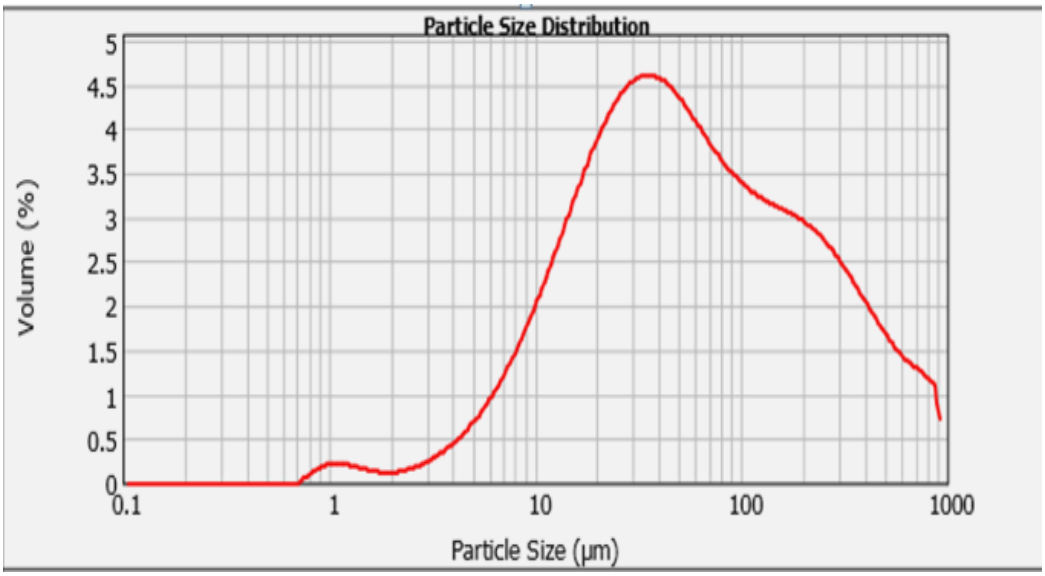


Figure 3.3 Particle size distribution of the solid in the settling zone of AnDMBR

Effluent VFA concentrations are presented in Figure 3.1c. Acetic, butyric, propionic, isobutyric, valeric, and capric acids were detected in the effluent. Acetic acid was the predominant VFA, present at levels higher than butyric and propionic acids when COD removal efficiency was higher than 85 %. Higher levels of propionic acid and other VFAs occurred as a result of decreasing treatment efficiency. During AnDMBR operation, total VFAs were 68 (phase 2), 707 and 391 (phase 4), and 759 mg COD/L (phase 6). These results show that high COD loading rates result in process instability and high VFA concentrations. VFA levels in the UASB and AnDMBR effluents did not differ significantly. Therefore, the AnDMBR had no significant effect on VFA removal.

3.1.2. Filtration performance

Steady flux levels were observed (51.5±3.9 L/m^{2}h), except for two days during the operation of the 70 µm pore size AnDMBR (Figure 3.4a). The flux decreased to 40 L/m^{2}h and 36 L/m^{2}h on days 134 and 148, respectively, because of the accumulation of lipids and particulates reduced the flow rate in the pipes. A very low CFV (0.06 m/h) was used during the operation of the 70 µm pore size AnDMBR and flux did not decrease during phase 2, suggesting that a significant cake layer did not form on the support material with a pore size of 70 µm. The flux values we obtained are consistent with those reported by Zhang et al., 2011 and Hu et al., 2018b, who applied fluxes of 65 L/m^{2}h and 22.5 L/m^{2}h in AnDMBRs with pore sizes of 61 and 75 µm, respectively. Because the 70 µm pore size AnDMBR did not effectively retain solids, support material with a pore size of 10 µm was submerged in the reactor on day 226 (phase 4). During reactor operation at this pore size, less effluent was produced on day 229 due to the accumulation of lipids. After the influent pipe was cleaned, the flux increased to 52.20 L/m^{2}h on day 233. During reactor operation with the 10 µm pore size support material, the same CFV (0.06 m/h) was applied to facilitate the build-up of the dynamic layer and to control cake layer thickness.

On day 235, the flux decreased and stabilized at 22.1 L/m^{2}h, along with the formation of a dynamic membrane on the support layer (Figure 3.4 b). The TMP was estimated at 100 mbar during reactor operation until day 235. Then it increased to 330 mbar (first period of phase 4), which was maintained for more than 3 days. Sun et al., 2018 applied similar operational conditions, and their stable flux levels were maintained for a longer period of time than ours. We were unable to prolong the filtration because when flux decreased

with DM formation, the resulting increase in water level caused a reactor overflow. The DM was then taken out of the system, and physically cleaned. The 10 μm pore size support material was resubmerged into the system, and in the second period of phase 4, the operation began with a lower flux value (46.22 L/m^{2}h) than in the first period (53.49 L/m^{2}h). This shows that fouling that had happened at the end of period 1 was irreversible, resulting in pore blockage of the support material. Pore blockage was not removed by physical cleaning (Meng et al., 2007), thus the membrane was not able to achieve its original flux value during the subsequent filtration period. A similar flux decline after the physical cleaning of the membrane module was observed by (Meng et al., 2007). During the second period of phase 4, the flux (44±4.3 L/m^{2}h) remained stable at a calculated TMP of approximately 97 mbar for 25 days. Then, the flux decreased sharply (12.79 L/m^{2}h) with a cake layer formation and a TMP of 399 mbar. The flux and TMP remained stable for two days (Figure 3.4b), after which the phase was completed. The flux values are consistent with (Quek et al., 2017), who applied fluxes of 30-50-100 L/m^{2}h during the operation of a 28 μm pore size AnDMBR. Furthermore, the operational TMP and flux values during phase 4 paralleled values from other AnDMBR studies that have been reviewed by (Hu et al., 2018a).In this experiment, we were able to operate the system at a high level of flux, which is an advantage for studying dynamic membrane (Ersahin et al., 2012). In addition, DM could be operated in lower pressure than conventional membranes. Thus, this reduced operational cost of system.

During synthetic wastewater treatment, our applied CFV of 0.06 m/h was lower than those reported for other studies, which ranged from 0.25 m/h to 360 m/h (Hu et al., 2018a). Hu et al., 2018b reported that a CFV of 0.85 m/h negatively affects compact cake layer formation. The CFV we applied was lower than that applied by Hu et al., 2018b, thus its effects on the DM have been ignored. As mentioned above, a more effective DM can be obtained by prolonging the operational time of our experiment.

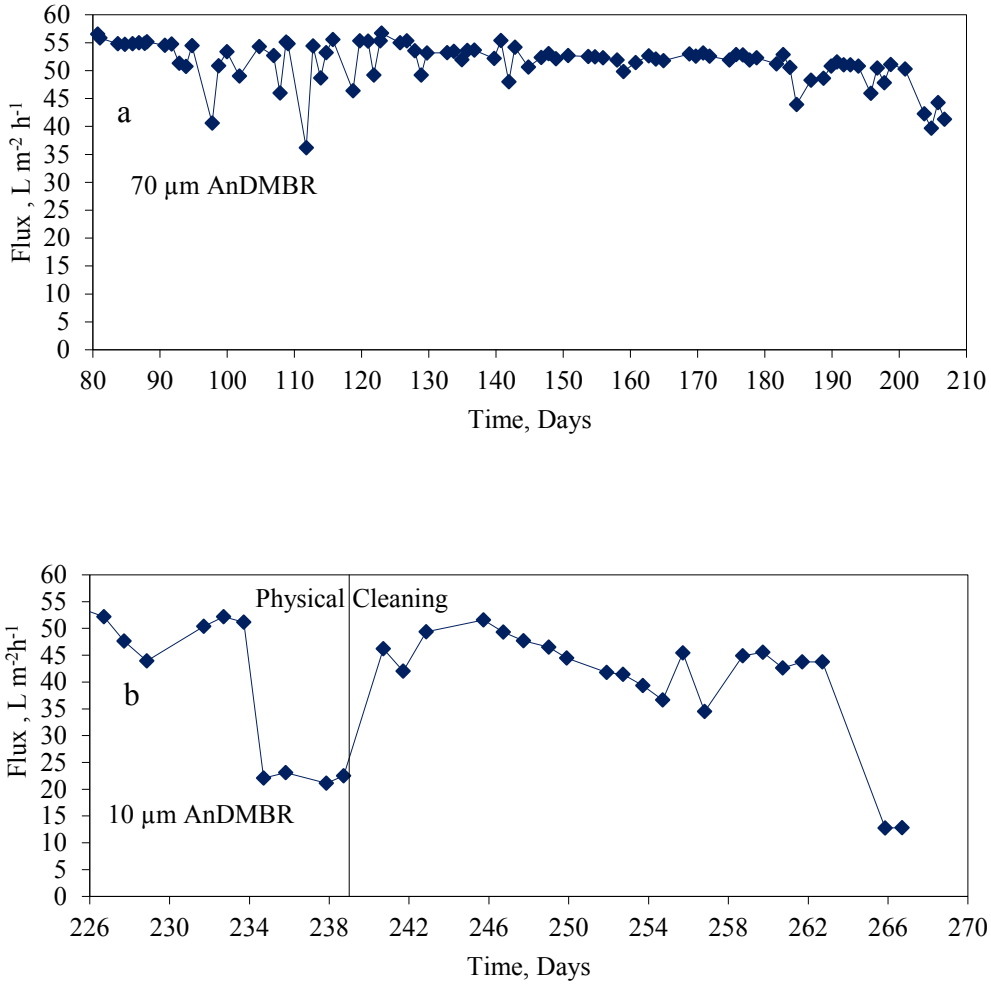


Figure 3.4 The Fluxes in AnDMBR, 70 µm (a, Phase 2) and 10 µm (b, Phase 4) during operation with synthetic wastewater

Our experiment shows that fouling can be controlled by applying a low CFV, which has a low-cost advantage. During phase 6, the initial flux decreased from 49 to 34.1 L/m^{2}h owing to the accumulation of suspended solids on the support material during the first 7 days; at this time, the measured TMP was in the range of 100 to 138 mbar (Figure 3.5). The CFV of 0.06 m/h at the beginning of phase 6 was increased to 44.58 m/h during treatment of real industrial wastewater. As the CFV increased, the flux increased to 48.3 L/m^{2}h on day 298. From day 299 to 311, the flux decreased because of the solids deposition on the support material. Then, the flux increased on day 312 at a CFV value of 44.58 m/ h. The TMP reached 240 mbar with the decrease in membrane permeability on day 313 and the flux decreased from 44.2 L/m^{2}h (day 312) to 29.7 L/m^{2}h on the

following day. The deposition of high levels of solids occurring at a high level of flux (44.2 L/m^{2}h) and the presence of a previously developed fouling layer induced both rapid increase in TMP and rapid decrease in flux on the following day (313), as seen in Figure 3.5b. These results indicate a rapid cake layer formation process. The AnDMBR operation continued for two more days before the DM was taken out of the system. The TMP values during phase 6 of our study are comparable to those measured by Alibardi et al., 2014; Zhang et al., 2011; Hu et al., 2018b who observed TMP levels increasing from 0 to 250-300 mbar. The TMP we observed in phase 6 was lower than that in phase 4, which may be due to the higher CFV during phase 6. Our CFV value during phase 6 is comparable to that reported by (Ersahin et al., 2014,2016a).

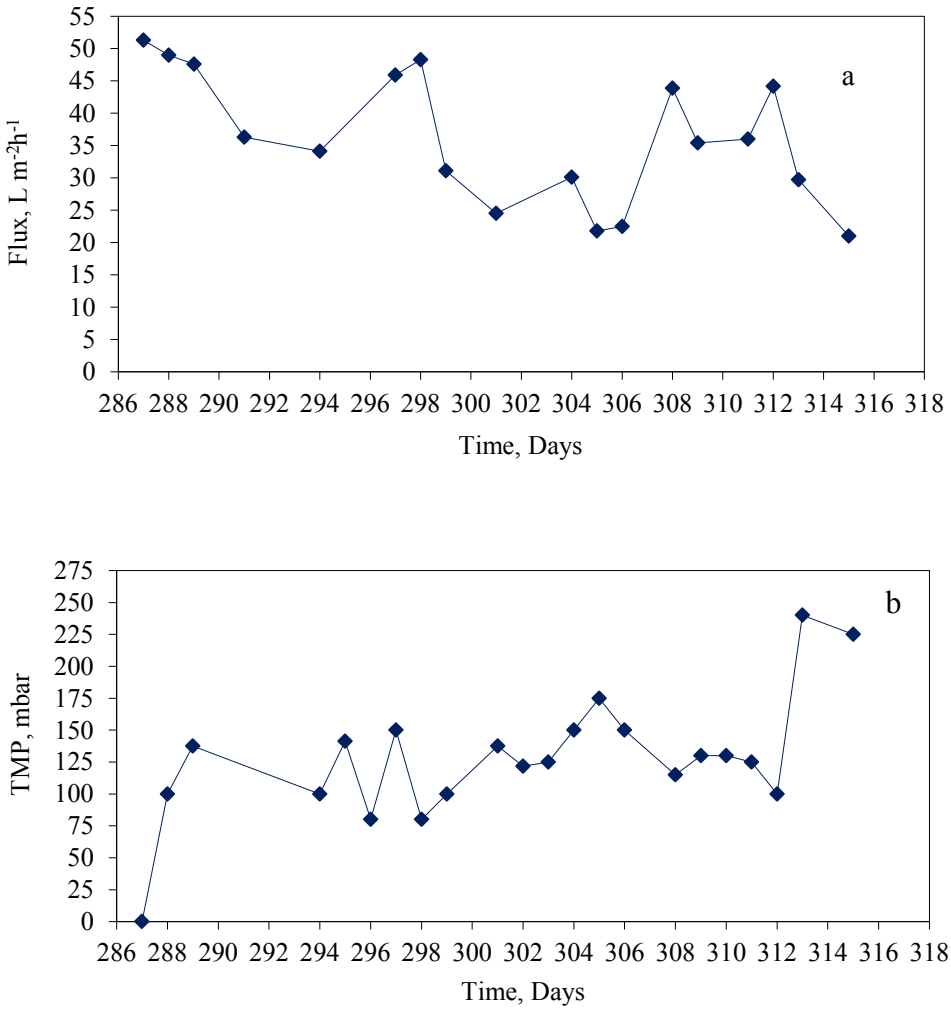


Figure 3.5 Membrane flux (a) and TMP (b) variations and the AnDMBR (10µm) during the treatment of diluted cheese whey (Phase 6)

The measured TMP values during phase 6 resulted in dynamic membrane resistance levels of $9.2x10^{10}$-37.9 $x10^{10}$ 1/m. These results agree with Zhang et al., 2010, Xiong et al., 2014 and Sun et al.,2018, who reported levels of 1.1-121.1 $x10^{10}$ 1/m, 3.5 x 10^{10} 1/m and 1.73 x 10^{10} 1/m, respectively. However, the levels we observed are lower than those reported by Ersahin et al., 2014, 2017; Wang et al., 2018; Sun et al., 2018. This could be due to the low level of suspended solids in the cylindrical tube where the DM was located in. Ersahin et al.,2014 reported that increasing the quality of small particles and sludge results in higher filtration resistance. Moreover, Alibardi et al.,2016 reported that the certain operational conditions relevant to the filtration module, such as wastewater characteristics and reactor configuration, can have an effect on the initial formation, consolidation, and filtration resistance of the DM.

3.1.3. Biogas generation

The generated biogas was measured for 184 days of operation, after which the entrance of oxygen (O_2) and nitrogen (N_2) into the reactor hindered biogas production. The production of biogas paralleled the removal of COD, that is, higher COD loading rates into the system resulted in higher biogas production, with a few exceptions. The reason for this result is likely due to biogas leakage. The UASB reactor and the AnDMBR did not differ in terms of biogas production, which produced CH_4 flows in the range of 6.72 ± 2.95 L/d to 3.94 ±1.72 L/d, respectively, during whole operational period (Figure 3.6). These levels are higher than those reported in previous studies. Alibardi et al., 2016 reported biogas production rates of approximately 0.025 to 0.175 L/d, while Ersahin et al.,2017 reported a CH_4 flow of 2.4 ± 0.1 L/d at a lower COD loading rate than that used in our study. According to Chen et al.,2016, substrate type, loading rate, reactor configuration, biogas collection method, and various operational parameters have effects on biogas production.

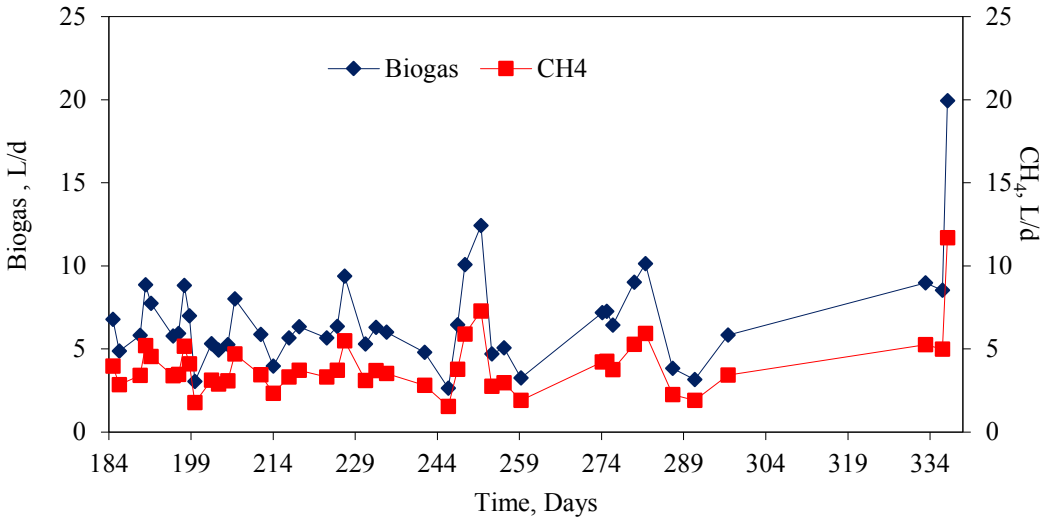


Figure 3.6 Biogas production and CH_4 concentration in the effluent of UASB and AnDMBR

In this experiment, a CH_4 yield of 0.26 L CH_4/$gCOD_{removed}$ was attained during reactor operation with the AnDMBR, and this value represents 66 % of the theoretical value of 0.395 L CH_4/$gCOD_{removed}$ at 35 °C (Figure 3.7).

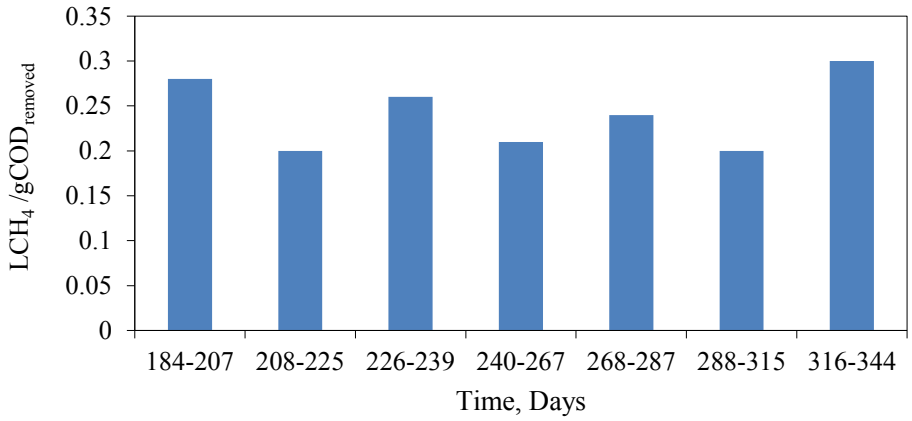


Figure 3.7 The methane (CH_4) yield during the operation

According to Ersahin et al.,2014, a certain amount of CH_4 is solubilised in effluent of the membrane, while another researcher reported that from 40% - 50% of total CH_4 produced in an AnDMBR can be dissolved in the membrane effluent (Smith et al.,2013). Mean reported CH_4 yields are in the range of 0.12-0.27 L CH_4/$gCOD_{removed}$ (Li et al.,2016), which is consistent with the results of this study (Figure 3.7).

3.2. Investigation of The Effect of Pore Sizes on DM Formation Time, and Cleaning Frequency

As it was mentioned in Section 3.1, cake layer formation took very long time with 70 µm pore size support material. On the other hand, DM formation was accomplished in short time on the support layer with smaller pore size (10 µm). Hence, in this section, DM properties and formation time were investigated in an external DM module. Before starting DM filtration experiments, critical flux was determined. The purpose was to accelerate DM formation. Then, a flux that was higher than the critical flux was applied during the following filtration experiments. By doing this, all pore sizes (10,20, 40 and 70 µm pore sizes) could be evaluated in terms of cake layer formation and filtration performance in short term operational period.

3.2.1. Critical flux

Results of the critical experiment is presented in Figure 3.8. As seen in Figure 3.8, flux was increased in stepwise, and TMP, that was correspond to the flux, was measured. After fouling has started on support material, TMP began to increase.

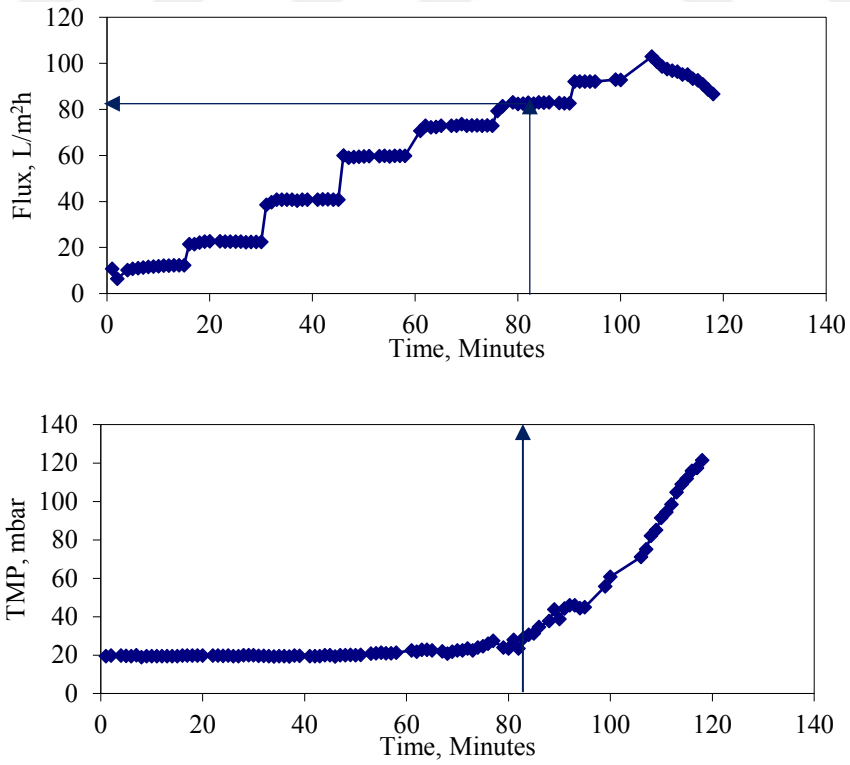


Figure 3.8 Critical flux determination for support material with 10 µm pore size

When the increasing of TMP became remarkable at a certain flux value (Figure 3.8b), this flux (critical flux) was determined as 83 L/m^{2}h.

3.2.2. Filtration and treatment performance of DM

The applied initial flux was 98 L/m^{2}h for 10 µm and 97 L/m^{2}h for 20 µm pore size, 95 L/m^{2}h for 40 µm pore size, and 93 L/m^{2}h for 70 µm pore size. Firstly, 10 µm experiments were conducted. During the operation, deposition of particles on support layer resulted increase in TMP and decrease in permeate flux (Figure 3.9a). As mentioned before TMP and flux are important indicators for membrane fouling. It should be remembered that the decline in flux in DM application happens due to the increase in membrane resistance by both gel layer formation that block the pores of the support layer and the cake layer formation over gel layer in. The pore blockage improves the membrane resistance whereas the cake formation produces an additional resistance layer. Both pore blocking and cake formation can be considered as two main mechanisms for membrane fouling in conventional membranes (Abdelrasoul et al., 2013) whereas they are also main mechanisms that form DM.

As seen in Figure 3.9a, the rapid increase in TMP happened and reached to 918 mbar at the end of half an hour of operation. Moreover, the stable turbidity (less than 20 NTU) was obtained at the end of 1.46 hours. Thus, it can be concluded that DM formation completed in 1.46 hours. DM operation continued for more 1.82 hours with an approximately TMP of 947±32 mbar. After DM was formed, flux continued to decrease gradually and it ended with a value of 21 L/m^{2}h (Table 3.2). The flux values were comparable with other reported DM studies (Hu et al., 2018a). As explained in previous experiment (Section 3.1), during synthetic wastewater treatment, prior to physical cleaning, DM formation on support layer with 10 µm pore size completed on 10 days. On the other hand, prior to physical cleaning, DM formation only took place in 1.46 hours during operation with 10 µm pore size in these experiment. The first reason was that the initial flux (93 L/m^{2}h) was higher than the initial flux that was applied during treatment of synthetic wastewater by AnDMBR with 10 µm pore size in previous experiment. (Section 3.1). Saleem et al. 2016, reported that applied high initial flux accelerated DM formation. It should be added that the initial applied flux was higher than the critical flux (83 L/m^{2}h) in this experiment and this flux resulted quick DM formation. The second

reason could be the operational temperature. In later experiment with 10 µm, the filtration operation was done at room temperature, which was lower than previous experiments given in Section 3.1. At lower temperature, particles have tendency to form membrane fouling due to decrease in Brownian diffusion back transport forces which particles were exposed to (Le Clech et al., 2006). Thus, the operation at low temperature could enhance particle accumulation on support material in these experiments. The third reason of quick DM formation could be related with the mixing. In this experiment, as mentioned in materials and methodology section, a mixer was used during the operation in order to improve solid contact with support layer (Figure 2.3). This could be also accelerated DM formation. Sabaghian et al., 2018 reported that mixing in reactor caused quick DM formation. Additionally, a negligible CFV (0.06 m/h) was applied to control cake layer thickness during 10 µm pore size operation, whereas the operation was done without CFV in this experiment. The cake layer formation without thickness control also could result quicker DM formation in this experiment.

After physical cleaning was done at the end of run-1, membrane module was reintegrated into the system in run-2. The initial flux was 84 L/m^{2}h in run-2 and this was lower than the flux of run-1 (98 L/m^{2}h). This was due to pore blocking (irreversible fouling) which could not be removed with physical cleaning. It could be inferred that some particles settled down or attached within pore walls and blocked the pore of support layer partially or completely. To sum up, due to attachment inside pore walls and blocked pores of support layer, irreversible fouling happened during run-1 (Di bella and Trapani, 2019).

In addition to this, there could be residual thin layer (a part of gel layer) over support layer that formed in run-1 that could not be removed physically. Thus, at the beginning of run-2, some pores of support layer were less than 10 µm due to this clogging that caused decreased fluxes owing to irreversible fouling.

In first 18 minutes of run-2, TMP was 868.5 mbar and it was increased to 968.5 mbar after 1.23 hours of operation (Figure 3.9a). TMP of run-1 (918 mbar) within the same hours was slightly lower than TMP of run-2 (968.5). Additionally, DM formation was also completed in 1.38 hours in run-2 that was a little quicker than previous run (run-1). In run-2, after DM formation, the initial flux decreased 69 % of its initial value, and turbidity became lower than 20 NTU. Besides, the flux continued in range of 26 and 15

L/m^{2}h after DM was formed, which were lower than the flux values (41-21 L/m^{2}h) monitored in previous run. As mentioned above, the support layer lost its original properties (pore size) in run-1 due to irreversible fouling.

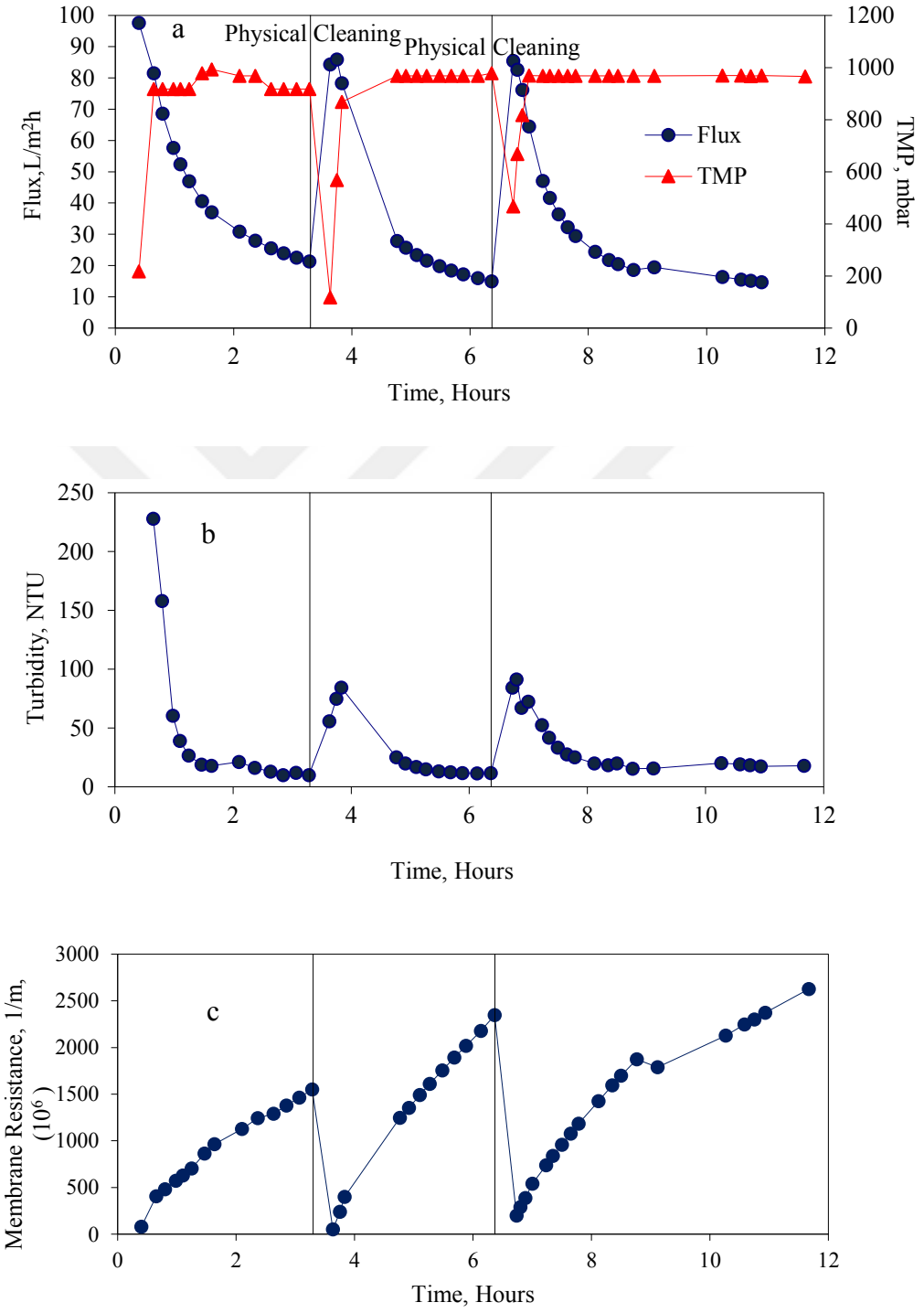


Figure 3.9 Change of Flux and TMP (a), Turbidity (b) and Membrane Resistance (c) versus time at support material with 10 µm pore size

The initial flux (85 L/m^{2}h) in run-3 was close to the initial flux observed in run-2 (Figure 3.9a). At the end of first 23 minutes of operation in run-3, TMP reached to 969 mbar. The rate of increase in TMP in run-3 was close to run-1 and run-2. After 1.7 hours of operation, turbidity became stable and DM formation completed. DM formation time was similar to the previous runs. After DM formation, the operation continued with fluxes in range of 24 and 13 L/m^{2}h that was similar to run-2. As mentioned above, the operation began with lower initial values in the following second and third runs due to irreversible fouling, taking place in first run. The similar results were observed by Meng et al., 2007. However, there was no big difference in the initial fluxes in run-1, run-2 and run-3 in our study. TMP and flux profiles were almost consistent with Gong et al., 2014, applying DM for filtration of sewage, in terms of the flux recovery and quick development of TMP after physical cleaning. Moreover, they also reported that regular physical cleaning was useful for flux recovery.

As seen in Table 3.3, TMP values in filtration experiments were higher than the values in critical flux experiment. This could be due to lower solid concentration in feed, led to low solid accumulation and resulted in lower TMP in critical flux.

Table 3.3 DM formation time for run-1, TMP and Flux after DM formation for run-1,2 and 3

	10µm	**20µm**	**40µm**	**70µm**
DM Formation Time (Run-1), hour	1.46	5.31	41.16	65.81
Average TMP After DM Formation (Run-1), mbar	947±32	768±0.8	1003±9.1	898±26
Average TMP After DM Formation (Run-2), mbar	970±3.6	868±51	997±1.9	852±34
Average TMP After DM Formation (Run-3), mbar	968±1.0	974±22	818	912±17
Flux After DM Formation (Run-1), L/m^{2}h	41-21	45-29	37-24	78-55
Flux After DM Formation (Run-2), L/m^{2}h	26-15	16-9	12-11	19-11
Flux After DM Formation (Run-3), L/m^{2}h	22-13	25-6	8-7	13-8

The turbidity is one of the important parameter to be used in order to detect DM formation (Li et al., 2017). During operation with 10 µm pore size, the initial and maximum turbidity in permeate was 228 NTU in run-1. It sharply decreased in the following hours (Figure3.9b) and became stable with DM formation. The average turbidity in permeate was 15±4 NTU from 1.46 hours till the end of operation. The maximum turbidity in permeate was 84.3 NTU in run-2. The irreversible fouling provided less turbidity in run-

2. In the beginning of run-2, some part of support layer covered by this fouling layer. Thus, this fouling layer resulted more solid retainment over the support layer. Therefore, turbidity in permeate in run-2 was lower than run-1 (Figure 3.9b). Similar to run-2, the maximum turbidity in permeate was 91.3NTU in run-3. The average turbidity in permeate was 15±5 NTU from 4.92 hours till the end of operation in run-2 and 18±2 NTU from 1.7 hours till the end of operation in run-3.

The filtration experiments were continued with 20 µm pore size support layer and the same steps were done for this pore size (Figure 3.10). The applied initial flux was 97 L/m^{2}h in run-1. The important increase in TMP happened after 2 hours of operation. DM formation took 5.31 hours during operation with 20 µm pore size that was longer than during operation with 10 µm pore size. This could be due to less solid retainment on support material with large pore size in the beginning of operation. Li et al., 2017 reported that DM with a large pore size had longer formation time and they added that small particles were less likely to be attached to mesh with large pore size during DM formation until detention of large particles. After DM formation, the flux continued in range of 45 and 29 L/m^{2}h with continuous increase in cake layer thickness. This flux (during operation with 20 µm pore size) was higher than fluxes during operation with 10 µm pore size (Table3.2). Furthermore, after DM formation, TMP was approximately 768±0.8 mbar during operation 20 µm pore size whereas TMP was approximately 947 mbar during operation 10 µm pore size in run-1 (Table 3.2). As mentioned by Alibardi et al., 2016, the studying with larger pore size support material enables operation with higher flux at lower TMP (Alibardi et al., 2016).

The initial turbidity in permeate was 129 NTU in run-1 during operation with 20 µm pore size. However, turbidity increased to 508 NTU after 2 hours of operation. In contrast to 10µm pore size, the spikes in turbidity were observed prior to DM formation (Figure3.10b) such that the small particles (less than 20 µm) passed through the filter. It could be inferred that support layer with 20 µm pore size had lower solid retainment capabilities than 10 µm pore size. Turbidity almost became stable with DM formation. The average turbidity in permeate was 23.05±4.4 NTU from 5.31 hours to the end of operation. The initial flux was 73 L/m^{2}h in run-2 that it was lower than initial flux value in run-1 whereas it was 91 L/m^{2}h in run-3. The higher initial flux was observed in run-3 than run-2. The presence of temporary irreversible fouling resulted lower initial flux,

taking place at the beginning of run-2 so the initial flux in run-3 recovered better than run-2.

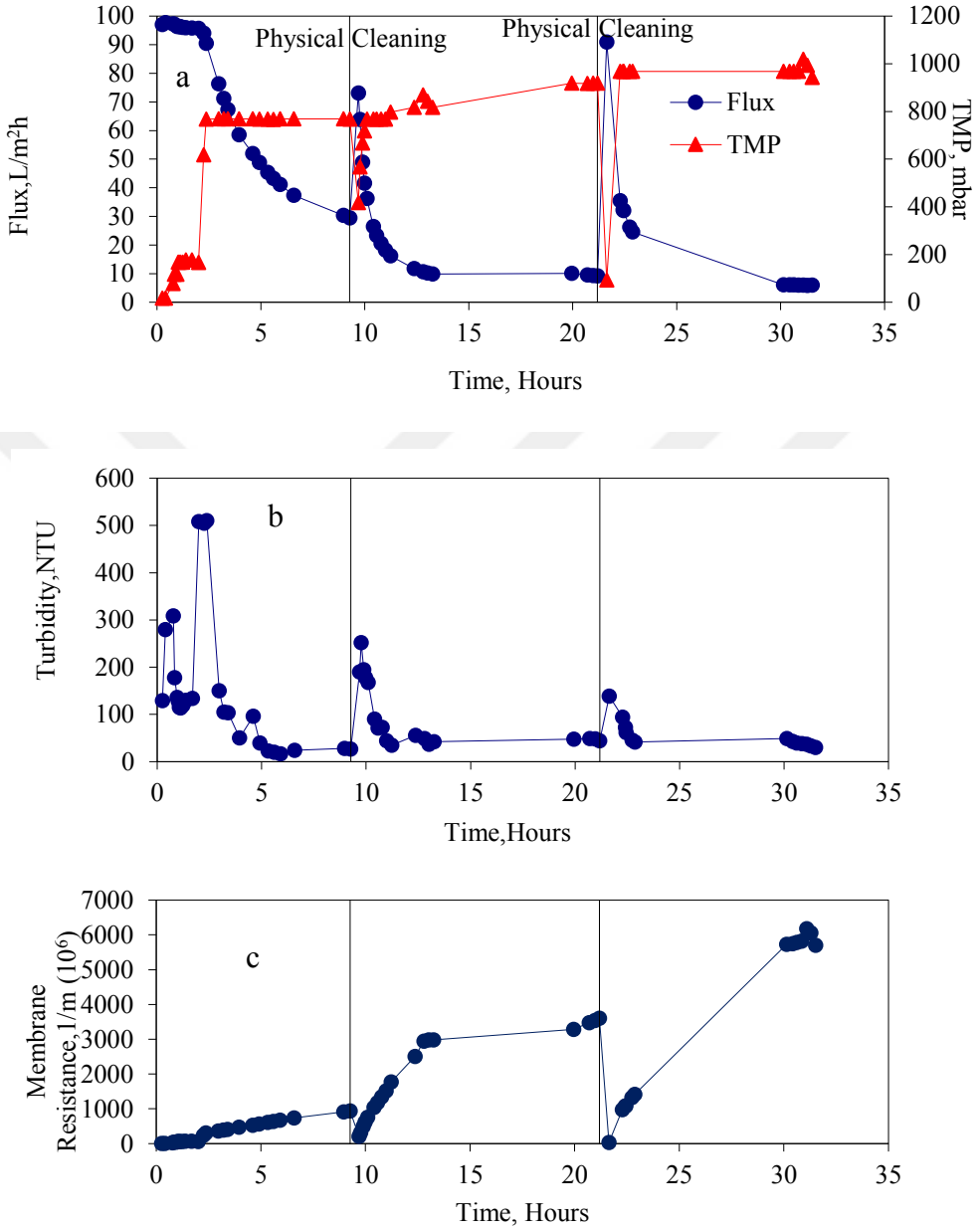


Figure 3.10 Change of Flux and TMP (a), Turbidity (b) and Membrane Resistance (c) versus time at support material with 20 µm pore size

DM formation completed in 5.31 hours in run-1, whereas, it completed 1.71 hours in run-2 and 1.43 hours in run-3. DM formation completed faster in the following runs (run-2

and run-3) and this showed the effect of irreversible fouling on DM formation. As for TMP, it increased to 768 mbar in 2.4 hours and continued with this value till the end of operation in run-1. On the other hand, TMP increased to the same value in a shorter time (35 minutes) in run-2 and it reached to 919 mbar in 10.43 hours of operation (Figure 3.10a). In run-3, TMP raised to 969 mbar in 61 minutes (1 hours), continued with the value of approximately 974 mbar till the end of operation. It could be inferred that after physical cleaning, TMP improved quickly.

After DM formation, the flux continued to decrease (Table 3.3) because the increase in cake layer thickness proceeded. The rise in membrane resistance can be showed as evidence for this increase (Figure 3.10c).

The spikes in turbidity were not observed in run-2 and run-3. As seen in Figure 3.10b, more solid retainment was observed in run-3 compared to run-2 such that the maximum turbidity in permeate was 252 and 139 NTU in run-2 and run-3, respectively. As mentioned just before, the irreversible fouling on previous runs (run-1, run-2) caused more solid retainment in the following runs (run-2 and run-3). After DM was formed, the average turbidity in filtered effluent was 41±5 NTU in run-2, and 39±6 NTU in run-3.

The initial flux was 95 L/m^2h during operation with 40 μm pore size in run-1 (Figure 3.11a). In first half an hour of operation, TMP was 68 mbar. At the end of 7 hours of operation, TMP reached to 518 mbar due to increase in deposition of particles on support material. DM formation completed in 41.16 hours and it took longer time than DM formation on 10 and 20 μm pore size. During operation of 40 μm pore size in run-1, after DM formation completed, maximum value of TMP was 1018 mbar which was higher than recorded TMP value during operation with 10 and 20 μm pore size. This result could be due to longer operation time of 40 μm pore size that resulted more solid retainment, so higher TMP. The flux continued to decrease gradually with development of DM formation and ended with a value of 24 L/m^2h. As showed in Table 3.3, after DM formation, the flux values (40 μm) were lower than the flux values in smaller pore sizes (10, 20 μm), which could be related with TMP.

Prior to DM formation, the spikes in turbidity were observed during operation with 40 μm pore size in run-1 (Figure 3.11b) and it reached to 1000 NTU in 9.28 hours of operation. As mentioned before, larger pore size nylon mesh had low capability of solid

retainment. Moreover, it could be inferred that size of the most of the particles was lower than 40 µm. As mentioned before, feed, coming from UASB effluent, was used for filtration and the average particle size in UASB was 35 µm (Section 3.1). Thus, the important quantity of particles had size less than pores of support layer (40 µm).

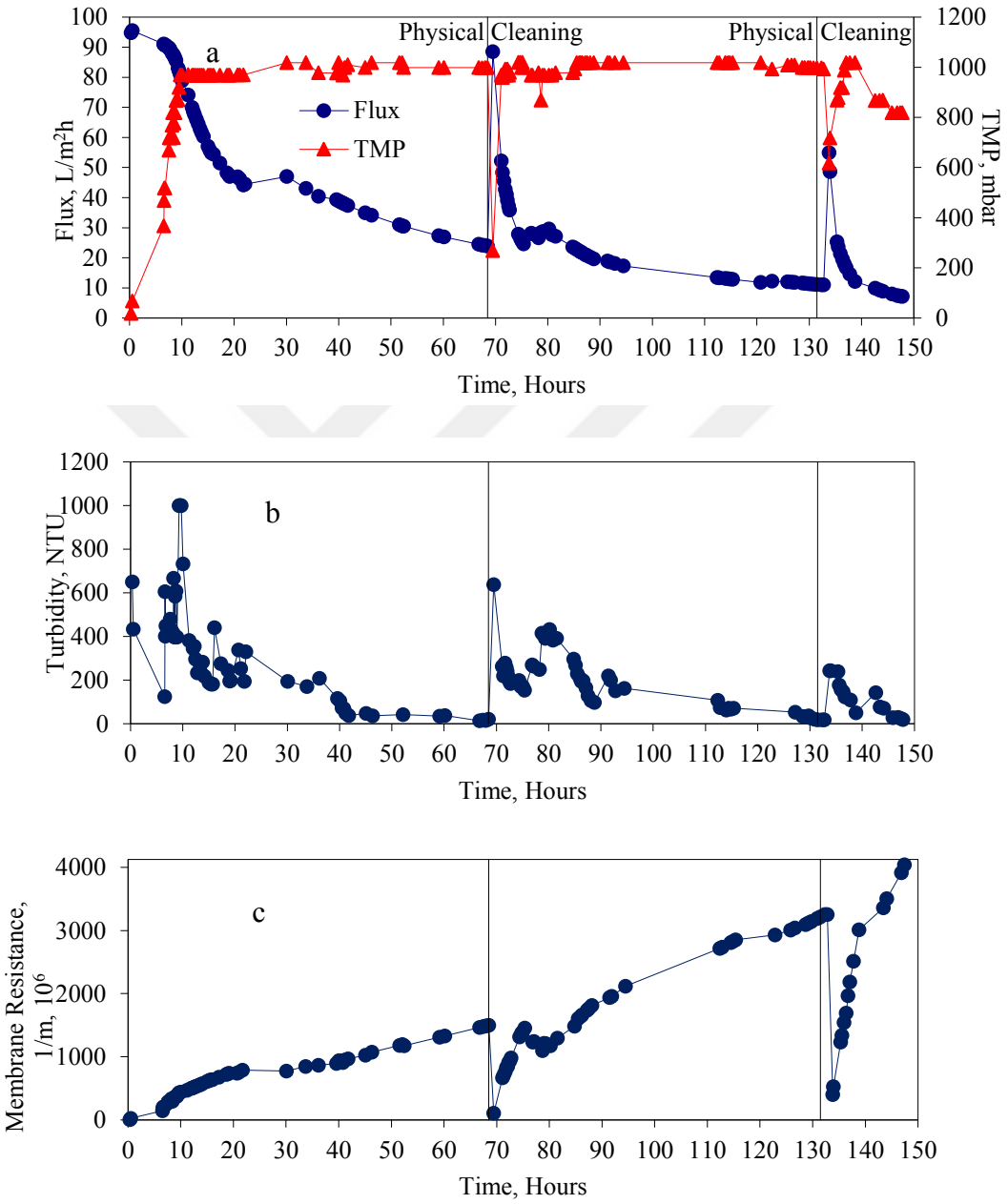


Figure 3.11 Change of Flux and TMP (a), Turbidity (b) and Membrane Resistance (c) versus time at support material with 40 µm pore size

As mentioned before, small particles that had lower size than pore size of support layer likely less attached inside pore of the support layer. Small particles passed through the

pores of support layer that these were observed as spikes in permeate turbidity (Figure 3.11b). As seen in Figure 3.11b, the variation in turbidity continued for a while. This showed that effective solid removal needed longer time for large pore sizes. Turbidity became stable with DM formation after 41.16 hours of filtration operation. Afterwards, the turbidity in permeate was 30±8 NTU in run-1. This value was higher than the values obtained during operation with 10, 20 μm pore size in run-1. It seems that support layer with smallest pore size resulted more solid retainment and lowest turbidity in permeate. Thus, the pore size effect on solid retainment was clearly observed in first run. However, the similar results were not observed in terms of turbidity in the following runs (run-2 and run-3) due to the fact that irreversible fouling changed the original pore size. Additionally, other factors such as the feed characteristics and operation time could affect solid retainment capability of membrane in the following runs (run-2 and run-3).

The initial flux was 89 L/m^{2}h in run-2 and 55 L/m^{2}h in run-3 (Figure 3.11a). The regular decrease in initial flux was observed after each run during operation with 40 μm pore size due to effective irreversible fouling. As for TMP, it sharply increased to 968 mbar in 2.4 hours of operation in run-2 whereas, it reached to 919 mbar in 9.47 hours in run-1. As mentioned in 20 μm pore size, after physical cleaning, quick increase in TMP occurred in run-2. Moreover, similar to run-2, in run-3, TMP reached to 988 mbar in 3.7 hours of operation. However, DM formation took 41.16 hours in run-1, 52 hours in run-2, and 12.8 hours in run-3. Despite the fast increase in TMP, DM formation took longer time in run-2 than run-1. This could be due to operational conditions. The feed, coming from UASB effluent, was not stable. Thus, low solid content in feed from time to time, could result in slow DM formation in run-2. Moreover, fast DM formation happened in last run (run-3) as expected. After DM formation, the flux was continued with range of 12 and 11 L/m^{2}h in run-2 and with range of 8 and 7 L/m^{2}h in run-3. Fluxes in run-2 and run-3 were lower than run-1. As mentioned before, the support layer lost its properties (pore size) at the end of run-1 due to irreversible fouling, and the fluxes after DM formation become lower on next runs (run-2 and run-3) than the first run. The initial turbidity was 638 NTU in run-2. The fluctuations in turbidity were observed in the following hours but these fluctuations in run-2 were lower than run-1. The turbidity in permeate decreased to 154 NTU in 6.6 hours of operation and increased to 432 NTU in 12 hours of operation in run-2. In the following hours, although some increase in turbidity was observed, turbidity decreased

continuously (Figure3.11b). The irreversible fouling, happened in run-1, improved solid retainment in the following runs. Thus, less variations in turbidity were observed in run-2.

In first 52 hours, the flux was approximately 95±1.25 L/m^2h during operation with 70 μm pore size in run-1 (Figure 3.12a). TMP values were about 19 mbar in the first 31 hours (Figure 3.12a). After 31 hours of operation, the increase in TMP started due to solid deposition on support material. TMP increased to 418 mbar in 35.65 hours of operation. Then, pressure drop happened from 35.65 hours to 50.47 hours of operation and it decreased to 18 mbar in 50.47 hours of operation. As a result, the sharp increase followed by decrease in TMP was due to temporary fouling, taking place over support layer between 31 hours and 35.65 hours of operation. A sharp increase in TMP was observed (after 51 hours) with effective solid deposition on support layer. TMP increased to 868.5 mbar in 53.95 hours of operation and continued to increase till 60.03 hours of operation. TMP decreased to 669 mbar within this hour and then kept on increasing. After DM formation, TMP continued with approximately 898±26 mbar till the end of the operation. The initial turbidity was 164 NTU in permeate. Similar to 40 μm, the spikes in turbidity were observed during operation 70 μm pore size. Turbidity reached to 1000 NTU in 51.60 hours of operation and continued at this value for more 52 minutes. As seen in Figure 3.11b, it was taken longer time (65.81 hours) for turbidity to become stable during operation with large pore size (70 μm). After DM was formed, the turbidity continued with a value of 29.28±7.15 NTU till the end of operation in run-1. This value were closed to the value in 40 μm pore size and higher than other pore sizes (10 and 20 μm).

DM formation time took longer time in 70 μm pore size than smaller pore sizes (10, 20 and 40 μm). As mentioned before, as pore sizes of support material increased, DM formation time increased. In addition to this, low solid content coming from UASB effluent could prolong DM formation time. In previous part of the study, (Section 3.1), DM formation took more than 207 days during operation with 70 μm pore size when AnDMBR operated with a lower flux. However, in this experiment, DM formation took 2.75 days (66 hours) with the same pore size. This showed that the operation conditions especially solids loading had an important effect on DM formation time as explained in 10 μm pore size.

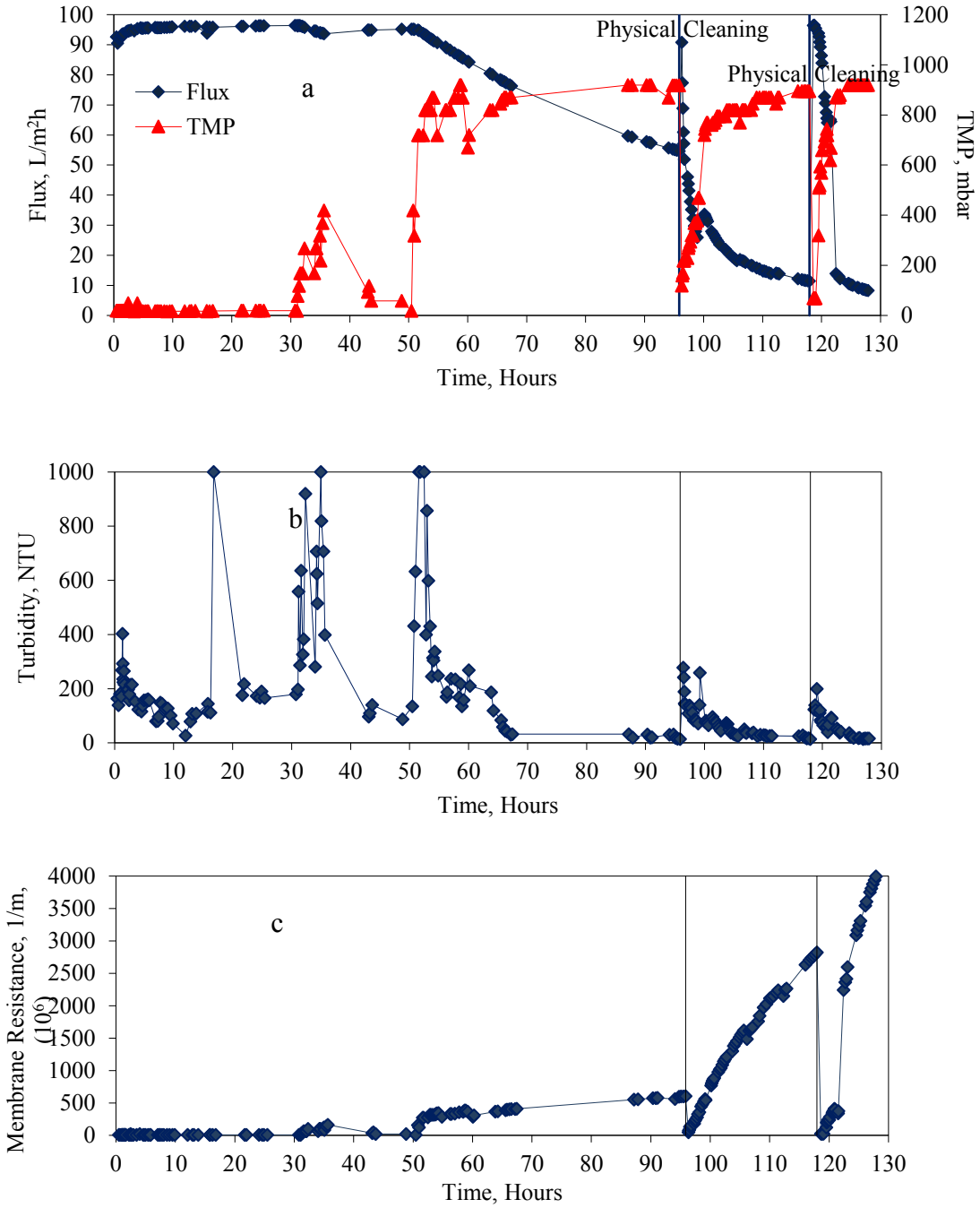


Figure 3.12 Change of Flux (a), TMP (b), Turbidity (c) and Membrane Resistance (d) versus time at support material with 70 µm pore size

The initial flux was 91 L/m^{2}h during operation with 70 µm pore size in run-2, and it was 96 L/m^{2}h in run-3. It should be stated that an important decrease in flux was not observed in first 52 hours of operation in run-1, whereas the initial flux began to decrease in a short time (in 17 minutes of operation) in run-2 and it began to decrease in 46 minutes of

operation in run-3. The result showed that, firstly, after physical cleaning, irreversible fouling resulted faster decrease in flux in the following runs (run-2 and run-3) than run-1 (Figure 3.12a). Secondly, despite faster decrease in flux happened in run-2 and run-3 than run-1, the initial flux recovered better in run-3 than run-2. It could be due to presence of temporary irreversible fouling in the beginning of run-2 as mentioned in 20 µm pore size. After DM formation, the flux continued in range of 78 and 55 L/m^{2}h in run-1, in range of 19 and 11 L/m^{2}h in run-2 and in range of 13 and 8 L/m^{2}h in run-3. As in other pore sizes, the fluxes in run-1 after DM formation was higher than in run-2 and run-3.

As for TMP, it was 119 mbar in first 12 minutes of operation and sharply increased to 719 mbar 4 hours later in run-2. TMP continued to increase in the following hours and reached to 875 mbar in run-2. Moreover, in run-3; TMP was 69 mbar in first of 50 minutes of operation and sharply increased to 319 mbar in 1.32 hours of operation and reached to 919 mbar in 6.33 hours of operation. This value was close to previous runs (run-1 and run-2). The irreversible fouling enhanced solid accumulation in the following runs (run-2 and run-3) that resulted in faster increase in TMP in run-2 and run-3 than run-1 (Figure 3.12a).

After DM formation, average TMP values for all pore sizes were between 750 and 1000 mbar (Table 3.3). TMP values were almost consistent with Salerno et al., 2017, who reported DM operation till TMP reached to 900 mbar. As to turbidity, as mentioned before, the spikes in turbidity were observed during DM formation in run-1 due to same reason as mentioned in 40 µm pore size (Figure 3.12b). Contrast to run-1, prior to DM formation, no important spikes in turbidity were observed in the following runs (run-2 and run-3). As seen in Figure 3.12b, DM formation took longer in run-1 than run-2 and run-3. DM formation took 65.81 hours in run-1, 9 hours in run-2, and 4.51 hours in run-3. As mentioned before, more solid retainment due to irreversible fouling resulted quick DM formation in the following runs similar to TMP (run-2 and run-3) (Figure 3.12a). After DM was formed, the turbidity continued with a value of 28±6 NTU and 23±8 NTU till the end of operation in run-2 and in run-3, respectively. Turbidity results for all pore sizes were explained above. Turbidity in permeate in our study was consistent with Ersahin et al., 2017, who reported the average permeate turbidity as 30±2 NTU in external AnDMBR with 10 µm pore size. In addition to this, Xiong et al., 2019 reported steady

turbidity effluent (20-50 NTU) after DM formation. All these results showed that turbidity values for all pore sizes in permeate were consistent values with those reported studies.

In run-1, fluxes (after DM formation) was lower in small pore sizes (10 μm) than large pore size (70 μm). In the following runs (run-2 and run-3), this discrepancy in flux between pore sizes decreased. It could be inferred that the nylon mesh lost its original properties (pore size) and the effect of pore size on filtration operation decreased. All these results showed that physical cleaning needed for regeneration of DM and continuity of operation. As mentioned by Hu et al., 2016, the end of runs (run-1, run-2) showed that physical cleaning was needed for regeneration of DM due to its important effects on the flux recovery and the stable operation of DM. As reported previous studies (Salermo et al., 2017; Sahinkaya et al., 2017), DM formation time in large pore sizes (40 μm, 70 μm) took longer than smaller pore size in first runs. The nylon mesh with pore size of 10 μm showed the lowest DM formation time and effluent turbidity. Generally, the formation of DM completed in a shorter time on next runs (run-2 and run-3) than first run for all pore sizes.

Some problems were encountered during operation with 70 μm pore size such that the low quality in membrane effluent was observed at the beginning of operation with large pore size support material (70 μm pore size). However, small pore size (10 μm) resulted in fast DM formation and produced low effluent. Sahinkaya et al., 2017, reported that this quick DM formation on low pore size support material result in rapid fouling. In addition to this, this can affect negatively the continuity of filtration operation without cake layer thickness control (such as CFV). During operation with large pore size, less cleaning was needed and provide longer continuous operation even lower effluent quality in the beginning. However, it should be stated that long formation time of DM means the decrease in the effluent quality for a while.

This study showed that low pore size (10 μm) formed quickly, whereas large pore size (70 μm) prolonged DM formation time that resulted in low effluent quality till DM formation completed. All these results showed that 20 μm pore size seemed to be optimum option considering DM formation time and treatment performance. Turbidity has been used to evaluate DM filtration performance in most of studies (Sun et al., 2018; Ersahin et al., 2014; Ersahin et al., 2017; Siddiqui et al., 2019; Yang et al., 2020). The

turbidity removal efficiency was similar (more than 92 %) and high for all pore sizes nylon meshes (Table 3.4). High turbidity removal (96-99%) can be obtained by conventional membranes (Cai et al., 2000; Noor et al., 2002; Horng et al., 2009). Similarly to conventional membranes, high turbidity removal was achieved by DM with low-cost operation.

Table 3.4 The turbidity removal with different pore size

Pore Size, µm	**Average UASB Effluent Turbidity, NTU**	**Initial Turbidity in Permeate, NTU**	**Maximum Turbidity in Permeate, NTU**	**The Final Turbidity in Permeate, NTU**	**Removal Rate, %**
10 µm	1000	228	228	9.97	99
20 µm	1000	129	510	26.6	97
40 µm	976	651	1000	20.4	98
70 µm	626	164	1000	14.4	98
Run2	**Average UASB Effluent Turbidity, NTU**	**Initial Turbidity in Permeate, NTU**	**Maximum Turbidity in Permeate, NTU**	**The Final Turbidity in Permeate, NTU**	**Removal Rate, %**
10 µm	1000	55.7	84.3	11.6	99
20 µm	1000	190	252	44.2	96
40 µm	389	638	638	17.6	95
70 µm	436	278	278	14.4	97
Run3	**Average UASB Effluent Turbidity, NTU**	**Initial Turbidity in Permeate, NTU**	**Maximum Turbidity in Permeate, NTU**	**The Final Turbidity in Permeate, NTU**	**Removal Rate, %**
10 µm	1000	84.4	91.3	17.9	98
20 µm	1000	139	139	30.5	97
40 µm	406	244	244	18.9	92
70 µm	678	110	471	14.7	98

Solid removal performance of DM was comparable with conventional membranes. The final SS in the membrane effluent was 14.58 mg/L (10 µm), 39 mg/L (20 µm) and 21 mg/L (70 µm) at the end of run-1. These results were much lower than other reported DM studies (Xie et al., 2014; Alibardi et al., 2016). In addition to turbidity, COD removal efficiency was determined for DM with 40 and 70 µm. In the end of 70 µm pore size nylon mesh operation, COD in the cylindrical tube and COD filtrated effluent was measured for all runs. COD in the cylindrical tube was 1000, 700 and 1425 mg/L, respectively.

COD in permeate was 75, 25 and 50 mg/L in the end of run-1, run-2 and run-3, respectively. COD removal was 93 % for run-1, and 96 % for run-2 and run-3. UASB reactor treated 85 %, 89 % and 78 %, respectively. DM with 70 µm pore size improved COD removal and more than 99 % COD was removed in this system. Moreover, COD in permeate was 25 (run-1), 43.75 (run-2) and 102.5 mg/L (run-3) in the end of DM

operation with 40 μm pore size operation. These results were consistent with Ersahin et al., 2017, Ersahin et al., 2014 and Wang et al., 2018. All these results showed that the application of DM could provide a good treatment performance with low-cost operation.

3.2.3. DM resistance

The membrane resistance is used to determine the filtration capacity of membranes (Xiong et al., 2016). It was calculated for all pore sizes applied in these experiments. The average membrane resistance of all pore sizes for each runs is presented in Table 3.5. Membrane resistance for 10 μm pore size, is showed in Figure 3.9c. Membrane resistance was $8x10^7$ 1/m in the early stage of DM. After DM was formed, the membrane resistance increased to $9x10^8$ 1/m in run-1. The operation ended with a value of $2x10^9$ 1/m. This value was lower than the values reported in other studies (Sun et al., 2018; Zhang et al., 2010). In addition to this, this value was lower than the value, obtained during treatment of cheese whey by AnDMBR with 10 μm pore size where the membrane was located internally. As a result, thicker cake layer was formed in previous experiment than this experiment. Lin et al., 2013 reported that sludge activity could improve membrane resistance. In this experiment, filtration was done with external DM where located in another cylindrical tube. Hence, there was no sludge activity in that tube and only solid/liquid separation was done during filtration. This lack of sludge activity could result in lower membrane resistance in this experiment. The membrane resistance increased further on the next runs (run-2 and run-3) during operation with 10 μm pore size (Figure 3.9c). The important reason increase in membrane resistance on next runs (run-2 and run-3) was irreversible fouling. This fouling layer caused more solid retainment in the following runs (run-2, run-3). As a result, more accumulation solid on filter resulted increase in membrane resistance. The same results about increase in membrane resistance in the following runs were observed for all pore sizes (20, 40 and 70 μm) as a result of irreversible fouling (Figure 3.10c, 3.11c and 3.12c).

This membrane resistance in 20 μm pore size was lower than 10 μm pore size in run-1 as expected (Table 3.5). The membrane resistance is governed by the membrane material itself. These are pore size of membrane, the surface porosity of membrane and the membrane thickness (Judd, 2006). Generally, small pore size membranes have high solid retainment capability that resulted in higher membrane resistance. Moreover, there are

other factors that can affect membrane resistance such as feed wastewater. Li et al., 2018 reported that feed wastewater with high particle concentration improved membrane resistance. Moreover, Ersahin et al., 2014 reported increase in small particles resulted in higher membrane resistance in the system. Thus, it can be inferred that the amount of small particles in feed affect membrane resistance more than the concentration of feed does. In the following runs (run-2 and run-3), the membrane resistance during operation with 20 μm pore size was higher than 10 μm pore size. The reason was, after first run, support layer lost its original properties (pore size) due to decrease in pore size as a result of irreversible fouling. In other words, the pore size of the support layer became less effective on membrane resistance on next runs (run-2, run-3) (Table 3.5). Moreover, other factors (such as feed concentration, blocked pores in run-1 and run-2) governed the membrane resistance. It should be added that, in run-2, the membrane resistance almost closed to each other for all pore sizes (10, 20, 40 and 70 μm). In run-3, the highest average membrane resistance was observed in 20 μm pore size (Table 3.5).

Contrary to expected, the membrane resistance during operation with 40 μm pore size was higher than 20 μm pore size in run-1 (Table 3.5). As mentioned before, TMP during operation 40 μm pore size was higher than 20 μm pore size. This could be due to occurrence of more solid deposition on nylon mesh and this improved TMP. The operation time in 40 μm pore size was longer than 20 μm pore size. Thus, long operation results more solid retainment on support layer that improves membrane resistance. It should be added that the highest membrane resistance was observed in 10 μm pore size in run-1. Thus, the pore size effect of support layer became clear for smallest pore size in first run.

Table 3.5 The membrane resistance, calculated during the operation with 10, 20, 40 and 70 μm pore size

	Average Membrane Resistance,1/m			
Pore Size	10 μm	20 μm	40 μm	70 μm
Run-1	$9x10^8 \pm 1.2x10^8$	$3.2x10^8 \pm 6x10^7$	$6.78x10^8 \pm 5x10^7$	$1.6\ x10^8 \pm 1.83x10^7$
Run-2	$1.5x10^9 \pm 2x10^8$	$1.9x10^9 \pm 3x10^8$	$1.87x10^9 \pm 1.2x10^8$	$1.3x10^9 \pm 1.07x10^8$
Run-3	$1.52x10^9 \pm 2x10^8$	$4x10^9 \pm 7.1x10^8$	$2.36x10^9 \pm 3.23x10^8$	$1.65x10^9 \pm 2.8x10^8$

The lowest average membrane resistance was observed in largest pore size (70 μm pore size) in run-1 (Table 3.5). Li et al., 2017 reported that mesh with large pore size had a filtration area and less filtration resistance than the mesh with small pore size. In addition to this, the amount and the particle size of solids are other factors that affect the membrane resistance. All these results showed that 10 μm pore size nylon mesh had highest solid retention capacity whereas 70 μm pore size nylon mesh had lowest solid retention capacity in run-1. However, the longer and sustainable operation are very important in filtration operations. Despite its advantages of working with smaller pore size, quick DM formation can result in shorter filtration operation and need more physical cleaning than large pore sizes (Sahinkaya et al., 2017). All things considered, this experiment shows the optimum pore size support layer should be selected in order to provide effective solid retention under continuous DM operation. In this experiment, as mentioned above, 20 μm pore size was found to be optimum pore size, when considering good solid retainment under continuous operation.

The filtration resistance of DM was remarkably much lower than that of MF/UF membranes in the range of 10^{12}–10^{14} 1/m during long-term sustainable operation (Lin et al., 2009). In addition to this, low filtration resistance in DM operation implies superior filtration capacity of DM over conventional membranes, and also reduction in energy consumption of the system (Sun et al., 2018).

The cake layer resistance effect on total membrane resistance was evaluated for 40 μm pore size (Table 3.6). Pore blocking resistance was calculated as 1.36 x 10^7 1/m and instinct membrane resistance was calculated as 7.13x10^6 1/m.

Table 3.6 The membrane resistance of 40 μm pore size; Total resistance, Pore blocking, Cake resistance and Virgin layer

Membrane Resistance,1/m	Run-3
Total Resistance	2.36x10^9
Cake Resistance (Reversible Fouling)	2.34x10^9
Pore blocking (Irreversible Fouling)	6.47 x10^6
Virgin Layer	7.13x 10^6

Cake layer resistance was calculated as by subtracting pore blocking (irreversible fouling) and virgin membrane resistances from the total membrane resistance. The determination

of pore blocking resistance was done at the end of run-3. Thus, cake layer resistance was calculated as 2.34x 10^9 for run-3 and it was 99.5 % of total resistance. According to the results, cake layer resistance composed most of the total resistance. This result was consistent with (Liu et al.,2012) reporting that cake resistance was responsible for over 98% of the total fouling. As mentioned by Chang and Kim, 2005, the cake layer formation was a major factor responsible for the overall flux decline. The cake layer formation was dominant mechanism that was responsible for DM formation.

3.3. The Effect of CFV on a Well-Formed DM Operation and The Characteristics of Well-Formed DM

3.3.1. The effect of CFV on a well-formed DM operation

The effect of pore size on the DM formation time and cleaning frequency were investigated in previous experiment and it was shown that DM was formed in short time with high flux. CFV is an important factor to control cake layer thickness in order to prevent sudden DM formation. In this experiment, filtration operation was done by controlling cake layer formation to enhance filtration time and decrease cleaning frequency.

The effects of CFV on DM formation and operation was investigated for 40 μm nylon mesh in this experiment. The system was operated in two runs. Physical cleaning was done between run-1 and run-2 (Figure 3.13). CFV was applied to control external DM thickness and permeability in this experiment. In other words, CFV was altered according to variation of turbidity in permeate, TMP and flux. The operation was done at room temperature in this experiment as in previous experiment, which the effect of pore size on DM formation was investigated. The temperature, which was lower than reactor temperature in first experiment (Section 3.1), increased tendency for membrane fouling. Such that this increase resulted quick DM formation in previous experiment that the effects of pore size on DM formation was investigated. Thus, CFV was applied to cake layer thickness and control permeability in wide range in this experiment.

The initial CFV was 39 m/h (Figure 3.13a). In the following hours, CFV was operated in range of 17 and 39 m/h. The turbidity in permeate was 139 NTU in first 1 hour of operation and no important decrease in turbidity happened on next hours. In first 4 hours,

TMP was 19 mbar (Figure 3.13a), then it began to increase. The turbidity was unstable at the same time (Figure 3.13b). Because no important change happened both in TMP and turbidity, CFV was decreased to 9 m/h in the end of 20 hours. CFV was kept at 9 m/h for 31 hours. As seen in Figure 3.13a, the fluctuations in TMP happened in the following hours and it continued with a range of 69 mbar and 219 mbar for a while. Then a sharp increase in TMP happened in 47.81 hours of operation.

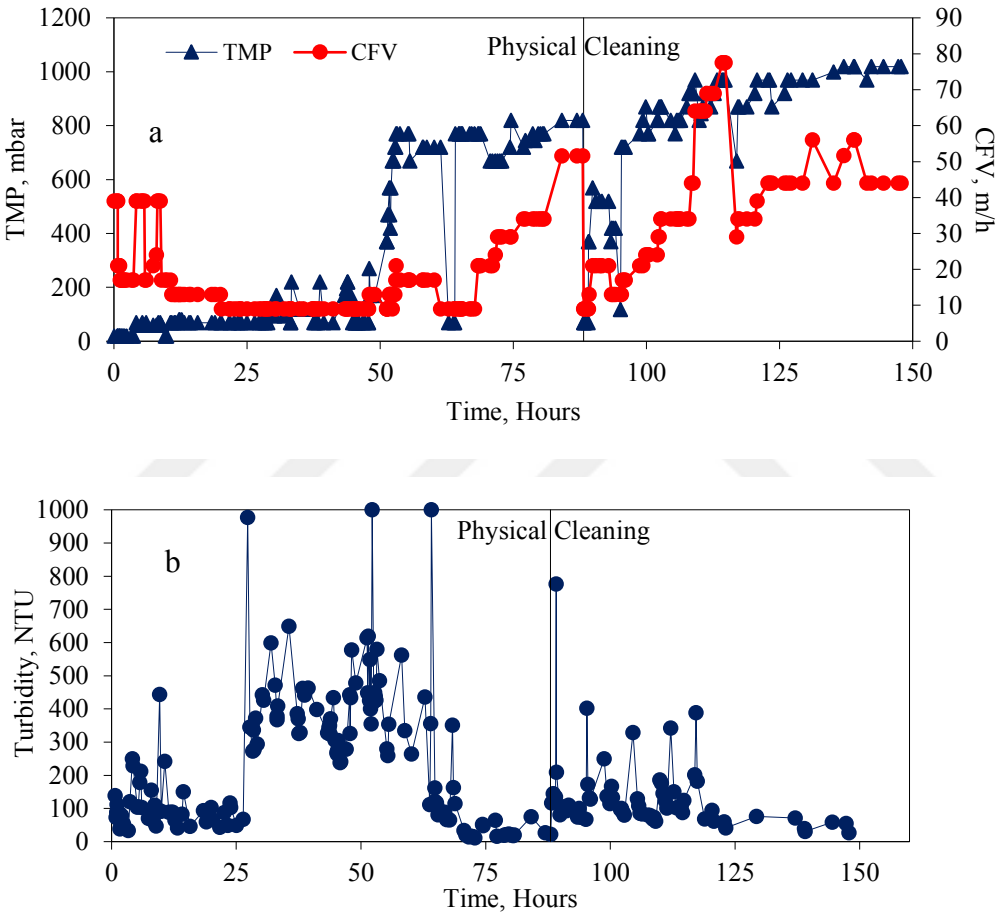


Figure 3.13 The variation in CFV and TMP (a) Turbidity (b) and during the operation

CFV was increased to 21 m/h in 53.03 hours of operation due to rise in TMP. However, this increase in CFV was limited to 21 m/h because turbidity in permeate was at high values, which was higher 200 NTU, simultaneously. Then CFV decreased to 9 m/h in 61.33 hours of operation and it kept at 9 m/h for 6.42 hours. However, a significant decrease in TMP was observed from 61.33 hours to 62.8 hours of operation such that TMP sharply decreased from 719 mbar and 69 mbar. TMP continued at this value for 1

hour. Then TMP began to increase and continued with values in range of 669 mbar and 819 mbar till the end of operation. When the effect of 40 μm pore size on DM formation was investigated in previous experiment, the fluctuation in TMP was not observed prior to DM formation. The reason of this fluctuation happened in TMP was application of CFV in this experiment. The application of CFV resulted in inefficient solid accumulation on support layer from the beginning of operation that this caused decrease in TMP from time to time.

As for flux, it did not change significantly and it was approximately 99 L/m^2h at first 54 hours of operation. Then as seen in Figure 3.14a, the decrease in flux started in the following hours. However, the decrease in flux happened in a shorter time for the same pore size in previous experiment where CFV was not applied.

The turbidity in permeate was less than 200 NTU in first 26.42 hours of operation. Then a sharp increase in turbidity happened and reached to 1000 NTU in 27.28 hours of operation. The turbidity reached to 1000 NTU two more time in 52.3 hours and 62.4 hours of operation. Then it sharply decreased. Although a limited increase in turbidity happened in 68.4 hours of operation, the decrease in turbidity continued in the following hours (Figure 3.13a). At the same time, flux also decreased considerably as a result of solid accumulation on support layer. Due to continuity of this high TMP and decrease in turbidity, CFV was started to increase in 67.75 hours of operation and it reached to 51.6 m/h in 84.15 hours of operation. As seen in Figure 3.13a, despite increase in CFV, TMP and flux were not affected by this increase. Thus, as mentioned by Alibardi et al., 2014, CFV lost its efficiency on TMP and flux after a while. In other words, the effect of shear force, created by CFV, became insignificant on solid accumulation (Sun et al., 2018). This was a sign of DM formation. Turbidity decreased to 34 NTU in 71 hour (2.96 day) of operation that this showed DM formation was completed. Then, turbidity was stabilized at 28±4 NTU. This turbidity value was similar to the value for the same size in experiment that the effect of pore sizes on DM Formation time was investigated. It should be stated that prior to DM formation, the spikes in turbidity were also observed for the same pore size in previous experiment where CFV was not applied. It could be inferred that, in comparation to CFV, size relationship between pore and particle is a significant factor, affecting permeate quality during the whole filtration.

After DM formation, the flux continued with a value of 82 and 67 L/m^{2}h. In end of operation, TMP reached to 819 mbar which was consistent with value reported by Salerno et al., 2017. In previous experiment where the effect of pore size on DM formation was investigated, DM formation on support layer with 40 µm pore size completed in 41.16 hours (1.72 days) and then the operation carried out in 68.43 hours. However, DM formation took longer in this experiment such that completed in 88 hours under operation with CFV. All things considered, CFV resulted in longer DM formation and thus prolonged filtration time in this experiment.

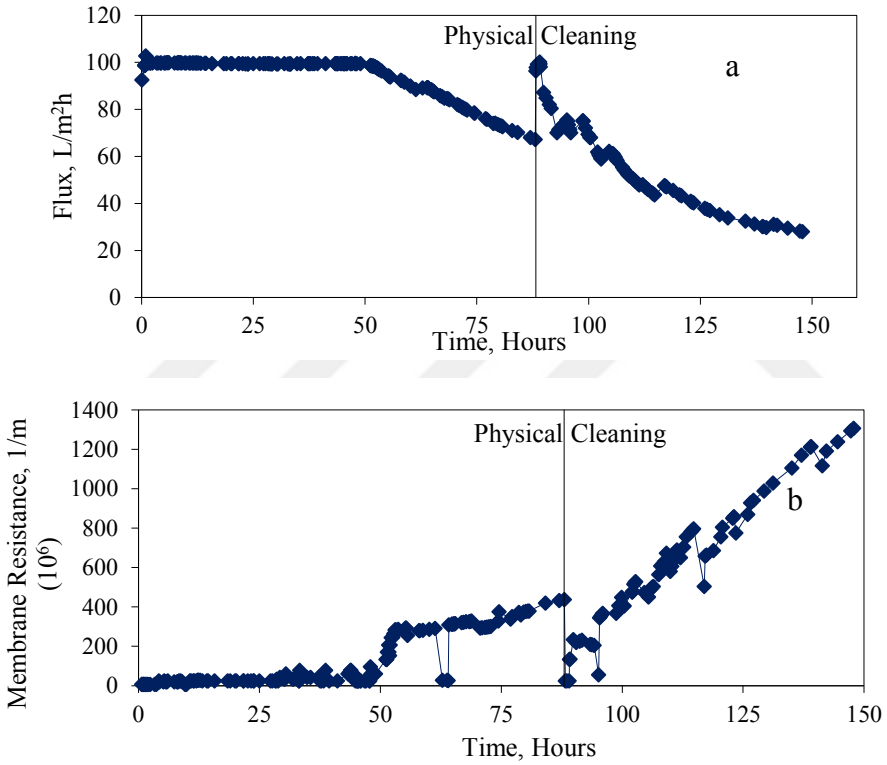


Figure 3.14 The variation in Flux (a) and Membrane Resistance (b) during the operation

Physical cleaning was done in the end of run-1, and the operation continued. The decreased flux in run-2 happened faster than run-1. The average flux was 99±1.4 L/m^{2}h in first 1.2 hours (72 minutes) of operation. Then the flux decreased continuously in the following hours. In contrast to previous run, the decrease in flux happened after a short time. The decrease in flux after physical cleaning was consistent with Chen et al.,2003. The operated flux was between 28 and 100 L/m^{2}h in run-2 (Figure 3.14a). The studied

flux values were consistent with reported studies (Hu et al.,2018a). In addition, TMP sharply increase to 569 mbar in first 1.5 hours of operation in run-2. Although, the sharp decrease was observed in the TMP after 5 hours, TMP increased to 719 mbar in 1.6 hours of operation. This increase continued in the following hours and it reached to 1019 mbar. Pore blockage, happened in previous run, could cause more increase TMP in run-2. Thus, higher CFV was applied to prevent sudden cake layer formation and sudden increase in TMP. During the whole operation, CFV values were lower than values reported in conventional membranes (Figure 3.13a). This was advantage of studies with AnDMBR. However, in this experiment, the higher CFV was applied than other AnDMBR studies (Hu et al.,2018a) due to studying at lower temperature that accelerated membrane fouling. DM formation completed in 51 hours, that was faster than previous run. This quick DM formation in run-2 was due to pore blockage. The small solids that blocked pore of the support layer, could not be removed by physically. Thus, irreversible fouling accelerated decrease in flux and DM formation in run-2. After DM formation, turbidity stabilized at 42±10 NTU. This value was higher than value in previous run. The applied higher CFV (9-77.52 m/h) in run-2 could result increase turbidity in permeate.

In previous experiment (Section 3.2), the operation completed in 147.26 hours totally during operation with 40 μm pore size and the physical cleaning was done three times. In this experiment, the operation carried out almost the same hours (148 hours) and the physical cleaning was done two times. It seems that CFV caused decrease in physical cleaning frequency.

As for membrane resistance, as seen in Figure 3.14b, depending on the variation of flux and TMP, membrane resistance continuously increased except two hours (in 63 and 64 hours of operation) in run-1. This decrease in membrane resistance in these hours was due to decrease in TMP. Similar to previous experiment that the effect of pore size was investigated, membrane resistance increased after physical cleaning due to irreversible fouling. Moreover, membrane resistance in this experiment was lower than the previous one for 40 μm pore size. This could be because of CFV. Xiong et al., 2016 reported that the membrane resistance was related to cake layer thickness. In addition to this, Mackley and Sherman, 1992 reported that higher CFV resulted in thinner cake layer. Thus, it could be inferred that the application of CFV resulted in lower membrane resistance. In end of run-2, COD test was done to determine organic matter removal. A sample of DM effluent

was taken for COD test. COD in this sample was determined as 37.5 mg/L. Another sample was taken in cylindrical tube, where DM was located in and was determined as 1440.9 mg/L. This showed the high organic removal efficiency (97 %) by well-formed DM.

3.3.2. The characteristics of well-formed DM

SEM images of DM are presented in Figure 3.15, SEM images showed a cake layer, formed on support layer. DM layer seemed to be dense (Figure 3.15). In order to verify the chemical components of the cake layer, elemental analysis was carried out to identify the major composition of the DM layer. SEM images are also presented in Appendix A at different magnifications.

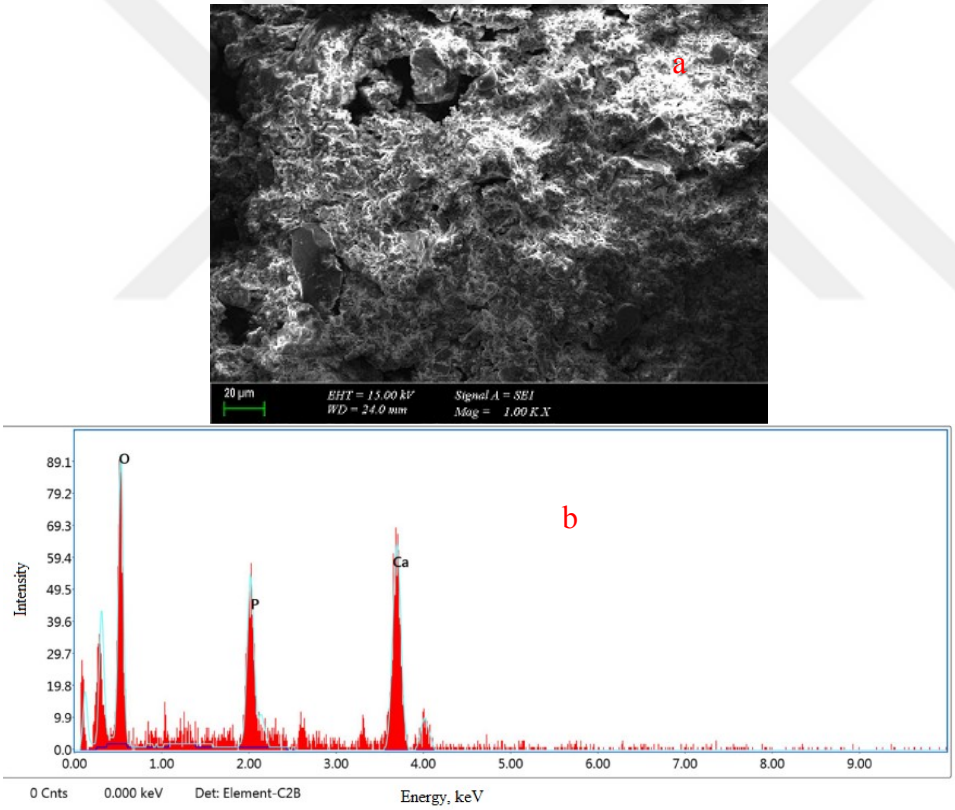


Figure 3.15 SEM Photo of DM Layer (Mag=1.00KX) (a) EDX analysis of the DM layer (40 µm) (b)

EDX analysis detected elements in selected points of DM layer (Figure 3.15). According to EDX analysis, the detected elements in DM was Ca (38.96 % in weight), P (14.14 % in weight), and O (46.91 % in weight). Ca^{+2} is one of the important cations that connect

with other biopolymers and cells and form dense cake layer (Meng et al., 2009). Figure 3.15a verified our result.

The FTIR spectrum of biopolymers in the cake layer is presented in Figure 3.16. The spectrum exhibited a broad region of absorption at 3272.6 cm^{-1} that was because of stretching of the O-H bond in hydroxyl functional groups. A sharper peak at 2912.6 cm^{-1} is due to stretching of C-H bonds (Gao et al.,2011). The peak at 1631.5 cm^{-1} and 1409.7 cm^{-1} presents amide I (Ersahin et al.,2016) and amide III (Mellamaca et al.,2014). Amide I groups consist of association of C=N and C=O bonds, whereas amide III stretching C-N (Lin et al.,2009). The peak at 1014.4 cm^{-1} shows the presence of polysaccharides, including C-O bonds (Ersahin et al.,2016). The results exhibited that components of cake layer were mostly polysaccharides and proteins. In addition to this, peak at 871.7 cm^{-1} showed carbonate ion, and peak at 597.8, 557.3 and 460.9 cm^{-1} showed sulfate ions (Coates et al., 2006), which were originated from feed wastewater.

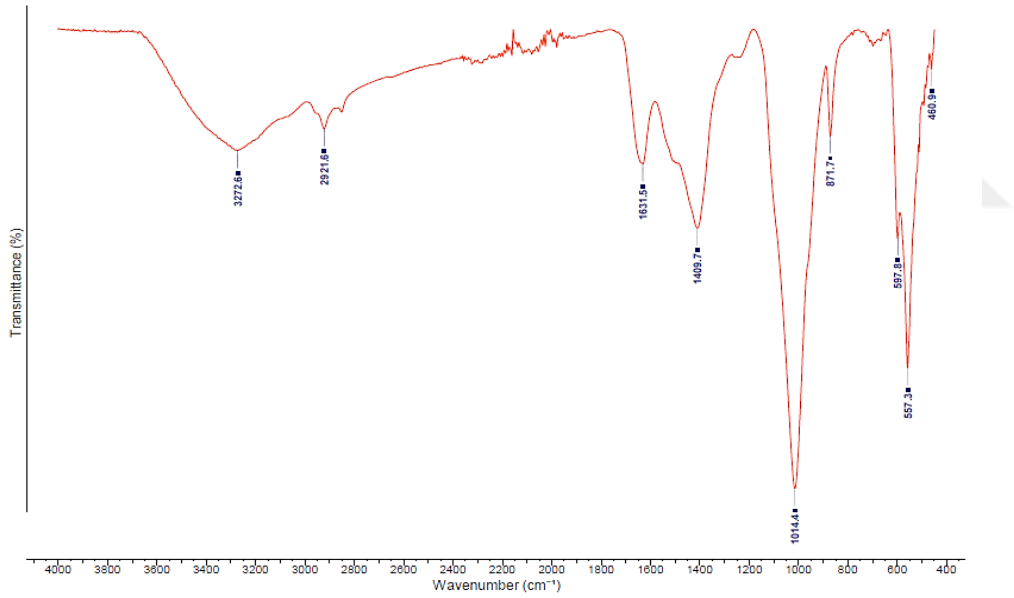


Figure 3.16 FTIR spectrum of DM layer

3.4. Blocking Mechanisms

DM is formed by combination of gel and cake layer that is a part of membrane fouling (Mahat et al., 2018). As mentioned before, pore blocking and solid accumulation over support layer causes gel/cake layer formation. When the particles block the pores of membrane surface and accumulate on the surface of membrane, the movement of the

water molecules through the pores of the membrane surface will be diminished. As a result, membrane permeability reduces (Ng et al., 2014). As mentioned before the TMP and flux are important indicators of membrane fouling. The decline in flux can be described by one of the membrane fouling mechanisms in conventional membranes (Charfi et al., 2012). There have been lots of studies that have been applied membrane fouling mechanisms in order to model the decrease in flux in conventional membranes. However, there are limited studies about application of membrane fouling mechanisms in DM application (Liu et al., 2009; Saleem et al., 2017; Gong et al., 2014; Huang et al., 2020). Mathematical modelling of fouling mechanisms that were responsible for the DM formation of different pore sizes were determined. Blocking mechanisms are used to define flux decline during filtration under constant pressure (Hermia,1982). The initial flux decline in membrane fouling happens as a result of standard blocking induced by the accumulation of particles within pores of membrane, it is followed by complete blocking, intermediate blocking, and finalized by a slower reduction in flux because of cake formation over the initial pore blocking (Bowen et al., 1995; Abdelrasoul et al., 2012). Additionally, membrane resistance deduces the membrane formation mechanisms (Xiong et al., 2016). In this experiment, membrane resistance was used to help in definition of blocking mechanism. The equations that are presented in Table 2.11 were used to detect blocking mechanism, that was responsible for DM formation. The linear fitting of obtained experimental data with blocking filtration mechanisms was tested.

3.4.1. Blocking mechanism for 10 µm

Firstly, blocking mechanisms were determined for 10 µm pore size. Linear fitting was applied to the data taken at different time intervals. These mechanisms were applied in separate time during operation. The equation associated with standard blocking were best fitted to the experimental data from the first 24 minutes to the end of the filtration time (R^2>0.99) (Figure 3.17a). The equations associated with complete blocking had best fit to the experimental data from the first 39 minutes to 75 minutes (1.25 hours) of the filtration time (R^2>0.99) (Figure 3.17b). The intermediate blocking fitted well with the experimental data during the whole operation (Figure 3.17c). From first 2 hours of filtration operation to the end of filtration operation (3.3 hours of operation), cake

filtration mechanisms fitted experimental data well. It can be concluded that cake filtration mechanism was not effective at the beginning of operation.

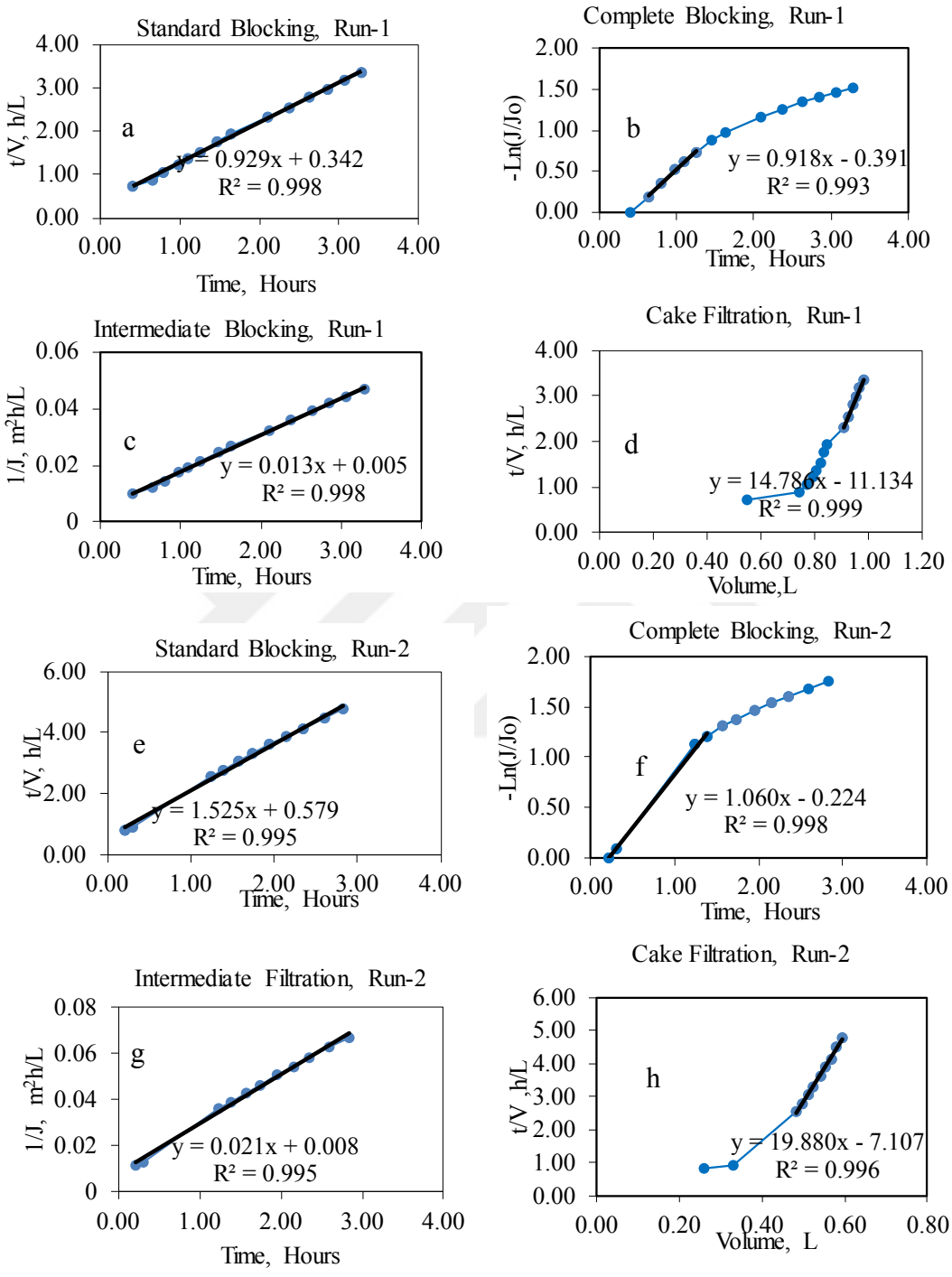


Figure 3.17 Flux decline rate (10 µm) for membrane fouling mechanisms in Run-1 and Run-2

As mentioned just before, the complete blocking happened for a certain period in run-1. Thus, this implies that some particles directly blocked the pores of support layer (complete blocking) for a certain period. On the other hand, the standard blocking and intermediate blocking mechanism were very effective on formation of membrane fouling during the whole run (run-1). It could be inferred that some particles attached inside the pore of support layer (standard blocking) and some particles directly blocked some pores of support layer and/or settled on other particles that had already blocked some pores of support layer (intermediate blocking) during the whole filtration operation. This shows that the occurrence of this membrane mechanisms depends on size of particles in feed. Thus, the particles size in feed can affect membrane fouling mechanisms. The pore blocking mechanisms (standard, intermediate and complete blocking) can happen in different times depend on particle size in feed. It should be remembered that the average particle size 35 μm in UASB (Section 3.1), where its effluent was used as feed. Moreover, the cake filtration accompanied both the standard blocking and intermediate blocking from 2 hours to the end of operation in run-1. According to the results, it could be deduced that the accumulation of particles resulted consolidated cake layer formation towards the end of filtration. The complete blocking and cake filtration accompanied with these mechanisms (intermediate and standard blocking) at different operational periods (Figure 3.17 a,b,c,d). It could be inferred that the formation of cake layer was not as effective in flux decline as intermediate pore blocking and standard pore blocking for the whole operation.

After physical cleaning, support layer lost its properties due to irreversible fouling. Till this time, the blocking mechanism for DM were only applied for virgin support layer (Liu et al., 2009; Gong et al., 2014; Sallem et al., 2017; Huang et al., 2020). In this experiment, the blocking mechanisms in reformed DM (run-2 and run-3) were also investigated. The standard blocking began in 13 minutes of operation in run-2 instead of 24 minutes of operation in run-1. Moreover, the standard blocking began in 7 minutes of operation in run-3. The same result was observed for complete blocking mechanisms. The semi-blocked and blocked pores, happened in run-1, accelerated the formation of blocking mechanisms in the following runs (run-2 and run-3). The standard and intermediate blocking fitted well to the experimental data during the whole operation in run-2 as in run-1. From first 1.2 hours of filtration operation to the end of filtration operation, cake

filtration mechanisms fitted well to experimental data (R^2>0.99) in run-2. This showed that cake filtration started in run-2 faster than run-1 as observed in blocking mechanisms. Furthermore, after physical cleaning, it was observed that the standard blocking and complete blocking happened again in run-2. However, the standard blocking and complete blocking are irreversible fouling and it can be expected not to happen on next runs (run-2 and run-3) (Di Bella and Trapani, 2019). All this considered, it can be inferred that all pores of support layer (10 μm) were not completely blocked at the end of previous run (run-1) and there were some unblocked and/or semi blocked pores, remained at the end of run-1. Thus, standard blocking and completely blocking were observed in the following runs (run-2 and run-3). In addition to this, intermediate pore blocking is semi-reversible fouling (Di Bella and Trapani, 2019). Thus, it can be expected reformation of intermediate pore blocking after physical cleaning.

In run-3, the standard blocking mechanism, complete blocking and intermediate blocking mechanism were happened simultaneously in first 1 hours of operation. Then the standard blocking and intermediate blocking maintained to happen for more 1.2 hours (Figure 3.18a). They were gradually substituted by cake layer filtration between 2.2 hours to 3.7 hours of filtration time. Finally cake filtration fitted best to experimental data in the following hours of operation (from 3.7 hours to 5.1 hours of filtration operation) (R^2>0.99) (Figure 3.18d). The rate of increase in membrane resistance versus time was faster in first 2.2 hours of operation than the following hours of operation (from 3.7 hours to the end of filtration time) in run-3 (Figure3.9c). Thus, rate of increase in membrane fouling versus time decreased during cake filtration stage (Figure 3.9c).

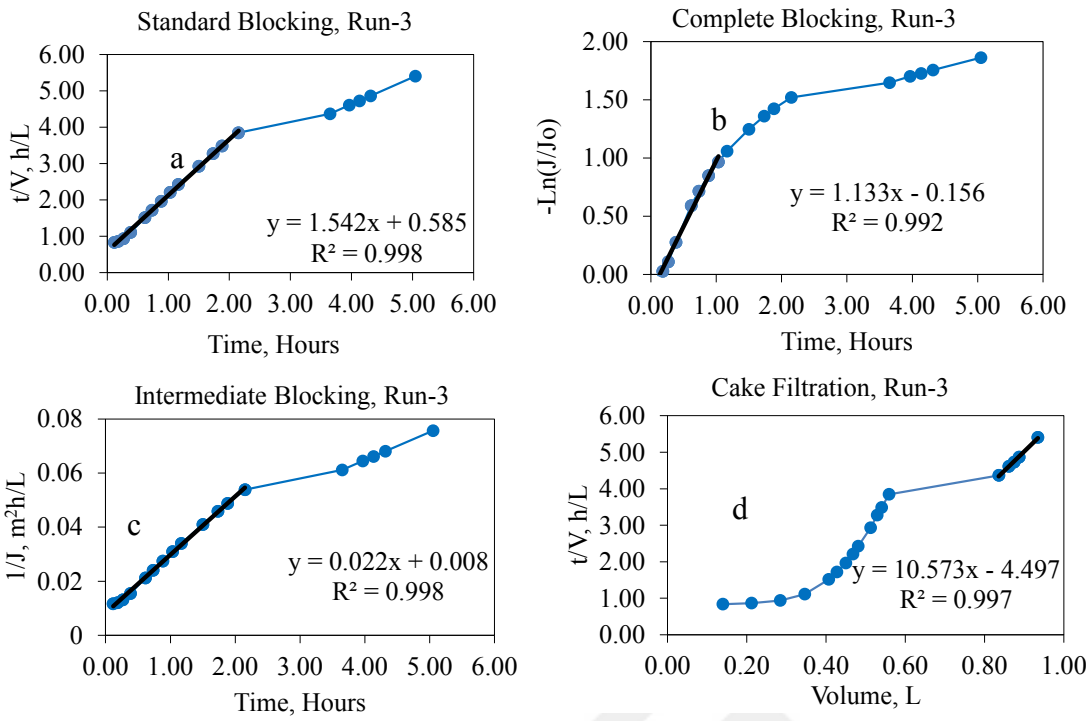


Figure 3.18 Flux decline rate (10 µm) for membrane fouling mechanisms in Run-3

The dominant mechanism towards the end of the operation was only cake filtration mechanism in run-3 and this was consistent with Liu et al., 2009. The transition between pore blocking and cake filtration mechanism became clearer in run-3 (Figure 3.18d) than in run-1 (Figure 3.17d) and run-2 (Figure 3.17h). However, as mentioned before, the intermediate pore blocking and standard pore blocking mechanism were effective during the whole operation in run-1 and run-2 (Figure 3.17). It seems that the intermediate pore blocking and standard pore blocking lost its effect in run-3 (Figure 3.18 a, c). This could be due to irreversible blocking. This irreversible fouling layer (previous runs) enhanced accumulation of solids over this layer. Thus, based on the R^2 value, the cake filtration model was seen as the best model to describe the flux decline mechanism in the last three hours of operation. An effective cake layer formation (due to irreversible fouling) improved cake layer resistance in the following runs (run-2 and run-3) (Figure 3.9c). Thus, membrane resistance increased by improving in cake layer formation on the following runs (Figure 3.9c) and this was clearly observed in run-3 with dominant cake layer formation in last hours of experiment (Figure 3.18d).

3.4.2. Blocking mechanism for 20 µm pore size

The membrane fouling mechanisms did not fit well to the experimental data in first 2 hours of operation in run-1. This was because no significant decline in flux happened in first 2 hours of operation. However, during operation with 10 µm pore size, the blocking mechanism fitted well to the experimental data from the beginning of the study. The standard and intermediate blocking showed its effect in decrease in flux from the beginning of 2 hours of operation during operation with 20 µm pore size. As seen in Figure 3.19, the standard blocking, complete blocking, and intermediate pore blocking happened together from 3 hours to 6.6. hours of operation. It can be inferred that some particles, which had smaller pore size than 20 µm, deposited inside the pore walls of support layer. In addition to this, some particles directly blocked the pores of support layer and/or accumulated other particles that had already blocked some pores of support layer. Cake filtration mechanism occurred from first 6.6 hours to the end of operation (9.3 hours of operation). It can be inferred that the particles deposited other particles that blocked surface of support layer. However, based on $R^2 > 0.99$, as mentioned above, the intermediate pore blocking occurred from 2 hours to the end of operation (9.3 hours of operation). As seen in Figure 3.19c, the intermediate blocking mechanism was the dominant mechanism in terms of time effect. The cake layer formation mechanism was not effective in flux decline as much as intermediate pore blocking. This was due to operational conditions. The operational time is an important factor in formation of blocking mechanism as mentioned in 10 µm pore size. Moreover, the sludge activity effect on cake layer formation should not be ignored.

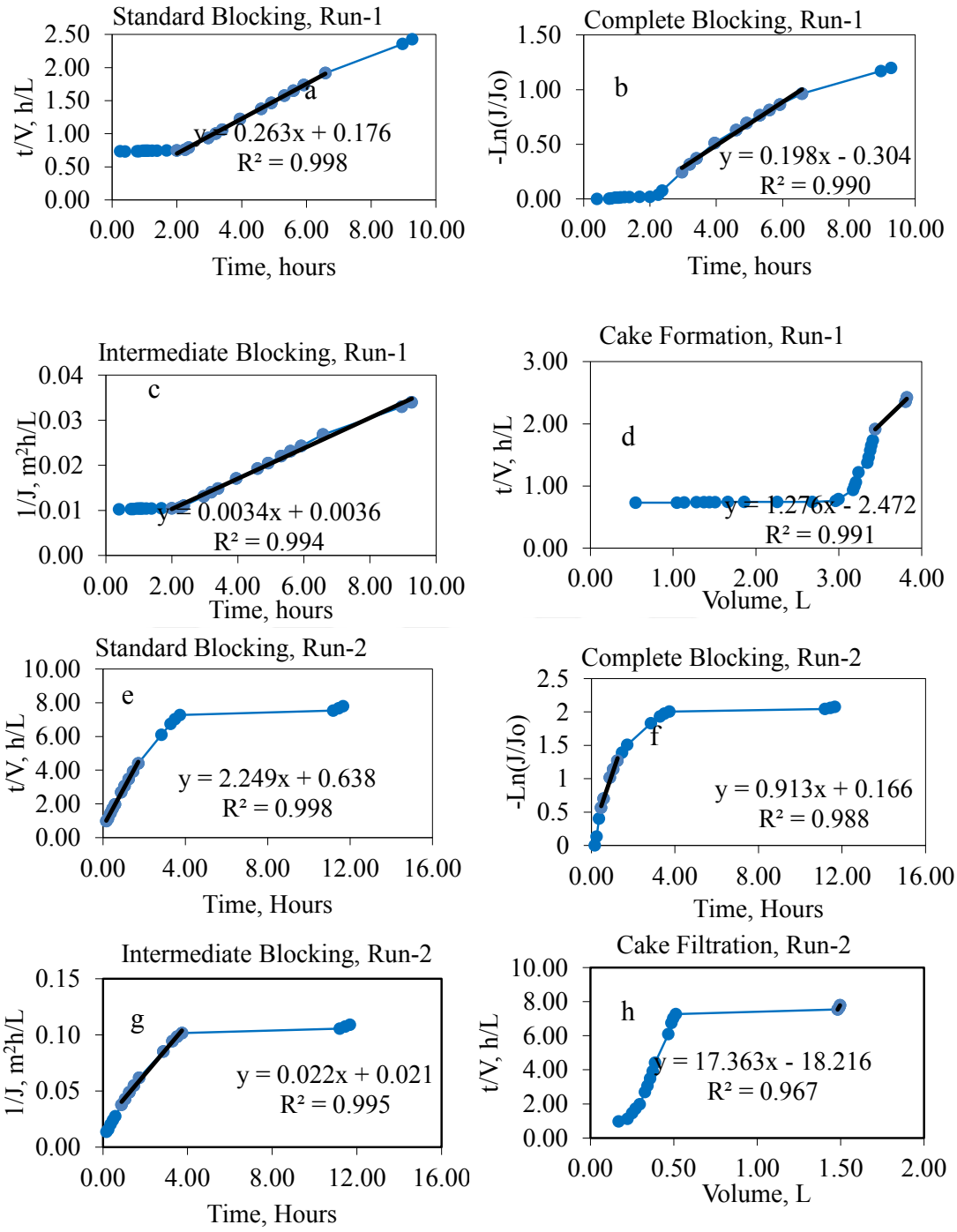


Figure 3.19 Flux decline rate (20 µm) for membrane fouling mechanisms in Run-1 and Run-2

The microbes produce EPS. The bound EPS allows microorganisms to attach to a membrane. These microorganisms aggregate and form biofilm, results in surface fouling. The high amount of EPS induces cake formation (Charfi et al., 2012). Thus, the sludge activity improves cake layer formation. However, in our study, the particles in feed,

having less EPS content, and they caused formation of inefficient cake layer formation. Moreover, Saleem et al., 2017 was reported that cake filtration was responsible for DM formation. That experiment was done in external DM that connected to reactor, where sludge activity took place. Boerlage et al., 2002 stated that standard blocking and complete blocking were expected to happen at the beginning of filtration operation and then intermediate blocking was expected to happen successively for a long time. In addition to this, they also reported that intermediate blocking was considered as transition phase between pore blocking (complete and standard blocking) and cake filtration till an effective cake layer developed. However, they reported that standard, complete, and intermediate blocking happened at the same time and finally, cake filtration developed during UF filtration. This was almost consistent with our result. All in all, the strong cake layer formation mechanism was not obtained in our experiment.

The blocking mechanisms happened in run-2 faster than run-1 (Figure 3.19e) due to irreversible fouling as mentioned in 10 µm pore size. The standard blocking began in 10 minutes (run-2) instead of 2 hours of operation (run-1). The standard blocking completed 4.6 hours in run-1 whereas, it carried out in 1.53 hours in run-2. The same results were observed in other blocking mechanisms (Complete blocking, intermediate blocking, and cake filtration mechanism).

Both intermediate pore blocking and cake filtration were effective mechanisms that governed the decline in flux in run-1 whereas, intermediate pore blocking fitted well to the experimental data for a certain time in run-2 (from 0.9 hours to 3.7 hours of operation). Then the intermediate pore blocking followed by cake filtration and the drop in the permeate flux was governed by cake layer formation till the end of operation (Figure 3.19h).

3.4.3. Blocking mechanism for 40 µm pore size

Similar to 20 µm pore size, the membrane fouling mechanism did not fit well to the experimental data in first 6 hours of operation in run-1 during operation 40 µm pore size. However, it should be stated that the blocking mechanism happened in 20 µm pore size faster than 40 µm pore size. This showed that important amount of particle in feed had smaller size than 40 µm pore size. Two mechanisms; standard blocking and complete blocking almost happened, simultaneously (from 7 hours to 22 hours of operation) (Figure

3.20a,b). Then, the intermediate blocking showed its effect 30 hours later from the beginning of operation.

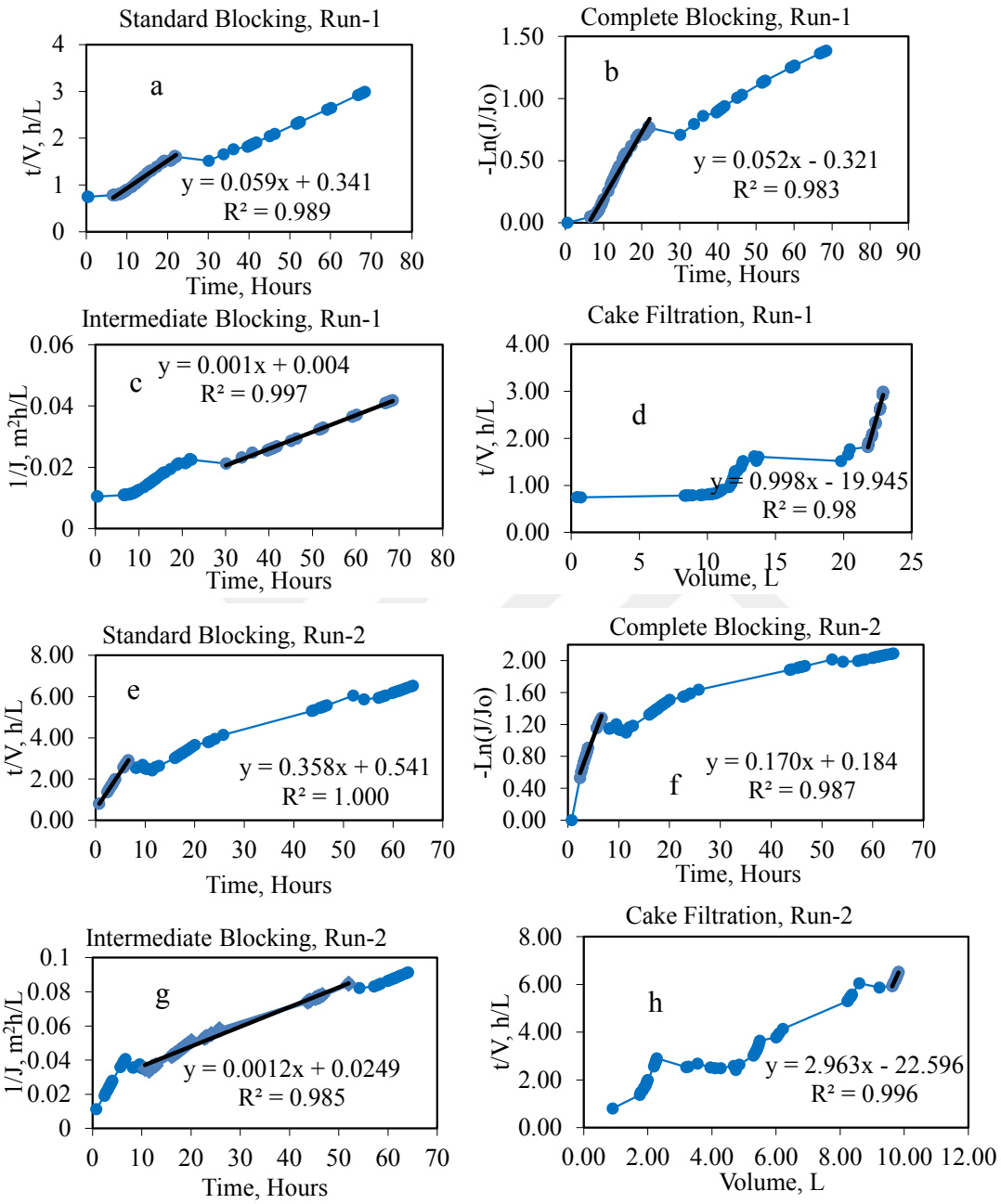


Figure 3.20 Flux decline rate (40 µm) for membrane fouling mechanisms in Run-1 and Run-2

The cake filtration began to occur 40 hours later from the beginning of operation. Both the intermediate blocking and cake filtration became the dominant mechanism from 40 hours to the end of operation. Similar to 20 µm pore size, both intermediate and cake

filtration were dominant mechanism in the last hours of operation during operation with 40 µm pore size in run-1.

As observed in other pore sizes, the blocking mechanism started early in the following runs (run-2 and run-3). Additionally, blocking mechanism occurred in run-2 faster than run-1, except intermediate blocking, during operation 40 µm pore size. For example, the standard blocking and complete blocking, and cake filtration happened in 7 hours, 6 hours, and 8 hours respectively in run-2, whereas they happened in 16 hours, 16.5 hours, and 29 hours respectively, in run-1.

The intermediate blocking mechanism fitted well to the experimental data from first 8 hours to 52 hours of operation (R^2>0.98) (Figure3.20g). Finally, the four blocking mechanisms happened in a shorter time in run-3 than run-1 and run-2 (Figure 3.21). Thus, it could be inferred that irreversible fouling accelerated membrane blocking formation time in the following runs (run-2 and run-3). The blocking mechanisms happened in run-3 are presented in Figure 3.21. Blocking mechanisms fitted well to the experimental data at different operational periods.

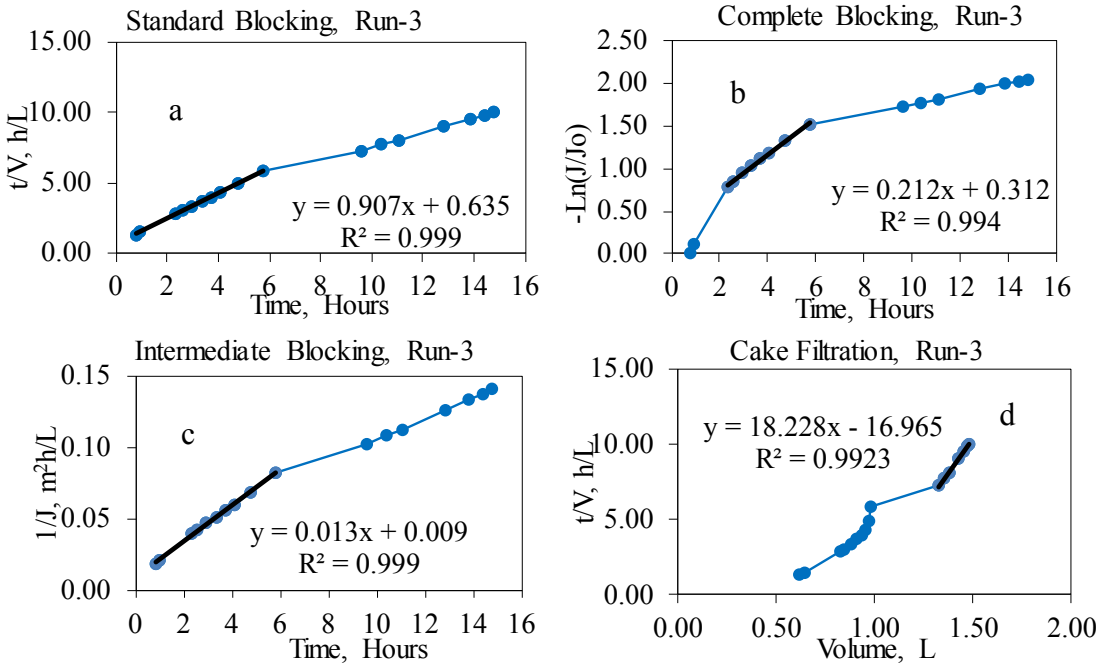


Figure 3.21 Flux decline rate (40 µm) for membrane fouling mechanisms in Run-3

3.4.4. Blocking mechanism for 70 µm pore size

Similar to 20 and 40 µm pore size, the membrane fouling mechanisms did not fit the experimental data well in first 50 hours of operation. Thus, blocking mechanisms started to happen later in 70 µm pore size than other pore sizes (10, 20 and 40 µm pore size). This showed that important amount of particle in feed had less size than 70 µm as mentioned in 40 µm pore size. The equations associated with standard, complete and intermediate blocking had best fit from the first 50.5 hours to the end of the filtration operation (Figure3.22a) (R^2>0.99). These three mechanisms started to happen simultaneously.

As seen in Figure 3.22d, cake filtration mechanism had an effect on decline in flux in last 32 hours of filtration. It can be deduced that some particles that accumulated on other particles that had already blocked partially the surface of support layer. As observed in 20 and 40 µm pore size, the blocking mechanisms began earlier and happened faster in the following hours (run-2 and run-3) than run-1. For instance, the standard blocking mechanisms started in the first 12 minutes in run-2 instead of 50.5 hours of operation in run-1. Additionally, it occurred in 26 minutes in run-2 whereas it occurred 46.4 hours in run-1. The same results were also observed for complete, intermediate blocking and cake filtration. As mentioned before, complete, and intermediate blocking occurred 46.4 hours in run-1 whereas, complete and intermediate happened in 2.33 hours and 12 hours, in run-2, respectively. Finally, cake filtration happened in 33.7 hours in run-1 whereas, it occurred 6.65 hours in run-2. Similar to other pore sizes (20, 40 µm), the blocking mechanisms in run-1 happened faster than run-1.

In the beginning of run-3, the equations associated with standard blocking mechanism had fit well to the data from the first 1.3 hours to 3.4 hours of the filtration operation (R^2>0.938) (Figure 3.23a). Moreover, the equations associated with complete blocking mechanism had best fit to the data from the first 1.3 hours to 1.9 hours of the filtration operation (R^2>0.99) in run-3 (Figure 3.23b). The standard blocking was gradually replaced by the intermediate blocking between 3.4 hours to 4.3 hours of filtration time. In the following hours, the intermediate blocking mechanism fitted the experimental data well (R^2>0.99) from 4.3 hours to the 14.23 hours of filtration time. As mentioned before, in contrast to run-3, the temporary irreversible fouling happened in run-2 (70 µm), this

could accelerate formation of blocking mechanism in that run. Thus, it was observed that blocking mechanisms started later in run-3 than run-2.

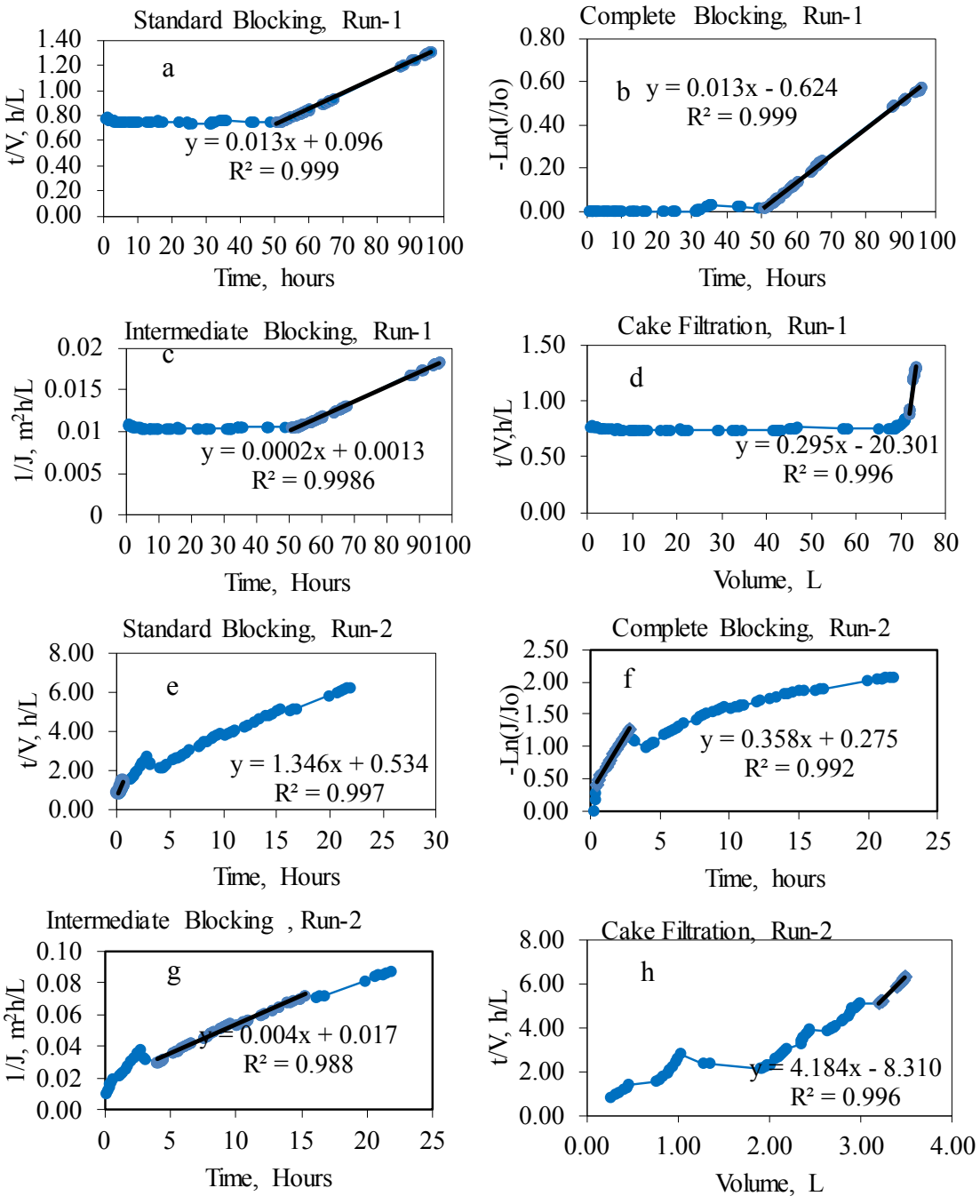


Figure 3.22 Flux Decline Rate (70 µm) for membrane Fouling Mechanisms in Run-1 and Run-2

As seen in Figure 3.23c, intermediate blocking mechanism was almost dominant mechanisms and it significantly affected permeate flux. Cake filtration mechanism did

not fit with the experimental data in run-3. As much as we understand, the operational conditions affected formation of membrane blocking mechanism. During operation with 70 µm pore size, the cake filtration mechanism was observed in run-1 and run-2. However, effective cake layer did not form during operation in run-3. Although, important increase in membrane resistance happened, an effective cake layer was not obtained in run-3.

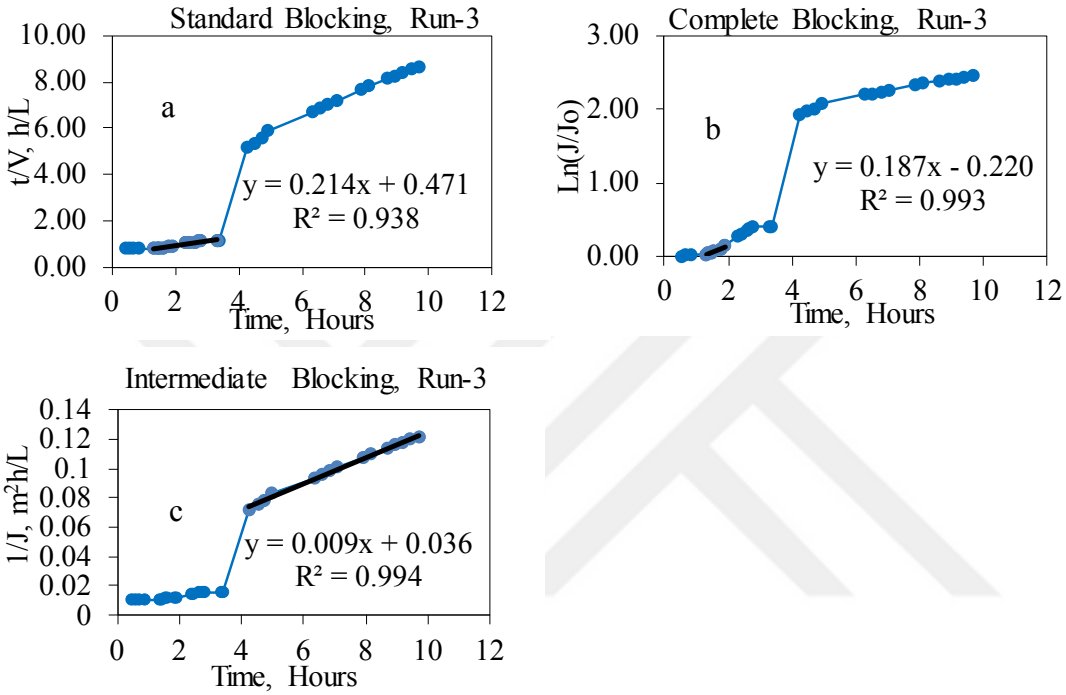


Figure 3.23 Flux decline rate (70 µm) for membrane fouling mechanisms in Run-3

El Rayess et al., 2012 reported that the thickness of cake enhances over time owing to the deposition of particles on the membrane surface. Moreover, Ng et al., 2014 reported that the cake layer thickness enhanced as the filtration time extended. When filtration time prolongs, cake layer formation more likely to happens (Ng et al., 2014). Thus, an effective cake layer was not observed due to insufficient filtration time in run-3 during operation 70 µm pore size.

To sum up, generally, the irreversibly deposited particles in previous runs (run-1), enhanced cake layer formation in the following runs (run-2, run-3). This can be seen in membrane resistance. The formation of cake layer improved membrane resistance (Figure 3.9c, Figure 3.10c, Figure 3.11c and Figure 3.12c). Moreover, this study showed that operational conditions had an effect on cake layer formation. Thus, it can be inferred that

in addition to operation time, sludge activity has an important role in cake layer thus DM formation.

As mentioned before, there have been lots of studies about application of blocking mechanism on conventional membranes to detect flux behaviors. Vela et al., 2008 reported that the operational conditions had an important effect on formation of fouling mechanism in conventional membranes. Griffiths et al., 2014 summarized the reported studies. They reported that combination of pore blocking (complete blocking and intermediate blocking) formed first in conventional membrane. Then cake layer was formed. In another study, pore constriction formed first, then pore blocking followed them and finally, formation of cake layer happened (Griffiths et al., 2014). Moreover, Liu et al.,2009 reported that DM fouling was formed in order of a standard blocking, complete blocking, intermediate blocking, and cake filtration step. In our study, the blocking mechanism almost followed this order, and pore blocking mechanisms almost happened simultaneously. Our results were partially consistent with Liu et al., 2009. In addition to this, our result was also consistent with Salazar-Pelaez et al., 2015, who reported the pore blocking mechanisms happened at the same time. Besides, generally, intermediate pore blocking was dominant mechanism in our experiment. The combination of intermediate blocking and cake filtration was found to be dominant mechanism that formed DM (Huang et al., 2020). Gong et al., 2014 reported that complete blocking was the main blocking mechanism during DM operation with 50 μm pore size, and added that cake filtration became main blocking mechanism during DM operation with 1 and 10 μm pore size. Thus, it could be inferred that the particle size, and pore size of support material had an important effect on formation degree of membrane fouling. However, as mentioned above, filtration time is another important factor. For example, cake filtration mechanisms were observed both during operation with almost all pore sizes. The important difference between these pore sizes in terms of cake layer formation was DM formation time. PSD analysis in UASB reactor could give a hint about particles that formed DM. The median particle size based on volume was 35 μm (in UASB reactor, Section 3.1). Thus, the solids, which were within the size range, could be retained on the support material with a 10 μm and 20 μm pore size in a short time. However, DM formation took longer on support material with pore size higher than 35 μm.

The equation constants (a, b) that obtained by linear fitting of experimental data for all pore sizes were different (Figure 3.17, 3.18, 3.19, 3.20, 3.21, 3.22, 3.23, 3.24). As mentioned in Material and Methodology section, these constants depend on mainly TMP, hydraulic resistance of membrane, membrane surface area, the concentration of sludge, specific cake resistance and the slope of the best fit of the linear equation (Liu et al., 2009). In our study, TMP was not constant. Only constant parameters were hydraulic resistance of virgin membrane and membrane surface area. Thus, it was normal to observe different constant values (a,b) in mathematical equations of blocking mechanisms for all runs.

3.4.5. Blocking mechanism for 40 µm pore size operated under CFV

The pore blocking mechanism was determined for DM with 40 µm pore size, operated with CFV (Section 3.3). As seen in flux (Figure 3.14a) and membrane resistance (Figure 3.14b), an important membrane fouling did not happen at first 51 hours. As shown in Figure 3.24, during operation period of 51 and 61 hours, based on R^2=0.991, the equations associated with standard blocking and complete blocking had best fit to experimental data. It means the standard blocking and complete blocking happened at the same time.

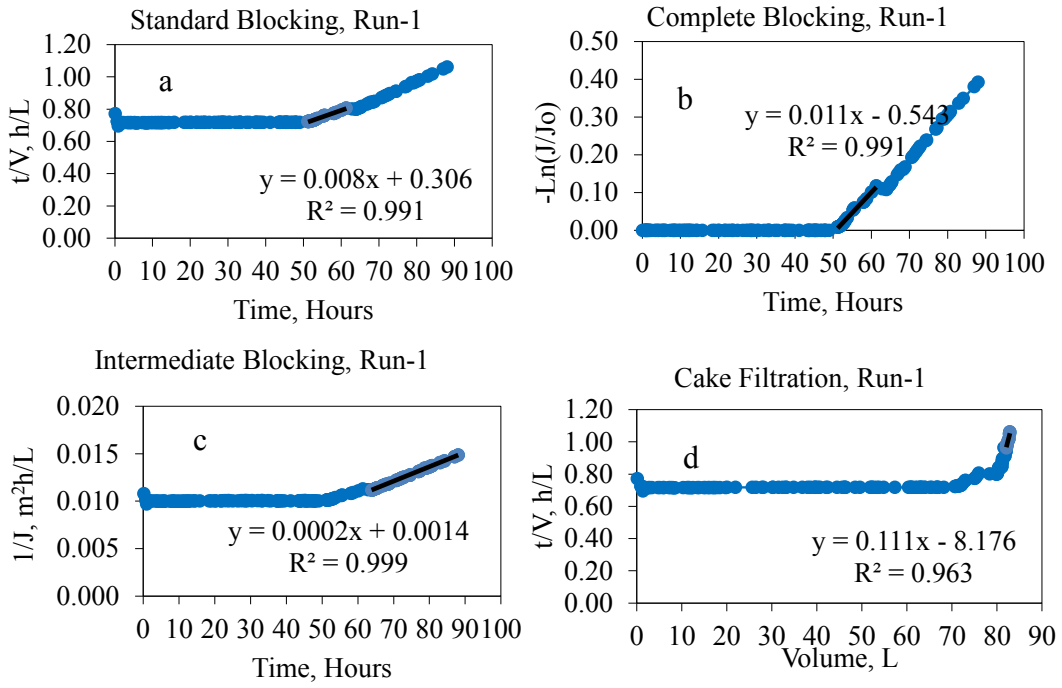


Figure 3.24 Flux decline rate for membrane fouling mechanisms in Run-1 during operation with 40 µm pore size

The particles, having smaller particles than pore size of support layer, deposited within the pores. Moreover, the particles that was similar or larger particle size than pore size of support layer, blocked the pores of support layer at the same time. In the following hours (from 64 hours to 88 hours of operation), the intermediate pore blocking showed the best fit to the experimental data (R^2>0.99). Thus, the particles accumulated on particles that had already blocked the pores of support layer within these hours. In last 9 hours of operation, based on R^2= 0.96, the cake layer filtration occurred. However, the dominant mechanism was almost intermediate pore blocking during the whole operation.

After physical cleaning, blocking mechanisms began earlier and happened faster than run-1. A significant decrease in membrane flux happened after 1 hours of operation in run-2 instead of 51 hours of operation in run-1. The standard blocking (Figure 3.25a) and complete blocking (Figure 3.25b) happened in 5 hours in run-2 whereas, they happened 11 hours in previous run (run-1). Based on R^2>0.98, the intermediate blocking fitted data well from 7 hours to the end of operation whereas in last 7 hours of operation, the cake filtration showed its effect on decline in flux.

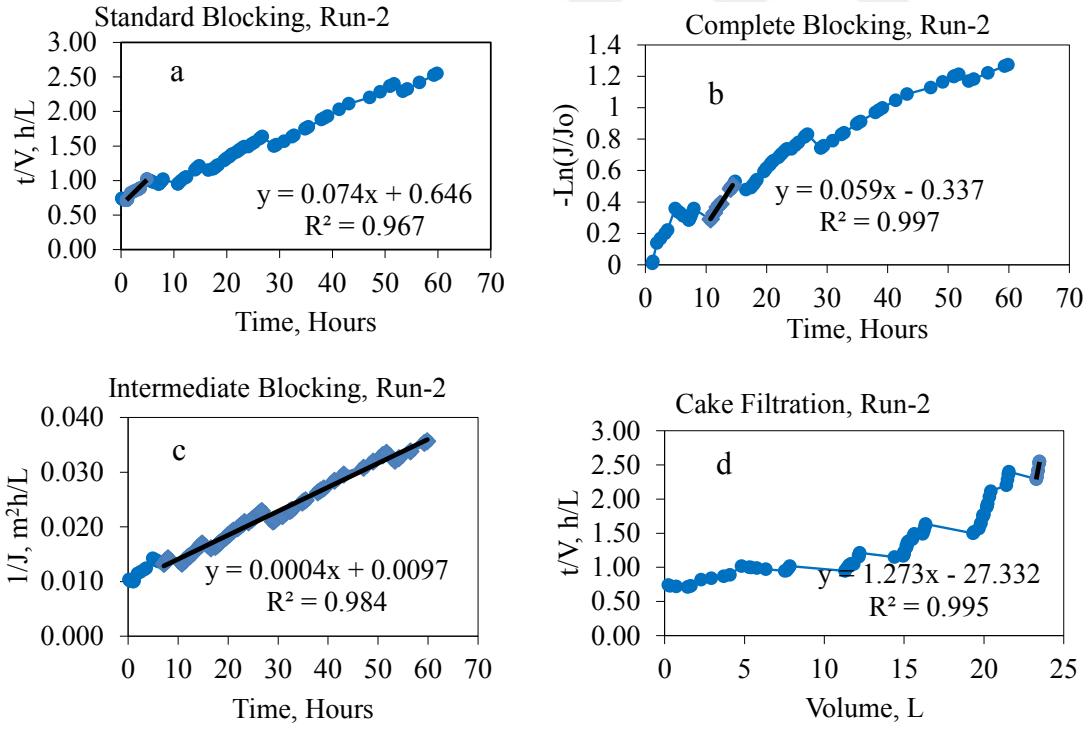


Figure 3.25 Flux decline rate for membrane fouling mechanisms in Run-2 during operation with 40 µm pore size

The dominant mechanism was intermediate pore blocking. As seen in Figure 3.25d, cake filtration mechanism did not fit to the data perfectly. Thus, it seems as if the formation of cake filtration never happened.

To sum up, cake layer filtration was not effective as much as pore blocking mechanisms in formation of DM layer and the dominant mechanism was intermediate blocking mechanism in this experiment. This result is almost similar our previous runs (10, 20, 40 and 70) such that intermediate pore blocking almost dominant mechanism even the filtration was operated under CFV or not. It could be inferred that the application of CFV did not affect the blocking formation mechanism importantly. The intermediate blocking is formed by blocking of pores of support layer and/or deposition of particles on other particles that had already blocked the pores of support layer. The larger particles (such as sludge flocs) enhance cake layer formation. However, the average particle size of feed, coming from UASB effluent, was 35 µm, and they had low EPS, SMP content. Thus, an effective cake layer could not be expected. All these results showed that in contrast to application of CFV, other operation conditions (such as feed characteristics, properties of support layer) had an effect on formation of blocking mechanisms.

3.5.Performance of DM Treatment in Long-Term Operation and Analyzing Characteristics of DM for Dairy Wastewater

In this experiment, 20 µm pore size tubular polyester nylon mesh was integrated into the system for dairy wastewater treatment. In Investigation of Treatment Performance of Synthetic Wastewater and Cheese Whey in UASB and AnDMBR experiment, effective DM was not formed on support layer with 70 µm pore size. In Investigation of the Effect of Pore Sizes on DM Formation Time, and Cleaning Frequency experiment, DM formation time on 20 µm pore size was a little more higher than 10 µm pore size. A quick DM formation was not observed. Therefore, 20 µm pore size tubular nylon mesh was selected as a filter in this experiment. When the effect of CFV on well-formed DM was investigated in previous experiment, it was observed that filtration time prolonged under CFV during operation 40 µm pore size. Thus, CFV was applied to control cake layer thickness for longer filtration operation in this experiment. The filtration operation was done uninterruptedly for 92 days. Filtration performance was evaluated by flux, TMP,

and membrane resistance. During operation COD, SS, VFA and biogas production was done to detect treatment performance. Turbidity was used to indicate DM formation.

3.5.1. Effect of CFV on DM formation

The CFV was changed three times to control cake layer formation on support layer with 20 μm pore size by the combination of increasing and decreasing its value within a wide range. As mentioned below, we studied with lower pore size and higher OLR than some reported AnDMBR studies (Hu et al., 2018a; Yang et al.,2020). Thus, we applied wide range of CFV for continuity of operation. The membrane flux decreased abruptly three times during the DM formation phase. The initial flux was approximately 11 $L/m^2 \cdot h$ (Figure 3.26a). As soon as the AnDMBR was put into operation, a sharp decrease in flux (decline of 25 % in the initial flux in 1 d) was observed on day 2 owing to pore blocking of the support layer by effluent solids (Figure 3.26a). The permeation drag force that was induced by the membrane flux uses force on the particle by way of the water permeating through the membrane (Ramon and Hoek,2012) thereby resulting in both adsorption and deposition of solids on the surface. Thus, this accumulation caused a decrease in flux. The CFV was similar between days 1 and 3, and it increased gradually and reached 54 m/h (day 5) (Figure 3.26b). The reason for the increase in CFV was that it enhanced shear force that caused back-transport of loosely accumulated solids (large particles) on the support material and slowed the membrane fouling. Another reason for the increase in CFV was that it also broke up the large particles (biological floc), thereby generating fine colloids and microbial cells, which formed a denser cake layer on the membrane (Chang et al., 2002).

As the permeability was restored on day 5, the CFV decreased gradually in the following days to accelerate the decrease in effluent turbidity and cause less energy consumption during operation. A high CFV (54.1 m/h) on day 5 broke up the large particles and formed small particles. The CFV decreased gradually to 5 m/h (day 11) from 54 m/h (day 5). The CFV remained at 5 m/h for 2 days. The decrease in CFV diminished back-transport forces. However, it is known that larger particles are subjected to back transport forces more effectively than small particles. In addition to this, shear forces are less effective in particles, which are smaller than the pore of support layer (Wang et al., 2020). It could be inferred that the small particles were less exposed to back transport forces and

deposited over the support layer in the experiment. The decline in flux was observed after day 5. Between day 5 and day 13, the membrane flux gradually declined, which corresponded to a flux reduction of 7%/d.

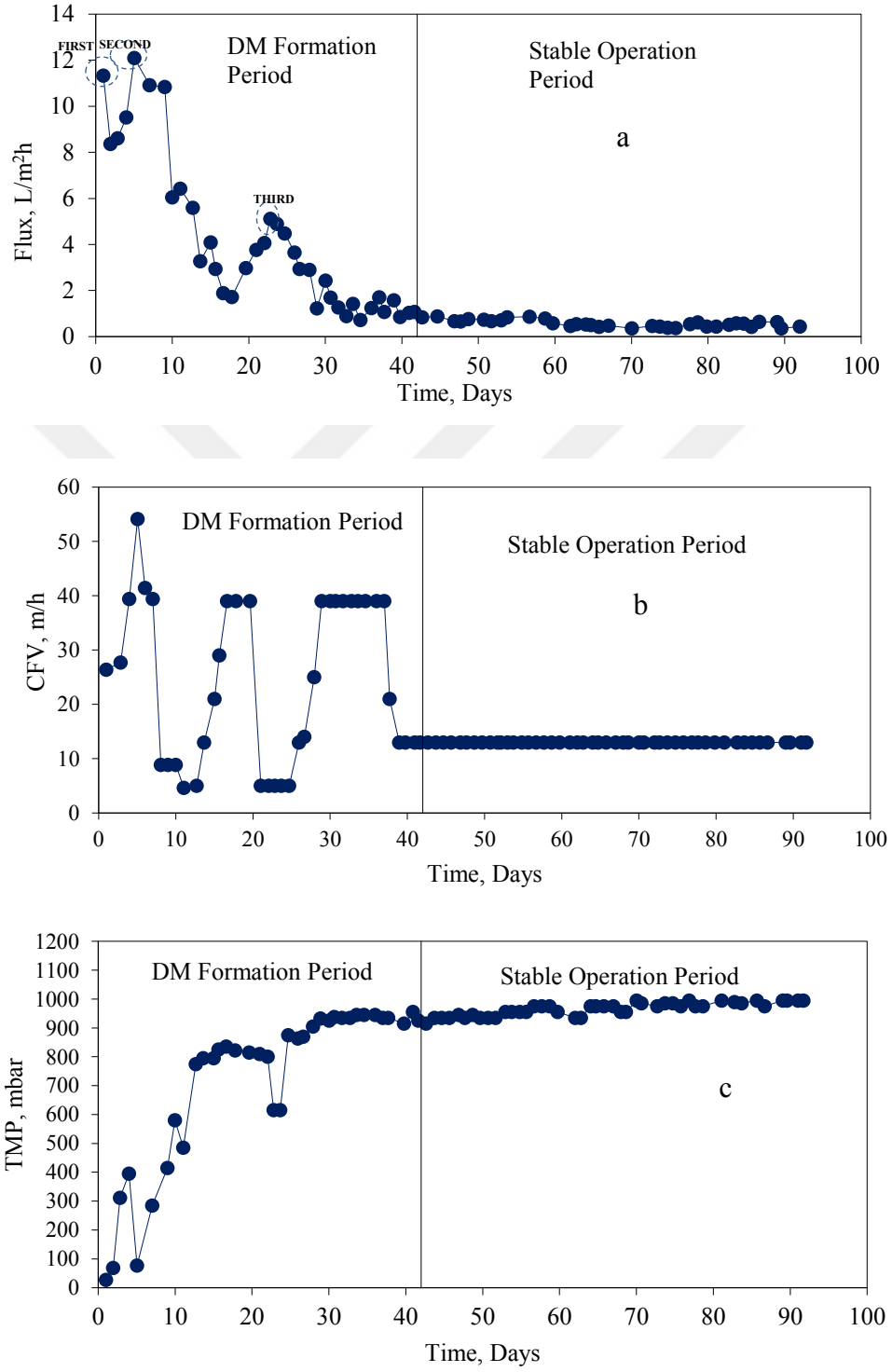


Figure 3.26 Flux (a), CFV (b) and TMP (b) determined during the AnDMBR operation

The second decline in flux was slower than the first. As a result, this procedure (increase followed by decrease in CFV) enhanced the effective cake layer formation. In order to control the flux decline, the CFV increased gradually from 5 m/h (day 13) to 39 m/h (day 17). The CFV remained at this value for more 3 days. A gradual recovery of flux (from 1.71 L/m^2h on day 18 to 5.10 L/m^2h on day 23) was observed. For this period, a limited improve in flux occurred, although the CFV was kept at a high level (39 m/h) between day 17 and day 20. This confirmed that particulates with sizes smaller than the pore size of the support layer had already deposited on the pores and formed a strict gel layer. Thus, even a high CFV was not sufficient to deform this layer, and resulted in a limited increase in flux. This was also a sign of the formation of the cake layer. However, during the periods of increased CFV, turbidity spikes were observed owing to broken solid depositions formed on the support material. Thus, small quantities of accumulated solids on the DM layer were removed. Due to the fact that flux showed increase trend, CFV was decreased after day 20. In order to study low-cost operation and not disturb the DM, the reactor continued to operate at a low CFV of 5 m/h for 5 days. The third decline in membrane flux began after day 23. In order to prevent sudden membrane fouling, the CFV was gradually increased (from 5 m/h on day 25 to 39 m/h on day 29). The CFV was maintained at 39 m/h for 9 d. The membrane flux continued to decrease and became almost stable, and no considerable change in effluent turbidity occurred. The CFV was not as effective as the previous CFVs, and lost its efficiency as the consolidated cake layer was formed. This showed that the CFV lost its effect on membrane permeability. As mentioned by (Alibardi et al.,2014), the consolidated cake layer decreases the effectiveness of the CFV. The CFV was decreased from 39 m/h (day 37) to 13 m/h (day 39). The CFV was maintained at this value until the end of the operational period. The membrane flux continued to decrease at a very slow rate. The membrane flux declined to 1 L/m^2·h on day 42, and continued to decrease very slowly.

The TMP was also manipulated throughout the operational period. The change in CFV affected the TMP similar to the membrane flux. As shown in Figure 3.26c, the TMP increased gradually throughout the operation, except for three times (day 5, day 23, and day 24). The rise in membrane permeability caused a decrease in the TMP on those three days. The TMP increased sharply to 875 mbar on day 25. In the following days, a slight increase in TMP to 925 mbar occurred during the DM formation period.

In the DM application, cake layer formation is a significant factor that determines the flux. Thus, other factors such as biological operational conditions, temperature, and substrate type have less of an effect on the flux (Jeison and van Lier ,2007; Ersahin et al.,2012). It is very important to control the cake layer thickness to obtain efficient solid retention and stable filtration with DM technology. This is because cake layer formation offers solid retention inside the bioreactor but also induces an increase in the filtration pressure (Ersahin et al.,2012). The CFV was found to be very beneficial for cake layer formation. The CFV provided mixing in the reactor and contact between solids (solutes and colloids) and the support layer. However, Hu et al., 2018b reported that CFV is not necessary for DM (75 μm) operation.

The applied CFV was less than 1.8 m/h in UASB integrated DM studies with pore size of 65 μm (Zhang et al.,2011) and 75 μm (Hu et al.,2018b; Yang et al.,2020). This could be due to reactor characteristics. Such that the membrane was integrated into top of UASB reactor in these studies whereas, the membrane was located in narrow membrane compartment in our experiment. The narrow cross-section of the membrane compartment caused high CFV in our experiment. However, Alibardi et al.,2014 performed a low CFV of 1 m/h for cake layer formation in the beginning of operation and increased CFV up to 360 m/h for controlling cake layer thickness and membrane permeability in CSTR integrated DM study. Moreover, there have reported CSTR integrated DM studies where constant CFV was applied (10-30 m/h) (Saleem et al., 2017; Hu et al.,2018a; Saleem et al., 2018).

CFV was carried out in wide range (up to 54 m/h) during DM formation stage and constant CFV (13 m/h) was applied during stable stage in this experiment (Figure 3.26b). CFV in stable stage operation was convenient with reported studies (Hu et al.,2018a). However, CFV was applied in wide range during DM formation stage to control cake layer thickness and membrane permeability. The low CFV induced cake layer formation and high CFV reduced particle size, cause a dense and compact cake layer formation. In addition to this, the recycle, which induced CFV, provide more sludge in suspended in the reactor. Thus, as recycle was increased, more particles overflowed into membrane compartment. This improved solid contact with membrane surface in this experiment.

Moreover, DM forms faster on smaller pore size support material and thus a high pollutant removal can be obtained by a small pore size (Li et al.,2017). A well-developed DM was obtained in our study with a smaller pore size by controlling the effective CFV in wide range. In contrast to the findings of (Hu et al.,2018b), the CFV was understood as an important factor for fertile AnDMBR operation in dairy wastewater treatment. All these results showed that reactor configuration seemed to be important factor for CFV application procedure.

3.5.2. DM formation and the stable operation phase

As the cake layer was formed on the support layer, the filtrated water become cleaner. The turbidity decreased to 31 NTU on day 42 (Figure 3.27). This was called the DM formation period. The permeate flux decreased from 12.1 L/m^2·h to 1.1 L/m^2·h at the end of this period. In the following days, the turbidity became almost stable (25 ± 6 NTU), which indicated that the DM was formed (Rezvani et al.,2014). After DM formation (day 42), the membrane flux continued to decrease more slowly than in the previous period. The membrane flux decreased to 0.5 L/m^2·h on operation day 62. The membrane flux continued at this average value (0.50 ± 0.08 L/m^2·h) from that day (day 62) until the end of the operational period. This period was concluded after 50 d and ended with a membrane flux of 0.43 L/m^2·h. This period was called the stable operational period (Figure 3.26a). In DM application, cake layer permeability is a significant factor that manages the membrane flux. The change in flux during the study confirmed the observations reported by Tang et al.,2017 and Sun et al.,2018. Moreover, the membrane flux was comparable to the value reported by (Jeison et al.,2008), who obtained stable fluxes between 0.5 L/m^2·h and 3.0 L/m^2·h during operation of an AnDMBR with pore sizes of 15 µm and 20 µm, respectively. Satyawali and Balakrishnan, 2008 obtained stable fluxes between 0.8 L/m^2·h and 0.9 L/m^2·h operating a DMBR equipped with a submerged membrane module characterized by a nominal pore size (30 µm).

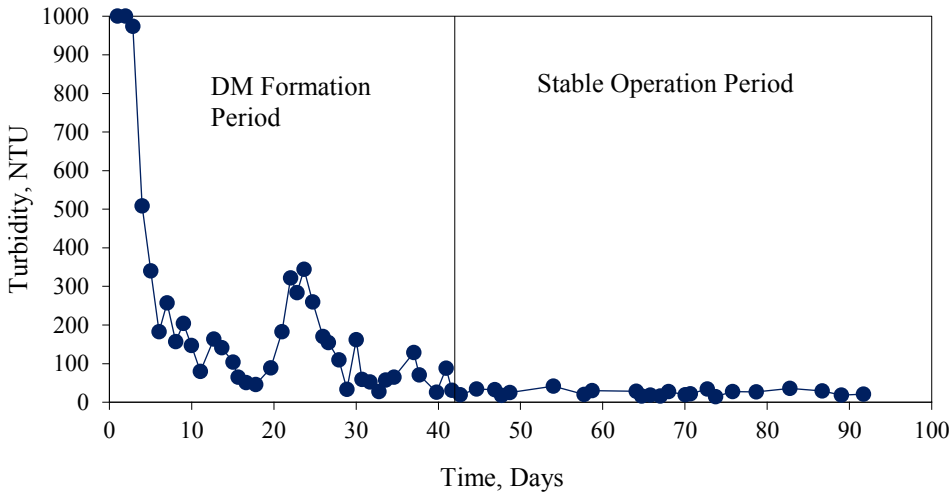


Figure 3.27 Turbidity during the AnDMBR operation

A low flux of 0.1 L/m^2·h was reported by Kooijman et al.,2017 during the operation of a laboratory-scale AnDMBR treating waste activated sludge. The pore size in this experiment was parallel with these reported pore sizes. Li et al., 2017 reported that DMs formed on a larger pore size mesh usually possessed a somewhat greater flux, and the selected pore size had an effect on the filtration flux. In this experiment, we obtained a low flux by using a small pore size.

3.5.3. Membrane resistance

As mentioned in Section 3.5.1, the TMP reached 925 mbar on day 42 owing to the decrease in membrane permeability, and was approximately 964 ± 23 mbar in the stable operational period (Figure 3.26c). The TMP progress in our study validates the TMP profile reported by Ersahin et al.,2014. Our value was higher than those in some previous studies, which were in the range of 20 mbar to 800 mbar (Hu et al.,2018a). This could have been due to the use of a higher loading rate because the accumulation of more solids on the support material could increase the TMP value. Moreover, our value was lower than that in a study conducted by Pillay et al.,1994. The typical operating pressure was reported to be 1000–4000 mbar for MF and 2000–7000 mbar for UF. Our studied DM pressure was lower than those reported in conventional membranes. This showed the advantage of DM operation owing to its low energy cost.

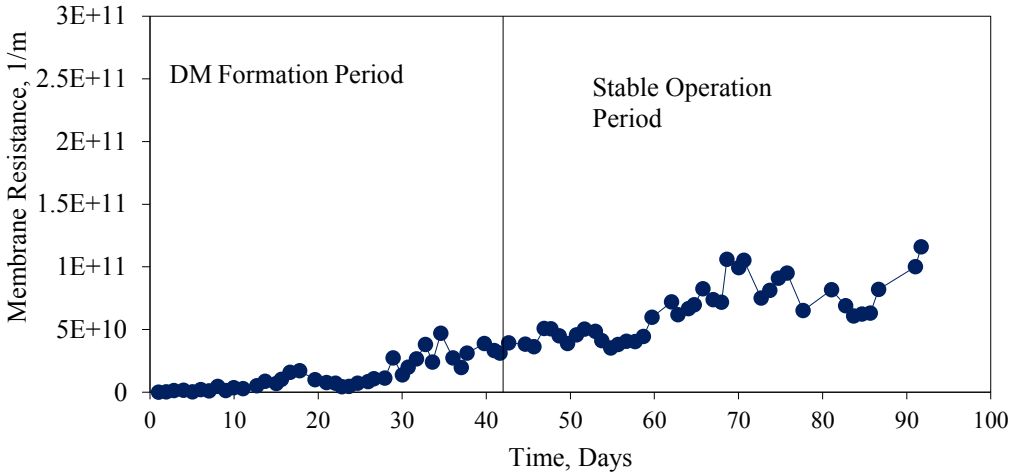


Figure 3.28 Membrane resistance during the AnDMBR operation

The formation time of DM in this experiment was higher than that in some previous studies (Ersahin et al.,2014; Alibardi et al.,2016). This could have been due to the low contact of solids with the support material. As mentioned by Ersahin et al.,2014, the time needed to develop an effective DM layer could be related to the morphology and concentration of the sludge, characteristics of the support material, feed type, and operational conditions. Moreover, membrane resistance is an important indicator for effective cake layer formation. As solutes and colloids were adsorbed and deposited on the support layer, membrane resistance began to increase in the DM formation period and continued to increase in the stable operational period. The membrane resistance reached 4.83×10^{10} 1/m and 1.28×10^{11} 1/m in the DM formation and stable operational periods, respectively (Figure 3.28). The change in CFV caused fluctuations in the TMP and flux until it lost its efficiency in DM operation. After the DM was formed, the membrane resistance improved with a very slow decrease in flux and increase in TMP as a result of the solids accumulation on the DM layer. As mentioned by Sun et al., 2018, the DM filtration resistance was affected by the deposited solid mass. Thus, the slight increase trend in the stable stage was explained by continuity of accumulation of solids on DM. Our membrane resistance values were consistent with (Zhang et al.,2010) (1.1×10^{10}-12.12×10^{11}). Sun et al.,2018 calculated the membrane resistance as 1.73×10^{10} 1/m and 6.68×10^{10} 1/m at the end of DM formation and the end of sustainable flux (30 µm) coupled with CSTR, respectively. The membrane resistance in this experiment was

slightly higher than that found by Sun et al., 2018. This could have been due to the pore size of the studied support material. Membrane resistance is governed by the membrane pore size and membrane surface porosity (Judd, 2006). As the pore size increases, the membrane resistance decreases. Moreover, biomass characteristics (PSD) and operational conditions (HRT) are other important factors for cake resistance (Lin et al., 2013). These factors are inversely proportional to cake resistance. The reported MF/UF membrane resistance was in the range of 10^{11}–10^{14} 1/m (Sun et al., 2018). Thus, as mentioned by (Sun et al.,2018), this lower membrane resistance in the DM shows superiority over other conventional filtration units in terms of the high-energy savings and filterability of the AnDMBR. As a result, it is possible to achieve high efficiency of the DM in wastewater treatment applications, which provides both high organic matter removal and low operating costs.

3.5.4. System treatment performance

The COD concentration both in the reactor (settling part of the reactor) and in the membrane effluent during the operational period are presented in Figure 3.29. In the DM formation period, the COD concentration was approximately 818 mg/L in the membrane effluent and the COD removal efficiency was 85 ± 9 %. From operation days 42 to 92, the COD removal was 99.0 ± 0.6 % (Figure 3.29b). The average COD concentration was 1467 ± 350 mg/L (Figure 3.29a) in the settling zone of reactor, whereas the average COD concentration was 127 ± 31 mg/L in the membrane effluent during the stable operation phase (Figure 3.29b). This showed that the membrane module improved the COD removal in the effluent.

The cake layer formed on the support layer caused both biodegradation in the DM layer and solid retention. As mentioned by Ersahin et al., 2016b, an effective combination of solid retention and biomass activity in the DM layer was liable for the higher COD removal in this system. Organic matter, such as polysaccharides, proteins, and microorganisms (colloidal matter), accumulated on the support layer, and a biofilm formed. The biofilm provided both solid-liquid separation and organic matter removal; thus, it improved the COD removal efficiency. Arceivala and Asolekar,2007, reported an expected COD removal efficiency of 75–85 % with a COD loading rate of 5 kg COD/m^3d and 10 kg COD/m^3d for wastewater treatment by a UASB reactor. A greater amount of

organic matter was removed with a COD loading rate of 8.1 ± 1.5 kg/m^{3}d in this experiment. Elangovan and Sekar, 2012 reported that a UASB reactor could achieve 70–90 % COD removal with 2–15 kg COD/m^3·d and an HRT of 8–50 h during dairy effluent treatment. Thus, in our experiment, COD reduction of dairy processing wastewater was improved by the help of an inexpensive DM module. The obtained COD removal efficiency in this experiment was higher than those reported in AnDMBR studies with higher COD loading rates.

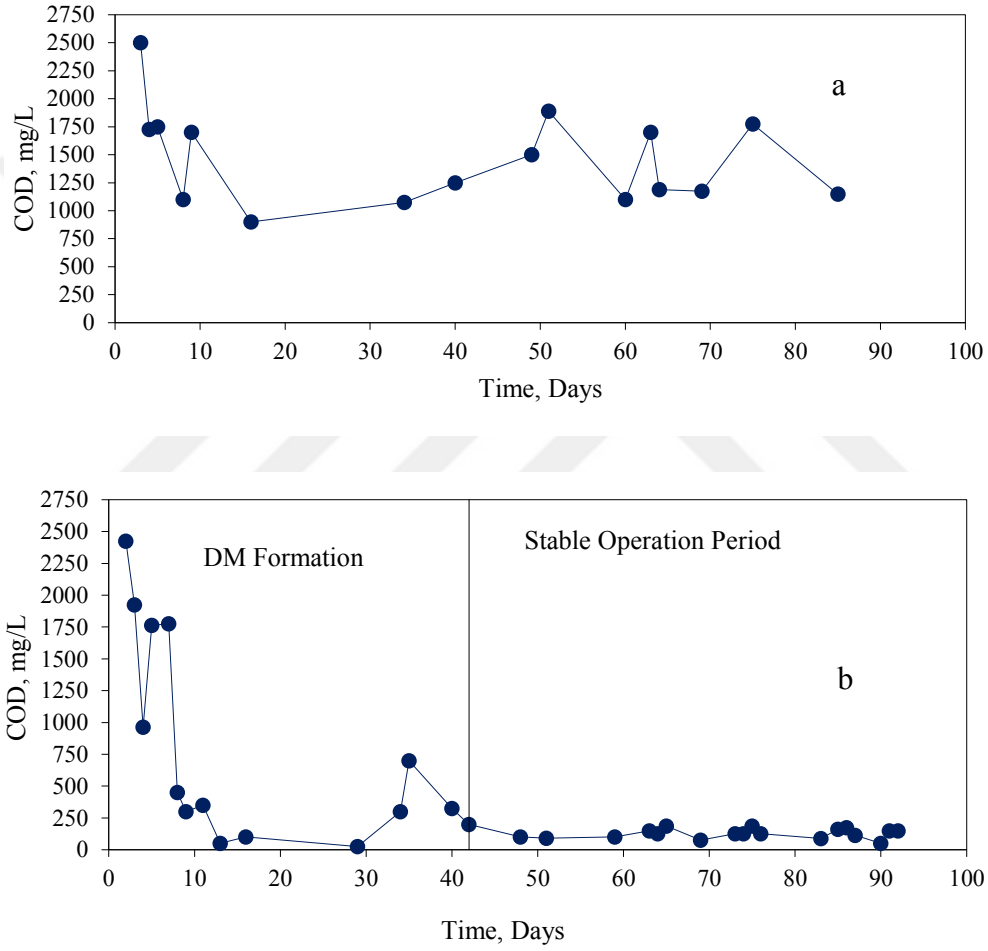


Figure 3.29 COD in the settling zone of the reactor (a) and COD in membrane effluent (b) during the AnDMBR operation

Couras et al., 2015 obtained 81 ± 5 % and 85 ± 6 % COD removal with COD loading rates of 3 kg COD/m^3 and 10 kg COD/m^3, respectively, with two UASB reactors treating diluted semi-skimmed milk. Kundu et al., 2013, achieved 78 % COD removal with a COD loading rate of 2.22–31.00 kg COD/m^3 and HRT of 0.75–5.00 d during simulated milk

treatment by an AFBR. In another study, synthetic dairy wastewater was treated with a COD removal rate of 64–76 %, HRT of 0.5–1.0 d and COD loading rate of 1-2 kg COD/m^3 d by a hybrid AnBR (Zielinska et al., 2013). In comparison to the results of reported dairy wastewater treatment studies, high-strength wastewater (diluted milk) could be treated by only a reactor equipped with a low-cost membrane. This showed the superiority of AnDMBRs over other reactors in terms of their high treatment performance and low operational cost.

Our COD removal efficiency was higher than the reported values for wastewater treatment by DM-coupled UASB systems. Quek et al., 2017, obtained COD removal efficiencies of 71 % (HRT: 6h) and 64 % (HRT: 3h) with OLRs of 1.5 kg COD/m^3·d and 3.0 kg COD/m^3·d during AnDMBR operation, respectively. (Hu et al., 2018b), reported a COD removal efficiency in the range of 72 % and 92 % (HRT:8h) during municipal wastewater treatment with COD loading rates of 0.88, 1.55, and 3.01 kg COD/m^3·d. A COD removal rate of 74.4% (HRT: 8 h), 77.3 % (HRT: 4h), 70.6 % (HRT: 2h) and < 60.4 % (HRT:1h) were obtained by Yang et al.,2020 during domestic wastewater treatment with a COD loading rate of 0.82–6.80 kg COD/m^3·d. Longer HRTs result in higher COD removal rates. Disadvantage of increasing OLR is accumulation of VFA and short HRT may lead to VFA accumulation (Maaz et al.,2019). Thus, we found convenient to study with higher HRT than these reported studies under higher OLRs. Studies have found that DM-coupled CSTR systems obtain COD removal efficiencies higher than 89 % (Hu et al., 2018a; Sun et al., 2018). Until now, COD removal efficiency has exhibited limited performance in DM-coupled UASB systems. In this experiment, high COD removal exceeding 99 % was obtained by a DM-coupled UASB system. This was because internal recycling provided SS and increased contact between the solids and support material. This caused efficient cake layer formation. A well-developed DM caused high organic matter removal in the DM-coupled UASB system. In addition, COD in the membrane effluent met the industrial wastewater effluent discharge regulations in Turkey.

SS concentrations measured in the settling zone of the reactor and membrane effluent are presented in Figure 3.30. At the beginning of the operational period, the initial SS concentration in the membrane effluent was 510 mg/L. The effluent solid concentration began to decrease owing to solid-liquid rejection on the support material. The effluent SS concentration then increased on day 31 with an increase in CFV and decreased to below

50 mg/L with the formation of an effective DM layer in the following days (Figure 3.30b). The effluent SS concentration was maintained at a low level (48 ± 13 mg/L) throughout the stable operation phase. The operation ended with a SS concentration of 27 mg/L in membrane effluent in this experiment.

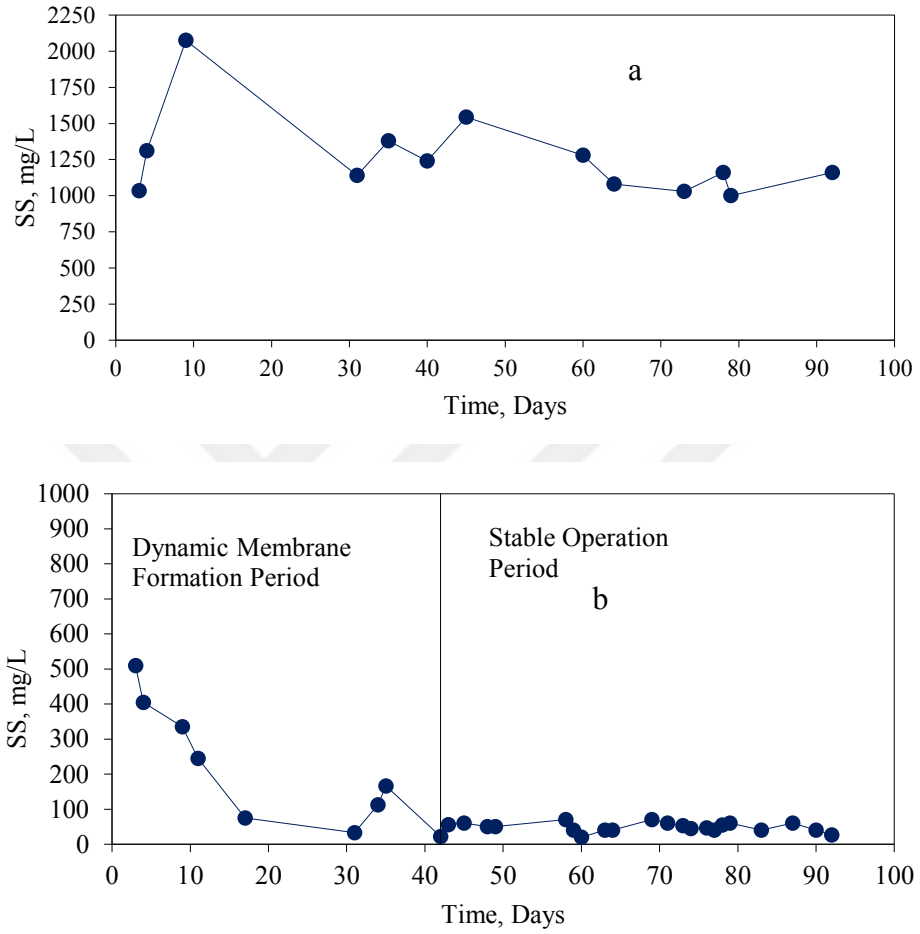


Figure 3.30 Suspended solid concentration in the settling zone of the reactor (a) and Suspended solid concentration in the membrane effluent (b) during the AnDMBR operation

Alibardi et al.,2016 reported an effluent SS concentration of lower than 40 mg/L with a well-formed DM layer at the end of the operational period. Moreover, the effluent SS concentrations were comparable with those of other AnDMBR studies (Hu et al., 2018a). However, as mentioned by Alibardi et al., 2014, we could not obtain absolute SS removal by the AnDMBR in comparison with conventional membrane systems. The SS concentration in the settling zone reactor was measured (1264 ± 289 mg/L) to detect the

effect of DM on the solid retainment in system during the operational period (Figure 3.30a). After DM formation, the DM-coupled UASB removed nearly 99 % of SS. In addition, 96 % of SS in the reactor was retained by well-formed DM. This showed that the DM could attain efficient solid rejections during high-strength wastewater treatment. Studies have reported dairy wastewater treatment by conventional anaerobic processes. Sivakumar and Sekaran, 2015 achieved 86 % SS removal with an HRT of 5.21 d with a UASB reactor treating synthetic milk wastewater. Bhuyar et al., 2015 treated milk wastewater using a UASB reactor with a 75 % SS removal efficiency and an HRT of 24 h. The SRT and HRT in AnDMBRs become completely independent (Hu et al.,2018a). Therefore, a high sludge concentration can be obtained even with a short HRT (Liu et al., 2005).

A high sludge concentration can result in significant solids removal. In addition, escaped solids from the settling zone can be retained by the membrane module. Thus, in our study, higher SS removal was obtained with an HRT of 26 ±2 h. which was lower than that in previously reported studies.

The biogas production was 9.00 ± 2.90 L/d and CH_4 production was 5.03 ± 1.75 L/d with a CH_4 content of 57 % (Figure 3.31a). This value was higher than that in some reported studies (Hu et al., 2018a) owing to operation with a higher COD loading rate. The CH_4 yield in this experiment was in the range of 0.10–0.28 L CH_4/g $COD_{removed}$ (Figure 3.31b). This was lower than the theoretical value of CH_4 yield. This showed that the amount of degraded COD transformed to CH_4 was lower than the amount of COD removed. Ersahin et al.,2014, indicated that up to 40–50 % of the CH_4 could be solubilized in the membrane effluent. The results of our study are consistent with those of AnMBR studies (0.12–0.270 L CH_4/g $COD_{removed}$) (Li et al.,2016). Yang et al.,2020 reported a CH_4 yield in the range of 0.08 L CH_4/g $COD_{removed}$ to 0.12 L CH_4/g $COD_{removed}$ during DM-coupled UASB reactor treatment.

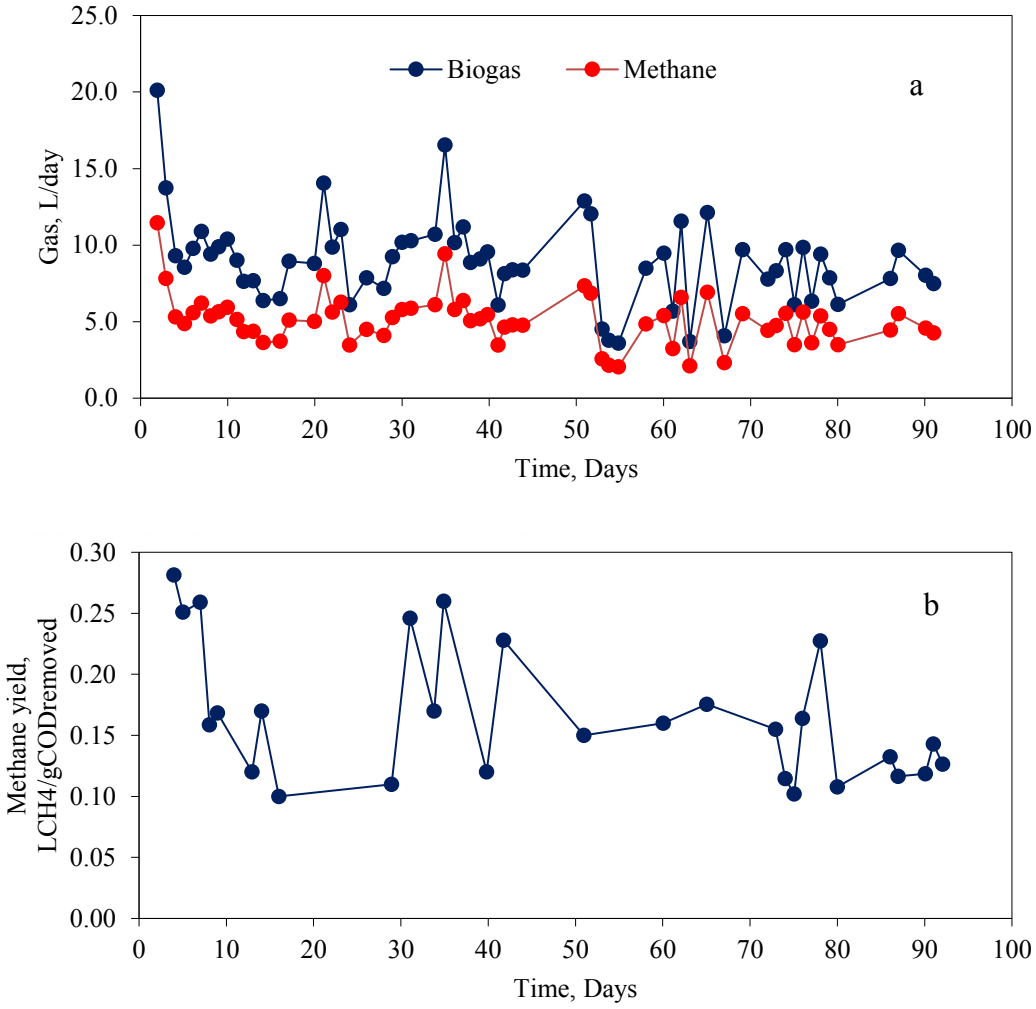


Figure 3.31 Biogas and CH_4 concentration (a) and CH_4 yield (b) in the AnDMBR effluent

The CH_4 yield fluctuated largerly during the operation. Thus, as mentioned by (Alibardi et al., 2014), the effect of negative pressure enforced by the effluent extraction pump on biogas loss through the effluent could be reason of this variation. The VFA effluent concentration was approximately 500 mg/L, and acetic acid was the dominant acid in the beginning of the operational period (first 7 d of operation). The VFA concentration was mostly under detectable limits (< 10 mg/L) and isobutyric acid was detected in the remaining operational period. Owing to the retention of methanogenic microorganisms in the membrane system, VFA was mostly converted into CH_4.

3.5.5. Morphological and chemical characteristics of the DM layer

3.5.5.1.PSD analysis of DM layer

The average particle sizes by volume were approximately 120 µm in the settling zone (Figure 3.32a). These results showed that the sludge particles that had a size larger than the 20 µm pore size support material could easily accumulate on the DM layer and significantly decrease membrane permeation.

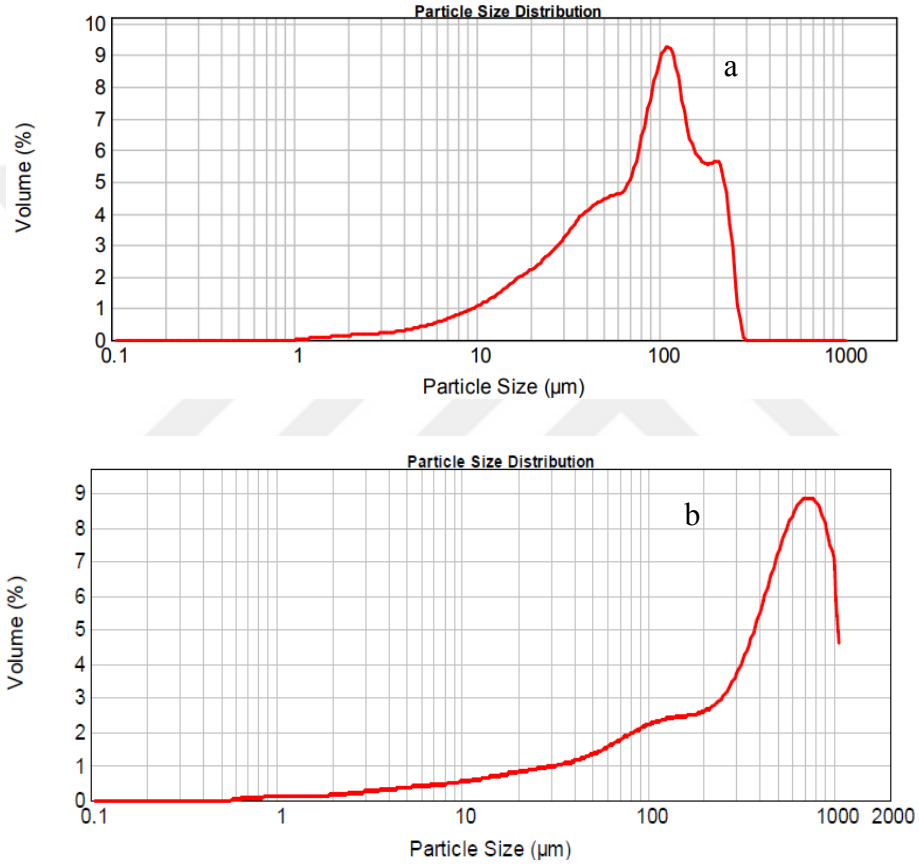


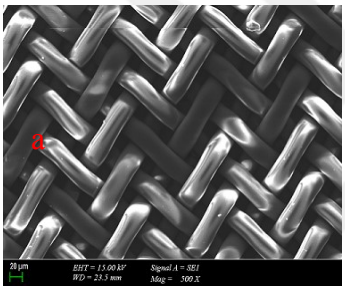
Figure 3.32 PSD of the settling zone of the reactor (a) and DM layer (b)

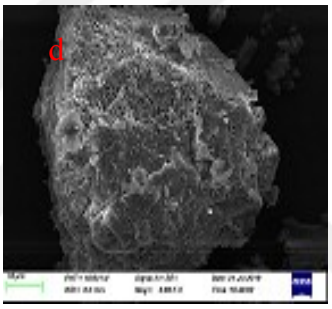
The support material of 20 µm pore size could result in rapid membrane fouling if the CFV and backwash were not applied. This showed the importance of cake layer control in long-term DM operation. Moreover, the medium particle size of the DM by volume were 700 µm pore size in the DM layer (Figure 3.32b). As mentioned above, the average particle sizes by volume were 120 µm in the settling zone of the reactor; thus, particle size on the DM layer was higher than on settling zone. This result was consistent with (Ersahin et al., 2016b). This is due to small particles could stick to each other since metal

ions may act as a bridge between biopolymers, microbial cells and, they formed strick cake layer. As mentioned (Ersahin et al., 2016b), the particle size may increase on support layer owing to this tight adherence.

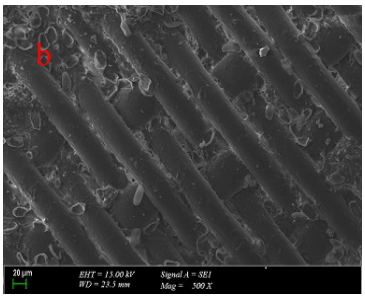
3.5.5.2.SEM-EDX analysis of DM layer

Figure 3.33a presents the SEM micrograph of the virgin layer, gel layer, and DM, and a picture of the DM. SEM images of gel layer (APPENDIX B) are presented in appendix at different magnifications (Mag.). A detailed figure of gel layer and cake layer is also presented in APPENDIX C. The surface of the virgin polyester nylon mesh is presented in Figure 3.33a, demonstrates the smooth structure and porosity of the regularly oriented nylon mesh fibers. C, Ca, P, and O deposited over the support material (Figure 3.33b).

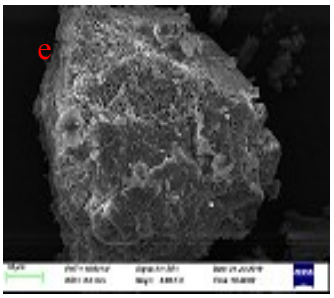




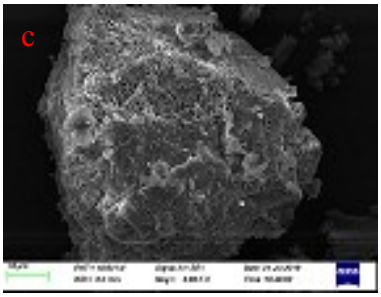
Element	Weight %
C	8.78
Ca	30.50
P	12.77
O	47.95



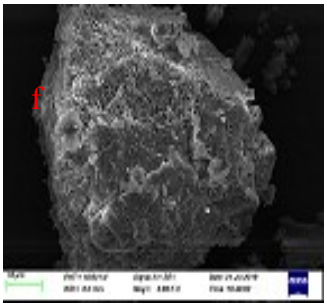
Element	Weight %
C	15.40
Ca	22.90
P	10.10
O	51.60



Element	Weight %
C	61.76
S	2.53
P	8.53
O	27.18



Element	Weight %
C	9.07
Ca	38.53
P	8.00
O	44.40



Element	Weight %
Ca	44.15
P	18.76
O	37.09

Figure 3.33 SEM Photos with EDX analysis (20 µm): Virgin support material (a), Gel layer (b) DM layer in the end of system operation (c, d, e, f)

EDX analysis of gel layer is presented in appendix (APPENDIX D). After the cake layer removed physically, it was observed that the residuals, which forming gel layer, adhered tightly to the support layer surface (Figure 3.33b). SEM analysis of the DM revealed deposition of solids on the DM as result of membrane flux (Figure 3.33c,d,e,f). Elemental analysis was performed to identify the major composition of the cake layer. EDX analysis detected C, Ca, P, O, S elements in selected points of the DM layer (Figure 3.34). The inorganic elements except S were originated from the feed wastewater owing to acting as a source of trace elements for healthy growth of bacteria. The cake layer is formed by interactions of divalent and trivalent cations (such as Ca^{+2}, Mg^{+2}, Fe^{+2}) with biopolymers. The organic foulants can catch metal ions via charge neutralization, and this enhances the formation of the cake layer (Meng et al., 2009). Organic substances and inorganic substances (Ca^{+2}, Mg^{+2}, Fe^{+2}) were responsible for strict cake layer formation in this experiment. It should be noted that Ca, Mg, and Fe elements were detected by ICP-MS. The ionisable groups in biopolymers such as CO_3^{-2}, PO_4^{-} and -OH were detected by FTIR analysis in this experiment.

As mentioned in Introduction (Section 1), these biopolymers catch these metal ions and inorganic fouling happens. As a result of all this, metal ions had a significant effect on the formation of cake layers that could bridge the deposited cells and biopolymers and then formed a dense DM layer. As mentioned above, these determined elements mainly arising from the feed, so the substrate type is significant for inorganic matter accumulation in DM. Thus, as mentioned by (Ersahin et al., 2016b), the amount of inorganic compounds in feed should be taken into account to handle DM control during the operation because these elements cause inorganic matter accumulation and improve cake layer formation.

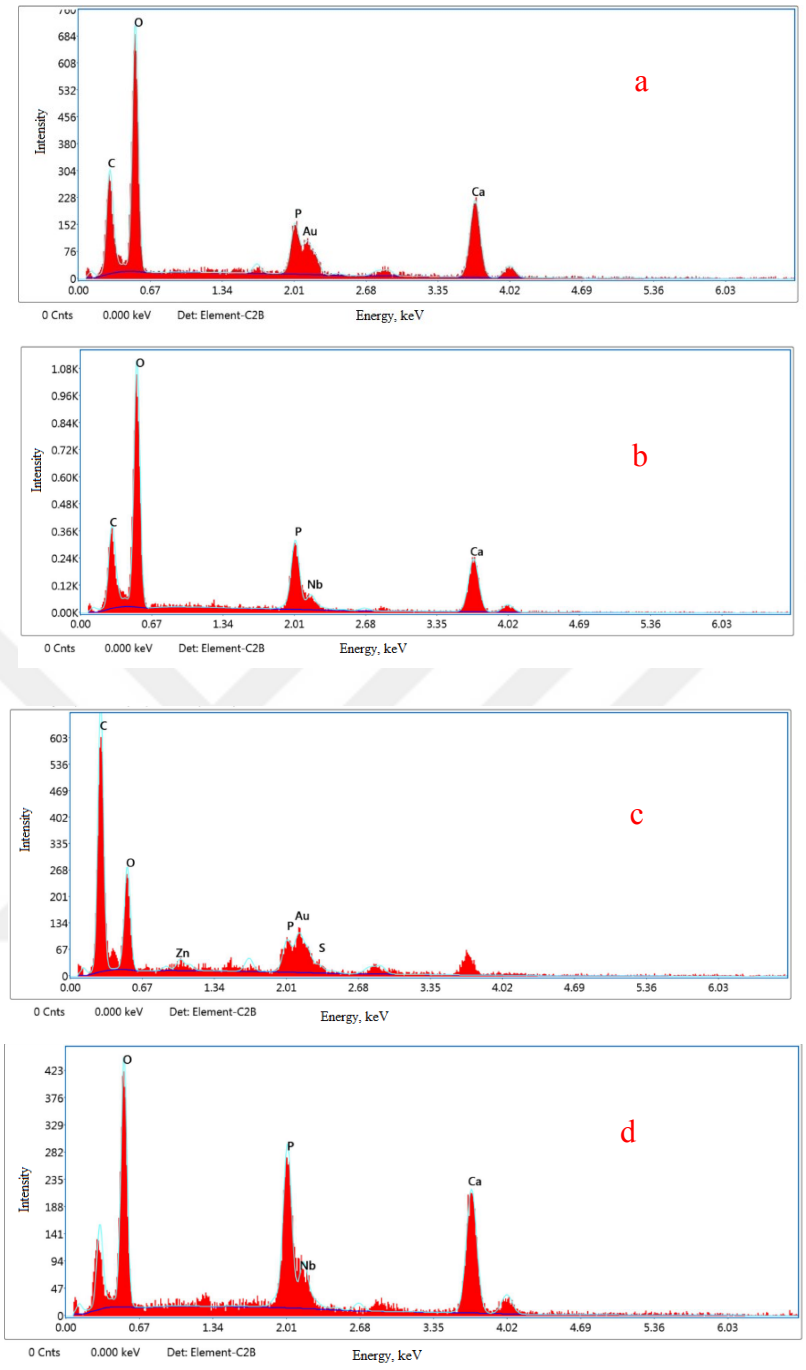


Figure 3.34 EDX analysis of the DM layer(a,b,c,d)

3.5.5.3. FTIR analysis of DM layer

The peak at 3272.6 cm^{-1} demonstrated -OH stretching of polysaccharides (Figure 3.35). In addition to this, the peak at 2920 cm^{-1} showed the presence of aliphatic C-H stretching

(Smidt and Meissl, 2007). The peak at 1629.5 cm^{-1} was in the region of 1700–1600 cm^{-1} in the spectrum, which is unique to the protein secondary structure of amides I (Alvarez et al., 2008). In addition, N-H wagging vibration at 711.6 cm^{-1} showed a secondary amide group (Smidt and Meissl, 2007). The peak at 1415.5 cm^{-1} and the band in the range of 1200 cm^{-1} and 1320 cm^{-1} presented the presence of amides III (C-N stretching and N-H bending) (Ersahin et al., 2016b). The broad peak at 1024 cm^{-1} and the band in the range of 1180 cm^{-1} and 1260 cm^{-1} indicated that the C-O bonds were showed the presence of polysaccharide or polysaccharide-like substances (Ersahin et al.,2016a).

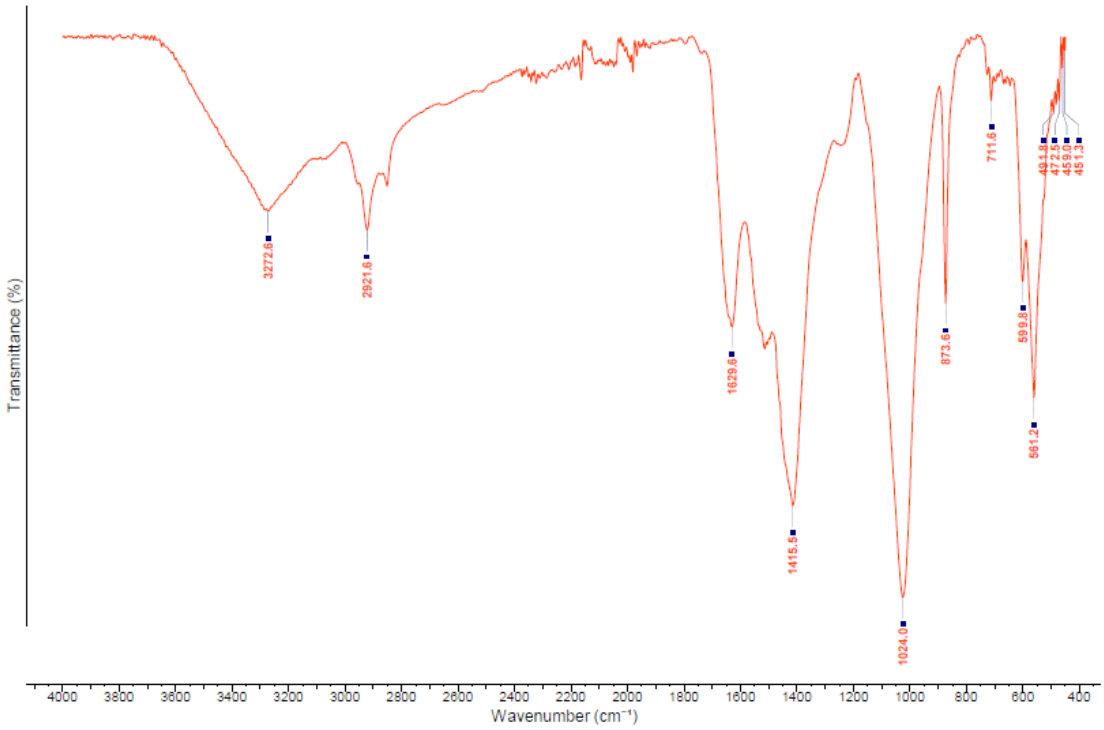


Figure 3.35 FTIR spectrum of DM layer

The results of the FTIR spectrum exhibited the presence of polysaccharide-like substances and proteins in the cake layer (Ersahin et al., 2016b). EPS are biopolymers produced by deposited cells in a membrane (Meng et al., 2017) that consist mainly of polysaccharides, proteins, and DNA (Costa et al., 2018). Taking into account all of this information, the FTIR spectroscopy and SEM results demonstrated the presence of EPS. Polysaccharides have properties such as large-size and gelation behavior. The gelling properties of polysaccharides strongly lead to their fouling tendency. The cross-linked chains in the polysaccharides creates the structure. Such that the gelling properties are

commonly formed by this structure. This gelation can be improved largely in the presence of divalent or multivalent cations due to the fact that these cations can play role as bridges for the carboxyl groups in polysaccharides. The presence of these cations can cause to the formation of impervious gels over the surface of membrane. In addition to this, the interactions between polysaccharides and proteins have high potential of membrane fouling. The protein can stick to the membrane so tightly that it cannot be physically removed (Meng et al., 2017). The peak at 873.6 cm^{-1} represented the carbonate ion. This inferred that the degradation of organic matter into biogas led to the release of inorganic compounds such as Ca, which reacted with carbonate ions and precipitated out (Marcato et al., 2008). Moreover, the sharp peak at 561.2 cm^{-1} was attributed to PO_4^{3-} groups (Mehdikhani and Borhani, 2014). Ca^{+2} and PO_4^{3-} originated from milk. In addition to this, peaks at 599.8, 491.8, 472.5, 459.0, and 451.3 cm^{-1} showed S-S stretching, originating from feed wastewater (Coates, 2006). It could be inferred that the substrate type affected importantly the contents of cake layer.

3.5.5.4.XRD analysis of DM layer

Calcium carbonate ($CaCO_3$) minerals were identified by XRD. The X-ray powder diffraction pattern of DM layer is presented in APPENDIX E. $CaCO_3$ had peaks at 2Θ of 29.70 and 30.94. $CaCO_3$ was found as a result of the reaction between Ca and carbonate in the DM layer. As mentioned by (Ognier et al., 2002), the high alkalinity of the activated sludge (pH = 8–9) could cause the precipitation of $CaCO_3$ in MBRs. That pH in membrane effluent was 8.08 ± 0.52 in our study. The XRD results showed that $CaCO_3$ minerals remained in the membrane during the process of DM formation.

3.5.5.5.ICP-MS analysis of DM layer

Metal ions play a very important role in dense cake layer formation because they make a connection between deposited cells and biopolymers (Meng et al., 2017). It was reported that the cake layer was formed by organic substances and inorganic elements such as Mg, Fe, Ca, etc .(Meng et al., 2009). Thus, the heavy metal ions were investigated in DM. ICP-MS detected 1.16 ± 0.08 % Na, 1.50 ± 0.09 % Mg, 0.76 ± 0.03 % K, 3.34 ± 0.11 % Ca, and 0.40 ± 0.01 % Fe in mass concentration. (Yang et al., 2020; Ersahin et al., 2016b)

were detected similar elements (Na, Mg, K, Ca and Fe) in DM layer. Consequently, the metal ions in the DM were one of the significant causes of the dense cake layer.

4.CONCLUSION

The aim of this thesis is to investigate DM technology applicability for dairy wastewater treatment and to evaluate the effect of operational conditions on the performance of DM formation and operation.

According to this purpose, a submerged AnDMBR was used to treat high-strength synthetic and real industrial wastewater (cheese whey) under anaerobic conditions to attain biogas production in first phase of this thesis. During high-strength synthetic wastewater treatment, AnDMBR with 70 µm obtained COD removal efficiencies of 96% and 78% with COD loading rates of 2.34 and 4.03 and kg/m^3 day, respectively. However, only a fair level of suspended solids removal was obtained AnDMBR with 70 µm in contrast to some reported studies due to slow DM formation on this large pore size support layer. Hence a smaller size, 10 µm pore size nylon mesh was integrated into system afterwards to compare the dynamic membrane formation and treatment performance. AnDMBR with 10 µm obtained 92% and 66% with COD loading rates of 3.16 and 5.02 kg/m^3day. 83% and 88% of suspended solids were removed by AnDMBR with 10 µm during period 1 and period 2, respectively. AnDMBR with 10 µm was used to treat real cheese whey wastewater, resulting in COD removal efficiencies ranging from 59% (4.32 kg/m^3day) to 97% (5.22 kg/m^3day). In addition, 85% of suspended solids were removed from real cheese whey wastewater by AnDMBR with 10 µm. The results show that AnDMBR with 10 µm can be used for treatment of real industrial wastewater successfully in terms of both COD and SS removal. DM pressure was lower than 400 mbar that was advantage of DM in low-cost operation. The AnDMBR produced methane flows in the range of 3.94 ± 1.72 L/day, respectively, during the whole operational period. In addition to this, a methane yield of 0.26 L CH_4/g $COD_{removed}$ was achieved during reactor operation with the AnDMBR. According to the results of the first phase of the thesis, it is understood that the pore size of support layer has an important effect on DM formation such that DM was formed on 10 µm pore size nylon mesh whereas insufficient DM formation happened on 70 µm pore size nylon mesh. Thus, in the second phase of the thesis, the effect of pore size on DM formation and operation was investigated. DM formation time has been significantly shortened by applying an operational flux that was higher than the critical flux determined in this study. The obtained results showed that as pore sizes of support

layer being taken into operation for the first time, decreased, DM formation time became shorter and filtration efficiency got higher. Additionally, after DM formation, support layer lost its original properties and its filtration characteristics became independent of pore size. Moreover, during operation with large pore sizes, cleaning frequency was decreased. Longer continuous operation was provided despite lower effluent quality in the beginning of experiment. Among the sizes tried, 20 μm was found to be optimum pore size considering DM formation time, flux, TMP and treatment performance.

The effects of CFV on a well-formed DM operation were investigated with using 40 μm nylon mesh as support material. The application of CFV resulted in longer DM formation time and filtration time and less cleaning was needed in comparison to previous experiment for 40 μm nylon mesh, which the effect of pore size on DM formation was investigated. During the whole operation, the studies CFV (9-77.52 m/h) was parallel with other reported DM studies and lower than values reported in conventional membranes. Additionally, it was observed that applications of CFV on the surface of membrane, decreased thickness of DM, DM resistance and increased DM formation time. To sum up, the operation of low pore size support material in conjuction with CFV extends clogging time of filter material and enables at low transmembrane pressure. EDX analysis detected Ca, P, O in DM layer such that Ca is one of the important elements, that contributes to effective DM layer formation. This showed that the application of CFV was found to be good at controlling cake layer thickness and feed component was important factor for well-developed DM formation. Moreover, the formation mechanism of DM was expressed by mathematical model. According to results, the combination of blocking mechanisms developed DM at room temperature. However, cake filtration did not fit well to the experimental data due to operational conditions and generally, intermediate pore blocking was almost dominant mechanism for all pore sizes.

In the first phase of the study, insufficient cake layer was formed on large pore size. When the effect of pore size on DM formation time and cleaning frequency were investigated, nylon mesh with 20 μm pore size was found to be convenient for DM formation and operation. Thus, in last phase of this study nylon mesh with 20 μm pore size was integrated into the system. This section includes two phases; DM formation phase and DM operation phase. The DM was formed in 42 d and the operation was continued for more than 50 d after. CFV (5-54 m/h) was applied more effectively than first phase of the

study in order to control permeability and cake layer thickness of DM. This study showed that the application of CFV was a key factor for fertile AnDMBR operation in dairy wastewater treatment. The applied CFV and TMP in this study were lower than those of conventional membranes. This contributed to the low cost of the operation. The COD removal efficiency was 85±9 % in the DM formation period (first 42 d). In the stable operational period, the COD removal improved by more than 10 % owing to the well-developed DM. In addition, DM application under anaerobic conditions not only obtained a high treatment efficiency, but also produced biogas (9.00 ± 2.90 L/d and CH_4 production was 5.03 ± 1.75 L/d), which made it an attractive technology for both the high-strength wastewater treatment and energy recovery. The analysis results showed that organic and inorganic materials such as biopolymers and Ca, P, S, contributed to the formation of a compact/dense cake layer.

All in all, the importance of this thesis and its contribution to the literature are summarized below;

AnDMBR showed high performance during treatment of high-strength synthetic and real industrial wastewater (cheese whey). Thus, DM technology is found to be applicable in dairy wastewater treatment. Taking advantage of anaerobic treatment and DM technology, a good treatment performance and biogas production could be attained with low-cost operation.

The operational conditions (operation mode of membrane, application of CFV, temperature, filtration time, feed characteristics, properties of support layer) are understood as important factor for DM formation and operation. This study shows that a convenient pore size should be selected for effective DM formation and operation in order to obtain good treatment. In addition to this, a well-developed DM and a continuous operation could be obtained by CFV. The type of feed is found to be important factor for compact DM formation. Thus, the wastewater can affect DM formation and system performance.

On account of this study, it is understood that DM technology is an effective method for dairy wastewater treatment. The varied reactor configurations and operation conditions can be developed for further DM applications for wastewater treatment. This DM technology can be improved for large scale applications.

REFERENCES

Abdelrasoul, A., Doan, H., Lohi, A. (2013). Fouling in membrane filtration and remediation, Nakajima, H., Editors.; Mass Transfer - Advances in Sustainable Energy and Environment Oriented Numerical Modeling, (pp.195-218). Intechopen.

Ahmad, T., Aadil, R.M., Ahmed, H., Rahman, V., Soones, B,CV., Souza, S.L.Q., Pimentel, T.C., Scudino, H., Gumaraes, J.T., Esmerino, E.A., Freitas, M.Q., Almada, R.B., Vendamel, S.M.R., Silva, M.C., Cruz, A.G. (2019). Treatment and utilization of dairy industrial wastes: A review. Trends in Food Science and Technology, 88, 361-372.

Ahmed, Z., Cho, J., Lim, B.R., Song, K.G., Ahn, K.H. (2007). Effects of sludge retention time on membrane fouling and microbial community structure in a membrane bioreactor. Journal of Membrane Science, 287, 211–218,

Alavi Moghaddam, M.R., Satoh, H., Mino, T. (2002). Effect of important operational parameters on performance of coarse pore filtration activated sludge process. Water Science and Technology, 46 (9), 229–236.

Alibardi, L., Bernava, N., Cossu, R., Spagni, A. (2016). Anaerobic dynamic membrane bioreactor for wastewater treatment at ambient temperature. Chemical Engineering Journal, 284, 130-138.

Alibardi, L., Cossu, R., Saleem, M., Spagni, A. (2014). Development and permeability of a DM for anaerobic wastewater treatment. Bioresource Technology, 161, 236-244.

Al-Malack, M.H., Anderson, G.K., Almasi, A. (1998). Treatment of anoxic pond effluent using crossflow microfiltration. Water Resource, 32 (12), 3738–3746.

Alvarez, P.A., Ramasway, H.S., İsmail, A.A. (2008). High pressure gelation of soy proteins: effect of concentration, pH and additives. Journal of food engineering, 88, 331-340.

American Public Health Association., Eaton, A.D., American Water Works Association., Water Environment Federation. (2005). Standard methods for the examination of water and wastewater. APHA-AWWA-WEF.

An.Y, Wang, Z., Wu, Z., Yang, D, Zhou, Q. (2009). Characterization of membrane foulants in an anaerobic non-woven fabric membrane bioreactor for municipal wastewater treatment. Chemical Engineering Journal, 155, 709–715.

Arceivala, S.J., Asolekar, S.R. (2007). Wastewater Treatment for Pollution Control and Reuse, 3nd ed., Tata McGraw-Hill Education, New Delhi.

Banu, J.R., Anandan, S., Kaliappan, S, Yeom, I.T. (2008). Treatment of dairy wastewater using anaerobic and solar photocatalytic methods. Solar Energy, 82, 812–819.

Barford, J.P., Cail R G., Callander, I.J., Floyd, E.J. (1986). Anaerobic digestion of high strength cheese whey utilizing semicontinuous digesters and chemical flocculant addition. Biotechnology and Bioengineering, 28, 1601-1607.

Belfort, G., Davis, R.H., Zydney, A.L. (1994). The behavior of suspensions and macromolecular solutions in cross-flow microfiltration. Journal of Membrane Science, 96, 1–58.

Berkessa, Y.W., Yan, B., Li, T., Jegatheersan, V., Zhang, Y. (2020). Treatment of anthraquinone dye textile wastewater using anaerobic dynamic membrane bioreactor: Performance and microbial Dynamics. Chemosphere, 238, 124539.

Bhuyar, K., Suka, S., Dawande, S. (2015). Treatment of milk wastewater using Up flow anaerobic packed bed reactor. Polish Journal of Chemical Technology, 17(2), 84-88.

Boerlage, S.F.E., Kennedy, M.D., Dickson, M.R., El-Hodali, D.E.Y., Schippers, J.C. (2002). The modified fouling index using ultrafiltration membranes (MFI-UF): characterization, filtration mechanisms and proposed reference membrane. Journal of Membrane Science, 197, 1-21.

Bowen, W.R., Calvo, J.I., Hernandez, A. (1995). Steps of membrane blocking in flux decline during protein microfiltration. Journal of Membrane Science, 101, 153–165

Britz, T.J., Van Schalkwyk, C, Hung, Y. (2006). Treatment of dairy processing wastewaters. Taylor and Francis Group, 1-28, https://edisciplinas.usp.br (15.03.2021)

Bruggen, B.V. (2018). Microfiltration, ultrafiltration, nanofiltration, reverse osmosis, and forward osmosis. In Luis, P. (Ed.), Fundamental Modelling of Membrane Systems, Membrane and Process Performance, (p.25-70). Elsevier.

Buffle, J., Leppard, G.G. (1995). Characterization of aquatic colloids and macromolecules.1. Structure and behavior of colloidal material, Environmental Science and Technology, 29, 2169–2175.

Cai, B., Ye, H., Yu, L. (2000). Preparation and separation performance of a dynamically formed MnO_2 membrane. Desalination, 128, 247–256.

Calabro, V., Basile, A. (2011). Fundamental membrane processes, science and engineering, Basile, A., Nuner, S.P. Editors.; Advanced Membrane Science and Technology for Sustainable Energy and Environmental Applications (pp.3-21), Woodhead Publishing Series in Energy.

Cao, D.W., Chu, H.Q., Jin, W., Dong, B.Z. (2010). Characteristics of the biodiatomite dynamic membrane (cake layer) for municipal wastewater treatment. Desalination, 250(2), 544-547.

Carvalho, F., Prazeres, A. R., Rivas, J. (2013). Cheese whey wastewater: characterization and treatment. Science of the Total Environment, 445–446, 385–396.

Casu, S., Crispino, N.A., Farina, R., Mattioli, D., Ferraris, M., Spagni, A. (2012). Wastewater treatment in submerged anaerobic membrane bioreactor. Journal of Environmental Science and Health - Part A. Toxic/Hazardous Substances and Environmental Engineering, 47, 204–209.

Chang, I., Kim, S. (2005). Wastewater treatment using membrane filtration-effect of biosolids concentration on cake resistance. Process Chemistry, 40, 1307-1314.

Chang, In-S., Le Lin Clech, P., Jefferson, B., Judd, S. (2002). Membrane fouling in membrane bioreactors for wastewater. Journal of Enviromental Engineering, 128(11), 1018-1029.

Chang, I.-S., Gander, M., Jefferson, B., Judd, S.J. (2001). Low-cost membranes for use in a submerged MBR. Process Safety and Environmental Protection, 79 (3), 183-188.

Charfi, A., Amar, N.B., Harmand, J. (2012). Analysis fouling of mechanisms in anaerobic membrane bioreactors. Water Research, 46, 2637-2650.

Chen, C., Guo, W., Ngo, H.H., Lee, D., Tung, K., Jin, P., Wang, J., Wu, Y., (2016). Challenges in biogas production from anaerobic membrane bioreactors. Renewable Energy, 98, 120-134.

Chen, J.P., Kim, S.L., Ting, Y.P. (2003). Optimization of membrane physical and chemical cleaning by a statistically designed approach. Journal of Membrane Science, 219, 27-45.

Choo, K. H., Lee, C. H. (1998). Hydrodynamic behaviour of anaerobic biosolids during crossflow filtration in the membrane anaerobic bioreactor. Water Resource, 32, 3387–3397.

Chu, H., Zhang, Y., Zhou, X., Zhao, Y., Dong, B., Zhang, H. (2014). Dynamic membrane bioreactor for wastewater treatment: Operation, critical flux, and dynamic membrane structure. Journal of Membrane Science, 450, 265-271.

Chu, H. Q., Cao, D.W., Jin, W., Dong, B. Z. (2008). Characteristics of bio-diatomite dynamic membrane process for municipal wastewater treatment. Journal of Membrane Science, 325(1), 271-276.

Chu, L., Li, S. (2006). Filtration capability and operational characteristics of dynamic membrane bioreactor for municipal wastewater treatment. Separation and Purification Technology, 51 (2), 173-179.

Coates, J. (2006). Interpretation of Infrared Spectra, A Practical Approach. Meyers, R.A. Editors.; Encyclopedia of Analytical Chemistry, (pp. 10815–10837). John Wiley & Sons Ltd.

Costa, O.Y., Roaijmakers, J.M., Kuramae, E.E. (2018). Microbial extracellular polymeric substances: Ecological function and impact on soil aggregation. Frontiers in Microbiology, 9, 1-14.

Couras, C.S., Louros, V.L., Gamerio, N.A., Silva, A., Capela, M.I., Arroa, L.M., Nadais, H. (2015). Anaerobic degradation of dairy wastewater in intermittent UASB reactors: influence of effluent recirculation. Environmental Technology, 36(17), 2227-2238.

Demirel, B., Yenigun, O., Onay, T.T. (2005). Anaerobic treatment of dairy wastewaters: A review. Process Biochemistry, 40, 2583-2595.

Dereli, R.K., van der Zee, F.P., Ozturk, İ., van Lier, J.B. (2019). Treatment of cheese whey by a cross-flow anaerobic membrane bioreactor: biological and filtration performance. Environmental Research, 168, 109–117.

Dereli, R.K., Loverdou, L., van der Zee, F.P., van Lier, J.B. (2015). A systematic study on the effect of substrate acidification degree and acidogenic biomass on sludge filterability. Water Resource, 82, 94–103.

Dereli, R.K., Ersahin, M.E., Ozgun, H., Ozturk, I., Jeison, D., van der Zee, F., van Lier, J.B. (2012). Potentials of anaerobic membrane bioreactors to overcome treatment limitations induced by industrial wastewaters. Bioresource Technology, 122, 160–170.

Di Benardino, S.E. (2019). Production of biogas/bioSNG from anaerobic pretreatment of milk-processing wastewater substitute. In Materazzi, M., Foscolo, P.U. Editors.; Substitute Natural Gas from Waste, (pp.397-424).Academic Press.

Di Bella, G., Di Trapani, D. (2019). A brief review on the resistance-in-series model in membrane bioreactors (MBRs). Membranes, 9 (2), 24, 1-29.

Dune, R., Cayetano, A., Park, J., Kim, S. (2020). Effect of shear velocity and feed concentration on the treatment of food waste in an anaerobic dynamic membrane Bioreactor: Performance Monitoring and microbial community analysis. Biosource Technology, 296, 122301.

Dvorák, L., Gómez, M., Dolina, J., Černín, A., Dolina, J. (2016). Anaerobic membrane bioreactors—a mini review with emphasis on industrial wastewater treatment: applications, limitations and perspectives. Desalination and Water Treatment, 57 (41), 19062–19076.

Elangovan, C., Sekar, A. (2012). Application of Up flow Anaerobic Sludge Blanket (UASB) Reactor Process for the Treatment of Dairy Wastewater – A Review. Nature Environment and Pollution Technology, 11, 409-414.

El Rayees, Y., Albasi, C., Bacchin, P., Taillandier, P., Mietton-Peuchot, M., Devatine, A. (2012). Analysis of membrane fouling during cross-flow microfiltration of wine. Innovative Food Science and Emerging Technologies, 16, 398-408.

Ersahin, M. E., Ozgun, H., Dereli, R.K., Ozturk, I., Roest, K., van Lier J B. (2012). A review on dynamic membrane filtration: materials, applications and future perspectives. Bioresource Technology,122, 196-206.

Ersahin, M. E., Ozgun, H., Spanjers, H., van Lier, J B. (2013). Effect of Support Material Properties on Dynamic Membrane Filtration Performance. Separation Science and Technology, 48(15), 2263-2269.

Ersahin, M.E., Ozgun, H., Tao, Y., van Lier, J.B. (2014). Applicability of DM technology in anaerobic membrane bioreactors. Water Resource, 48, 420- 429.

Ersahin M E, Gimenez J B, Ozgun H, Tao Y, Spanjers H, van Lier, J B. (2016a). Gas-lift anaerobic dynamic membrane bioreactors for high strength synthetic wastewater treatment: effect of biogas sparging velocity and HRT on treatment performance. Chemical Engineering Journal, 305, 46–53

Ersahin M E, Tao Y, Ozgun H, Spanjers H, van Lier, J B. (2016b). Characteristics and role of dynamic membrane layer in anaerobic membrane bioreactors. Biotechnology and Bioengineering, 113, 761-71.

Ersahin, M. E., Tao, Y., Ozgun, H., Gimenez, J. B., Spanjers, H., van Lier, J. B. (2017). Impact of anaerobic dynamic membrane bioreactor configuration on treatment and filterability performance. Journal of Membrane Science, 526, 387–394.

Fan, B., Huang, X. (2002). Characteristics of a self-forming dynamic membrane coupled with a bioreactor for municipal wastewater treatment. Environmental Science and Technology, 36(23), 5245-5251.

Fernandez, C., Cuetos, M.J., Martínez, E.J, Gomez, X. (2015). Thermophilic anaerobic digestion of cheese whey: coupling H_2 and CH_4 production. Biomass Bioenergy, 81, 55–62.

Field, R. W., Wu, D., Howell, J.A. Gupta B. B. (1995). Critical flux concept for microfiltration fouling. Journal of Membrane Science,100**,** 259-272.

Flemming, H.C., Schaule, G., Griebe, T., Schmitt, J., Tamachkiarowa, A. (1997). Biofouling – the Achilles heel of membrane processes. Desalination ,113 (2–3), 215–225.

Freilich, D., Tanny, G.B. (1978). The formation mechanism of dynamic hydrous Zr(IV)

oxide membrane on microporous supports. Journal of Colloid and Interface Science, 64, 362–370.

Gaddis, J.L., Spencer, H.G., Wilson, S.C. (1979). Separation of materials in dye manufacturing process effluent by hyperfiltration. American Institute of Chemical Engineers symposium series, 75 (190), 156-161.

Gannoun, H., Khelifi, E., Bouallagui, H., Touhami, Y., Hamdi, M. (2008). Ecological clarification of cheese whey prior to anaerobic digestion in up flow anaerobic filter. Bioresource Technology, 99, 6105–6111.

Gao, W.J., Lin H.J., Leung, K.T., Schraft, H., Liao, B.Q. (2011). Structure of cake layer in a submerged anaerobic membrane bioreactor. Journal of Membrane Science, 374,110–120.

Gong, H., Wang, X., Zheng, M., Jin, Z., Wang, K., (2014). Direct sewage filtration for concentration of organic matters by dynamic membrane. Water Science and Technology, 70(8), 1434-1440.

Groves, G.R., Buckley, C.A., Cox, J.M., Kirk, A., MacMillan, C.D., Simpson, M.J. (1983). Dynamic membrane ultrafiltration for the treatment of industrial effluents for water reuse. Desalination 47, 305–312.

Griffiths, I.M., A. Kumar, A., Stewart, P.S. (2014). A combined network model for membrane fouling. Journal of Colloid and Interface Science, 432, 10-18.

Hermia, J. (1982). Constant pressure blocking filtration laws—Application to power-law non-Newtonian fluids. Transaction of The Institution of Chemical Engineers, 60, 183–187.

Ho, J., Sung, S. (2009). Effects of solid concentrations and cross-flow hydrodynamics on microfiltration of ananerobic sludge. Journal of Membrane Science, 345 (1-2), 142-147.

Horng, R. Y., Huang, C., Chang, M.C., Shao, H., Shiau, B.L., Hu, Y.J. (2009). Application of TiO_2 photocatalytic oxidation and non-woven membrane filtration hybrid system for degradation of 4-chlorophenol. Desalination, 245, 619-182.

Hu, Y., Wang, X.C., Tian, W., Ngo, H.H., Chen, R. (2016). Towards stable operation of a dynamic membrane bioreactor (DMBR): Operational process, behavior, and retention effect of dynamic membrane. Journal of Membrane Science, 498, 20-29.

Hu, Y., Wang, C.X., Ngo, H.H., Sun, Q., Yang, Y. (2018a). Anaerobic DM bioreactor (AnDMBR) for wastewater treatment: A review. Bioresource Technology, 247, 1107–1118.

Hu Y, Yang Y, Yu S, Wang X, Tang J. (2018b). Psychrophilic anaerobic dynamic membrane bioreactor for domestic wastewater treatment: Effects of organic loading and sludge recycling. Bioresource Technology, 270, 62-69.

Hu, Y., Zang, Y., Yang, Y., Duan, A., Wang, X.C., Ngo, H.H., Li, Y., Du, R. (2020). Zero-valent iron addition in anaerobic dynamic membrane bioreactors for preconcentrated wastewater treatment: Performance and impact. Science of the Total Environment, 742, 140687.

Huang, C., Liu, H., Meng, S., Liang, D. (2020). Effect of PAC on the behavior of dynamic membrane bioreactor filtration layer based on the analysis of mixed liquid properties and model fitting. Membranes, 10, 420, 1-14.

Igawa, M., Seno, M., Takabashi, A., Yamabe, T. (1977). Reverse osmosis by dynamic membranes. Desalination 22, 281–289.

Ince, O. (1998). Performance of a two-phase anaerobic digestion system when treating dairy wastewater. Water Resource, 32, 2707–2713.

Jaffrin, M.Y. (2011). Hydrodynamic techniques to enhance membrane filtration. The Annual Review of Fluid Mechanics, 44, 77–96.

Jeison, D., van Lier, J.B. (2007). Cake formation and consolidation main factors governing the applicable flux in anaerobic submerged membrane reactors (AnSMBR) treating acidified wastewaters. Separation and Purification Technology, 56, 71-78.

Jeison D, van Lier, J.B. (2008). Feasibility of thermophilic anaerobic submerged membrane bioreactors (AnSMBR) for wastewater treatment. Desalination, 231, 227–235.

Jeison, D., Diaz, I., van Lier, J.B. (2008). Anaerobic membrane bioreactors: Are membrane really necessary? Electronic Journal of Biotechnology, 11(4), 1-9.

Jia, R., Sun, D., Dang, Y., Meier, D., Holmes, D.E., Smith, J.A. (2020). Carbon cloth enhances treatment of high-strength brewery wastewater in anaerobic dynamic membrane bioreactors. Bioresource Technology, 298, 1-7.

Jiraratananon, R., Uttapap, D., Tangamornsuksun, C. (1997). Self-forming dynamic membrane for ultrafiltration of pineapple juice. Journal of Membrane Science, 129, 135–143.

Joshiba, G.J., Kumar, P.S., Femina, C.C., Jayashree, E., Racchara, R., Sivanesan, S. (2019). Critical review on biological treatment strategies of dairy wastewater. Desalination and water treatment, 160, 94-109.

Judd, S. (2006). The MBR Book: Principles and Application of Membrane Bioreactors in Water and Wastewater Treatment. 1st Edition., Elsevier, Amsterdam, Holland.

Karadağ, D., Köroğlu, O.E., Ozkaya, B., Cakmakcı, M., Heaven, S., Banks, C., Sema-Maza, A. (2015a). Anaerobic granular reactors for the treatment of dairy wastewater: A review. International Journal of Dairy Technology, 68(4), 459-470.

Karadağ, D., Köroğlu, O.E., Ozkaya, B., Cakmakcı, M. (2015b). A review on anaerobic biofilm reactors for the treatment of dairy industry wastewater. Process Chemistry, 50, 262-271.

Karthiyen, K., Kandasamy, J. (2009). Up flow anaerobic sludge blanket (UASB) reactor in wastewater treatment. Water and wastewater treatment technologies, 2, 80-198.

Kessler, HG. (1981). Food Engineering and Dairy Technology. Verlag: Freisburg, Germany.

Kırdar, S.S., Karaca, O.B. (2017). An overview of the Turkish dairy sector. Indian Journal of Dairy Science, 70(3), 249-255.

Kim, M.M., Zydney, A.L. (2004). Effect of electrostatic, hydrodynamic, and Brownian forces on particle trajectories and sieving in normal flow filtration, Journal of Colloid and Interface Science, 269, 425–431.

Kishihara, S., Tamaki, H., Fuji, S., Komoto, M. (1984). Clarification of sugar solution through a dynamic membrane formed on a porous ceramic tube. Jonurnal of Membrane Science, 41, 103–114.

Kisielius, V. (2012). (Bio)fouling in cross-flow membrane system investigating the role of transparent exopolymer particles (TEP). Msc Thesis, Wageningen University, Holland, 58.

Kiso, Y., Jung, Y. J., Ichinari, T., Park, M., Kitao, T., Nishimura, K., Min, K. S. (2000). Wastewater treatment performance of a filtration bio-reactor equipped with a mesh as a filter material. Water Resource, 34(17), 4143-4150.

Kiso, Y., Jung, Y.J., Min, K.S., Wang, W., Simase, M., Yamada, T., Min, K.S. (2005). Coupling of sequencing batch reactor and mesh filtration: operational parameters and wastewater treatment performance. Water Resource, 39, 4887–4898.

Kooijman, G., Lopes, W., Zhou, Z., Guo, H., de Kreuk, M., Spanjers, H., van Lier, J. (2017). Impact of Coagulant and Flocculant Addition to an Anaerobic Dynamic Membrane Bioreactor (AnDMBR) treating waste-activated sludge. Membranes, 7 (2), 18.

Kundu, K., Bergmam, I., Hanke, S., Klocke, M., Shanma, S., Sreekrishran, T. (2013). Carbon source- a strong determinant of microbial community structure and performance of an anaerobic reactor. Journal of biotechnology, 168(4), 616-624.

Le Clech, P., Jefferson, B., Chang, I. S., Judd, S. J. (2003). Critical flux determination by the flux-step method in a submerged membrane bioreactor. Journal of Membrane Science, 227, 81-93.

Le Clech, P., Chen, V., Fane, T. A.G. (2006) Fouling in membrane bioreactors used in wastewater treatment. Journal of Membrane Science, 284, 17-53.

Lee J, Ahn W Y, Lee C H . (2001). Comparison of the filtration characteristics between attached and suspended growth microorganisms in submerged membrane bioreactor. Water Resource, 35, 2435-2445.

Leitao, R.C., Santaellla, S.T., van Haadal, A.C., Zeeman, G., Lettinga, G. (2006). The effects of hydraulic and organic shock loads on the robustness of up flow sludge blanket reactors treating sewage. Water Science and Technology, 54(2), 49-55.

Li N, Hu Y, Lu Y, Zeng R J, Sheng G. (2016). In-situ biogas sparging enhances the performance of an anaerobic membrane bioreactor (AnMBR) with mesh filter in low-strength wastewater treatment. Applied Microbiology and Biotechnology, 100(13), 6081-6089

Li, L., Xu, G., Yu, H. (2017). Dynamic membrane filtration: Formation, filtration, cleaning and applications. Chemical Engineering and Technology, 41(1), 7-18.

Li, L., Xu, G., Yu, H., Xing, J. (2018). Dynamic membrane for micro-particle removal in wastewater treatment: Performance and influencing factors. Science of the Total Environment, 627, 332-340.

Liao, B.Q., Bagley, D.M., Kraemer, H.E., Leppard, G.G., Liss, S.N. (2004). A review of biofouling and its control in membrane separation bioreactors. Water Environment Research 76 (5), 425–436.

Lin, H. J., Xie, K., Mahendran, B., Bagley, D.M., Leung, K. T., Liss, S.N., Liao, B.Q. (2009). Sludge proporties and their effects on Blocking in submerged anaerobic membrane bioreactors (SAnMBRs). Water Resource, 43, 3827-3837.

Lin, H.J., Xie, K., Mahendran, B., Bagley, D. M., Leung, K. T., Liss, S. N., Liao, B.Q. (2010). Factors affecting sludge cake formation in a submerged anaerobic membrane bioreactor. Journal of Membrane Science, 361, 126-134.

Lin H, Peng W, Zhang M, Chen J, Hong H, Zhang Y. (2013). A review on anaerobic membrane bioreactors: applications, membrane fouling and future perspectives. Desalination, 314, 169–188.

Liu, H., Fang, H.H.P. (2002). Extraction of extracellular polymeric substances (EPS) of sludges. Journal of Biotechnology, 95, 249-256.

Liu, R., Huang, X., Chen, L., Wen, X., Qian, Y. (2005). Operational performance of a submerged membrane bioreactor for reclamation of bath wastewater. Process Biochemistry, 40(1), 125-130.

Liu, H., Yang, C., Pu, W., Zhang, J. (2009). Formation mechanism and structure of dynamic membrane in the dynamic membrane bioreactor. Chemical Engineering Journal, 148, 290-295.

Liu, Y., Lui, Haining, Cui, L., Zhang, K. (2012). The ratio of food-to-microorganism (F/M) on membrane fouling of anaerobic membrane bioreactors treating low-strength wastewater. Desalination, 297, 97-103

Liu, H., Wang, Y., Yin, B., Zhu, Y., Fu, B., Liu, H. (2016). Improving volatile fatty acid yield from sludge anaerobic fermentation through self-forming DM separation. Bioresource Technology, 218, 92-100.

Ma, J., Wang, Z., Zou, X., Feng, J., Wu, Z., 2013. Microbial communities in an anaerobic dynamic membrane bioreactor (AnDMBR) for municipal wastewater treatment: Comparison of bulk sludge and cake layer. Process Biochemistry, 48 (3),510–516.

Maaz, M., Yasin, M., Aslam, M., Kumar, G., Atabari, A.E., Idrees, M., Anjum, F., Jamil, F., Ahmad, R., Khan, A.L., Lesage, G., Heran, M., Kim, J. (2019). Anaerobic membrane bioreactors for wastewater treatment: Novel configurations. Bioresource Technology, 283, 358-372.

Machado, R. M. G., Freire, V. H., Silva, P. C., Figuerêdo, D. V., Ferreira, P. E. (2002). Environmental Control in Small and Medium-Sized Dairy Industry (Controle ambiental nas pequenas e médias indústrias de laticínios) Segrac: Belo Horizonte, MG, p. 223 (In Portuguese).

Mackley, M.R., Sherman, N.E. (1992). Cross-flow cake filtration mechanisms and kinetics. Chemical Engineering Science, 47(12), 3067-3084.

Mahat, S.M., Omar, R., Idris, A., Kamal, S., Idris, A. (2018). Dynamic membrane applications in anaerobic and aerobic digestion for industrial wastewater: A mini review. Food and Bioproducts Processing, 112, 150-168.

Mallamace, F., Corsano, C., Mallamace, D., Vasi, C., Dugo, G. (2014). The role of water in protein's behavior: The two dynamical crossovers studied by NMR and FTIR techniques. Computational and Structural Biotechnology Journal, 13, 33-37.

Marcato, C.E., Mohtar, R., Revel, J.C., Poliech, P., Hafidi, M., Guirresse, M. (2008). Impact of anaerobic digestion on organic matter quality in pig slurry, International Biodeterioration and Biodegradation, 63, 260-266.

Marcinkowsky, A.E., Kraus, K.A., Phillips, H.O., Johnson, J.S., Shor, A.J. (1966). Hyperfiltration studies IV. Salt rejection by dynamically formed hydrous oxide membranes. Journal of the American Chemical Society, 88 (24), 5744–5750.

Martin-Garcia I, Monsalvo V, Pidou M, Le Clech P , Judd S. J., McAdam E. J., Jefferson, B. (2011). Impact of membrane configuration on fouling in anaerobic membrane bioreactors. Journal of Membrane Science, 382**,** 41–49.

Massé, A., Spérandio, M., Cabassud, C. (2006). Comparison of sludge characteristics and performance of a submerged membrane bioreactor and an activated sludge process at high solids retention time. Water Research, 40(12), 2405-2415.

McCarty, P.L., Bae, J., Kim, J. (2011). Domestic wastewater treatment as a net energy producer-can this be achieved? Environmental Science and Technology, 45 (17), 7199–17106.

Meng, F., Zhang, H., Yang, F., Liu, L. (2007). Characterization of cake layer in submerged membrane bioreactor. Environmental Science and Technology, 41, 4065-4070.

Meng, F., Chae, S.R., Drews, A.,Kramue, M., Shin, H.S., Yang, F. (2009). Recent advances in membrane bioreactors (MBRs): Membrane fouling and membrane material. Water Resource, 43, 1489-1512.

Meng, F., Wang, Y., Huang, L.N., Li, J., Jiang, F., Li, S., Chen, G.H. (2013). A novel nonwoven hybrid bioreactor (NWHBR) for enhancing simultaneous nitrification and denitrification. Biotechnology and Bioengineering, 110 (7), 1903–1912.

Meng, F., Zhang, S., Oh, Y., Zhou, Z., Shin, H.S., Chae, S.R. (2017). Fouling in membrane bioreactors: An updated review. Water Resource, 114, 151-180.

Najafpour, G.D., Hashemiyeh, B.A., Asadi, M., Ghasemi, M.B. (2008). Biological treatmentof dairy wastewater in an up flow anaerobic sludge-fixed film bioreactor. American-Eurasian Journal of Agricultural and Environmental Sciences, 4, 251–257.

Ng, C.Y., Mohammad, A.W., Ng, L.Y., Jahim, J. (2014). Membrane fouling mechanisms during ultrafiltration of skimmed coconut milk. Journal of Food Engineering, 142, 190-200.

Odlum, C.A. (1990). Reducing the BOD level from a dairy processing plant. Proceedings 23rd International Dairy Congress, October, Montreal, Canada.

Ognier, S., Wisniewski, C., Grasmick, A. (2002). Characterization and modeling of fouling in membrane bioreactors. Desalination, 146 (1-3),141-147.

Park, J.H., Anburajan, P., Kumar, G., Park, H.D., Kim, S.H. (2017). Biohydrogen production integrated with an external dynamic membrane: A novel approach. The International Journal of Hydrogen Energy, 1-7.

Pillay, V.L., Townsend, C.A., Buckley, C.A. (1994). Improving the performance of anaerobic digesters at wastewater treatment works: the coupled cross-flow microfiltration/digester process. Water Science and Technology, 30 (12), 329–337.

Polprasert C, Koottatep T. (2017). Organic waste recycling: Technology, management and sustainability. 4th Edition, IWA Publishing, London.

Poostchi, A.A., Mehrniac, M.R., Rezvani, F. (2015). Dynamic membrane behaviours during constant flux filtration in membrane bioreactor coupled with mesh filter. Environmental Technology, 36(14), 1751-1758.

Prazeres, A.R., Carvalho, F., Rivas, J. (2012). Cheese whey management: A review. Journal of Envrionmental Management, 110, 48-68.

Quek, P. J., Yeap, T.S., Ng, H.Y. (2017). Applicability of up flow anaerobic sludge blanket and DM-coupled process for the treatment of municipal wastewater. Applied Microbiology and Biotechnology, 101, 6531–6540.

Ramesh, A., Lee, D.J., Lai, J.Y. (2007). Membrane biofouling by extracellular polymeric substances or soluble microbial products from membrane bioreactor sludge. Applied Microbiology and Biotechnology, 74, 699–707.

Ramon, G.Z., Hoek, E.M.V. (2012). On the enhanced drag force induced by permeation through a filtration membrane. Journal of Membrane Science, 392-393,1-8.

Rezvani, F., Mehrnia, M. R, Pootschi, A.A. (2014). Optimal operating, strategies of SFDM formation for MBR application. Separation and Purification Technology, 124, 124-133.

Ribero-Pi, J., Campitelli, A., Badia-Fabregat, M., Jubany, I., Martinez-LIado, X., McAdam, E., Jefferson, B., Soares, A. (2020). Hydrolysis and methanogenesis in UASB-AnMBR treating municipal wastewater under psychrophilic conditions: Importance of reactor configuration and inoculum. Frontiers in Bioengineering and Biotechnology, 8, 1-14.

Rico, C., Munoz, N., Fernandez, J., Rico, J.L. (2015). High-load anaerobic co-digestion of cheese whey and liquid fraction of dairy manure in a one-stage UASB process: Limits in co-subtrates ratio and organic loading rate. Chemical Engineering Journal, 262, 794-802.

Sabaghian, M., Mehrnia, M.R., Esmaieli, M. Nourmohammadi, D. (2018). Influence of static mixer on the formation and performance of dynamic membrane in a dynamic membrane bioreactor. Separation and Purification Technology, 206, 324-334.

Sadr, S.M.K., Saroj, D.P. (2015). Advances in Membrane Technologies for Water Treatment. Membrane technologies for municipal wastewater treatment. Materials, Processes and Applications Woodhead Publishing Series in Energy, 443,463.

Sahinkaya, E., Yurtsever, A., Cinar, O. (2017). Treatment of textile industry wastewater using dynamic membrane bioreactor: Impact of intermittent aeration on process performance. Separation and Purification Technology, 174, 445-454.

Salazar-Pelaez, M., Morgan-Sagastume, J.M., Noyolan, A. (2015). Fouling layer characterization and pore-blocking mechanisms in an UF membrane externally coupled to a UASB reactor, Water S.A., 43(4), 573-580.

Saleem M, Alibardi L, Lavagnolo M C, Cossu R, Spagni A. (2016). Effect of filtration flux on the development and operation of a dynamic membrane for anaerobic wastewater treatment. Journal of Environmental Management, 180, 459–465.

Saleem, M., Alibardi, L., Cossu, R., Lavagnolo, M. C., Spagni, A. (2017). Analysis of fouling development under dynamic membrane filtration operation. Chemical Engineering Journal, 312, 136-143.

Saleem, M., Lavagnolo, M.C., Spagni, A. (2018). Biological hydrogen production via dark fermentation by using a side-stream dynamic membrane bioreactor: Effect of substrate concentration. Chemical Engineering Journal, 349, 719-727.

Salerno, C., Vergine, P., Berardi, G., Pollice, A. (2017). Influence ofair scouring on the performance of a Self Forming DynamicMembrane BioReactor (SFD MBR) for municipal wastewatertreatment. Bioresource Technology, 223, 301–306.

Satyawali, Y., Balakrishnan, M. (2008). Treatment of distillery effluent in a membrane bioreactor (MBR) equipped with mesh filter. Separation and Purification Technology, 63(2), 278-286.

Seghezzo L., Zeeman, G., van Lier, J. B., Hamelers, H.V. M., Lettinga, G. (1998). A review: the anaerobic treatment of sewage in UASB and EGSB reactors. Bioresource Technology, 65, 175-190.

Seo, G.T., Moon, B.H., Lee, T.S., Lim, T.J., Kim, I.S. (2002). Non-woven fabric filter separation activated sludge reactor for domestic wastewater reclamation. Water Science and Technology, 47(1), 133-138.

Siddiqui, M.A., Dai, J., Guan, D., Chen, G. (2019). Exploration of the formation of self-forming dynamic membrane in an up flow anaerobic sludge blanket. Separation and Purification Technology, 212, 757-766.

Siddiqui, M.A., Biswal, B.K., Saleem, M., Guan, D., Iqbal, A., Wu, D., Khanal, S.K., Chen, G. (2021). Anaerobic self-forming dynamic membrane bioreactors (AnSFDMBRs) for wastewater treatment-Recent advances, process optimization and perspectives. Bioresource Technology, 125101 (*In press*).

Sivakumar, R., Sekaran, V. (2015). Comparative study of performance evaluation of UASB reactor for treating synthetic dairy effluent at psychrophilic and mesophilic temperatures. Nature Environment and Pollution Technology, 14(3), 679-684.

Smidt, E., Meissl, K. (2007). The applicability of Fourier transform infrared (FT-IR) spectroscopy in waste management. Waste Management, 27, 8-276.

Smith A L, Skerlos S J, Raskin L. (2013). Psychrophilic anaerobic membrane bioreactor treatment of domestic wastewater. Water Resource, 47(4),1655–1665.

Strydom, J.P., Britz, T.J., Mostert, J.F. (1997). Two-phase anaerobic digestion of three different dairy effluents using a hydrid bioreactor. Water SA, 23, 151-156.

Song, L., Elimelech, M. (1995). Theory of Concentration Polarization in Crossflow Filtration. Journal of the Chemical Society, Faraday Transactions, 91(19), 3389-3398.

Sun, F., Zhang, N., Li, F., Wang, X., Zhang, J., Song, L., Liang, S. (2018). Dynamic analysis of self-forming DM (SFDM) filtration in submerged anaerobic bioreactor: Performance, characteristic, and mechanism. Bioresource Technology, 270, 383–390.

Tang, J., Wang, X.C., Hu, Y. Ngo, H.H., Li, Y. (2017). DM-assisted fermentation of food wastes for enhancing lactic acid production. Bioresource Technology, 234, 40-47.

Tanny, G.B., Johnson Jr., J.S. (1978). The structure of hydrous Zr(IV) oxidepolyacrylate membranes: poly(acrylic acid) deposition. Journal of Applied Polymer Science, 22, 289–297.

Vela, M. C.V., Blancoa, S. Á., García, J. L., Rodríguez, E. B. (2008). Analysis of membrane pore blocking models applied to the ultrafiltration of PEG. Separation and Purification Technology, 62, 489-498.

Vidal, G., Carvalho, A., Mendez, R., Lema, J.M. (2000). Influence of the content in fats and proteins on the anaerobic biodegradability of dairy wastewaters. Biosource Technology, 74, 231-239.

Waktole, Y., Yan, B., Li, T., Jegatheesan, V., 2020. Treatment of anthraquinone dye textile wastewater using anaerobic dynamic membrane bioreactor: Performance and microbial dynamics. Chemosphere 238, 124539.

Walker, M., Banks, C.J., Heaven, S. (2009). Development of a coarse membrane bioreactor for two-stage anaerobic digestion of biodegradable municipal solid waste. Water Science and Technology, 59 (4), 729–735.

Wang, S., Rao, N.C., Qiu, R., Molett, R. (2009). Treatability and kinetic analysis of anaerobicmoving bed biofilm reactor treating high strength milk permeate. Desalination and Water Treatment, 4, 1–3.

Wang, L., Liu, H., Zhang, W., Yu, T., Jin, Q., Fu, B., Liu, H. (2018). Recovery of organic matters in wastewater by self-forming dynamic membrane bioreactor: Performance and membrane fouling. Chemosphere, 203, 123-131.

Wang, J., Cahyali, A., Wu, B., Pee, W., Fane, A.G., Chew J.W. (2020). The roles of particles in enhancing membrane filtration: A review, Journal of Membrane Science, 595, 117570.

Wendorff, W.L. (2001). Treatment of dairy wastes, In Applied Dairy Microbiology, 2nd Edition., Marth, E.H., Steele, J.L. Editors.; Marcel Dekker Inc., New York, USA.

Xie, Z., Wang Z, Wang Q, Zhu C. (2014). An anaerobic dynamic membrane bioreactor (AnDMBR) for landfill leachate treatment: performance and microbial community identification. Bioresource Technology,14, 29–39.

Xiong, J., Fu, D., Singh, R. P. (2014). Self-adoptive dynamic membrane module with a high flux and stable operation for the municipal wastewater treatment. Journal of Membrane Science, 471, 308-318.

Xiong, J., Fu, D., Singh, R.P., Ducoste, J. J. (2016). Structural characteristics and development of the cake layer in a dynamic memrbane bioreactor. Separation Science and Technology, 167, 88-96.

Xiong, J., Yu, S., Hu, Y., Yang, Y., Wang, X.C. (2019). Applying a dynamic membrane filtration (DMF) process for domestic wastewater preconcentration: Organics recovery and bioenergy production potential analysis: Organics recovery and bioenergy production potential analysis. Science of the Total Environment, 680, 35-43.

Xu, H.L., Wang, J.Y., Zhang, H., Tay, J.H. (2003). A comparative study of anaerobic digestion of food waste in a single pass, a leachate recycle and coupled solid/liquid reactors. Water Science and Technology, 47(1), 319-324.

Yamagiwa, K., Oohira, Y., Ohkawa, A., 1994. Performance evaluation of a plunging liquid jet bioreactor with crossflow filtration for small-scale treatment of domestic wastewater. Bioresource Technology, 50 (2), 131–138.

Yan, J. Q., Lo, K. V., Liao, P.H. (1990). Anaerobic digestion of cheese whey using an up flow anaerobic sludge blanket reactor: III. Sludge and substrate profiles. Biomass, 21, 257–271.

Yang, Y., Hu, Y., Wang, X., Ngo, H. (2020). Up flow anaerobic dynamic membrane bioreactor (AnDMBR) for wastewater treatment at room temperature and short hrts: Process characteristics and practical applicability. Chemical Engineering Journal, 383, 123-186.

Ye, Y., Le Clech, E., Chen, V. (2005). Fouling mechanisms of alginate solutions as model extra cellular polymeric substances. Desalination, 175, 7-20.

Yu, Z., Hu, Y., Dzakpasu, M., Wang, X.C., Ngo, H.H. (2019). Dynamic membrane bioreactor performance enhancement by powdered activated carbon addition: Evaluation of sludge morphological, aggregative and microbial properties. Journal of Environmental Science, 75, 73-83.

Yurtsever, A., Basaran, E., Ucar, D., Sahinkaya, E. (2021). Self-forming dynamic membrane bioreactor for textile industry wastewater treatment. Science of Total Environment, 751, 141572.

Zayed, G., Winter, J. (2000). Inhibition of methane production from whey by heavy metalsprotective effect of sulphide. Applied Microbiology and Biotechnology, 53, 726–731.

Zhang, X., Wang, Z., Wu, Z., Lu, F., Tong, J., Zong, L. (2010). Formation of dynamic membrane in an anaerobic membrane bioreactor for municipal wastewater treatment. Chemical Engineering Journal, 165, 175-183.

Zhang, X., Wang, Z., Wu, Z., Wei, T., Lu, F., Tong, J., Mai, S. (2011). Membrane fouling in an anaerobic dynamic membrane bioreactor (AnDMBR) for municipal wastewater treatment. Characteristics of membrane foulants and bulk sludge. Process Biochemistry, 46(8), 1538-1544.

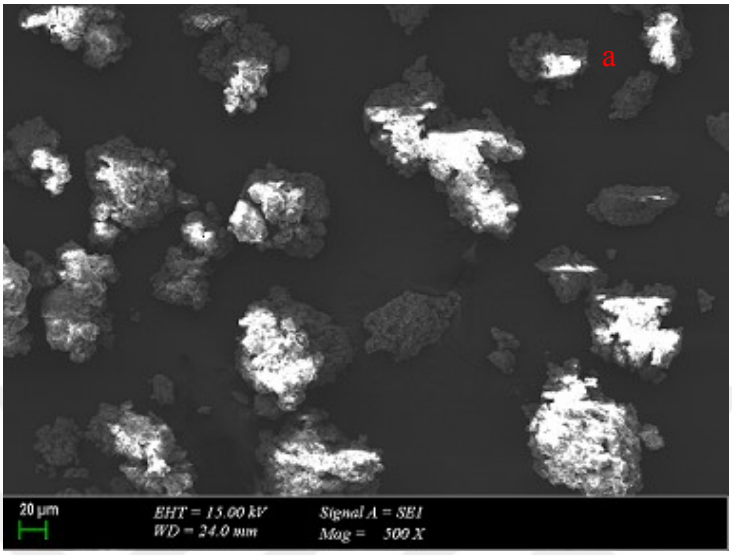
Zhang Y, Zhao Y, Chu H, Dong B, Zhou X. (2014a). Characteristics of dynamic membrane filtration: structure, operation mechanisms, and cost analysis. Chinese Science Bulletin, 59 (3), 247–260.

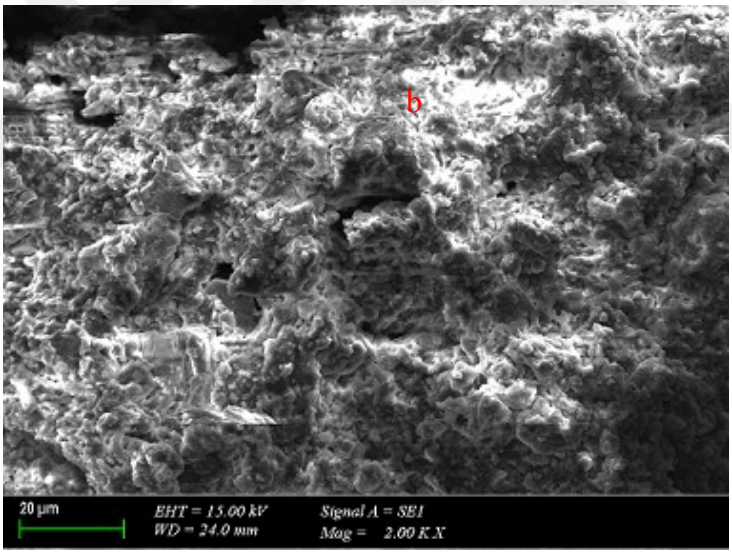
Zhang, X., Xu, R., Li, J. (2014b). Optimization of anaerobic micro-mesh separation bioreactor. Environmental Science and Technology, 39 (9), 59–63

Zielinska, M., Cydzik-Kwiatkowska, A., Zielinski, M., Debowski, M. (2013). Impact of temperature, microwave radiation and organic loading rate on methanogenic community and biogas production during fermentation of dairy wastewater. Bioresource Technology, 129, 308– 314.

APPENDIX A

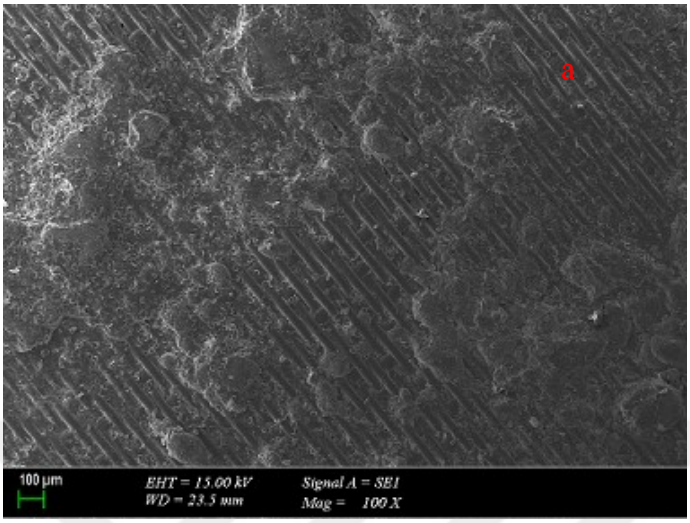
SEM Image of DM layer (40 µm) (Mag=500X (a), Mag=2.00KX(b))

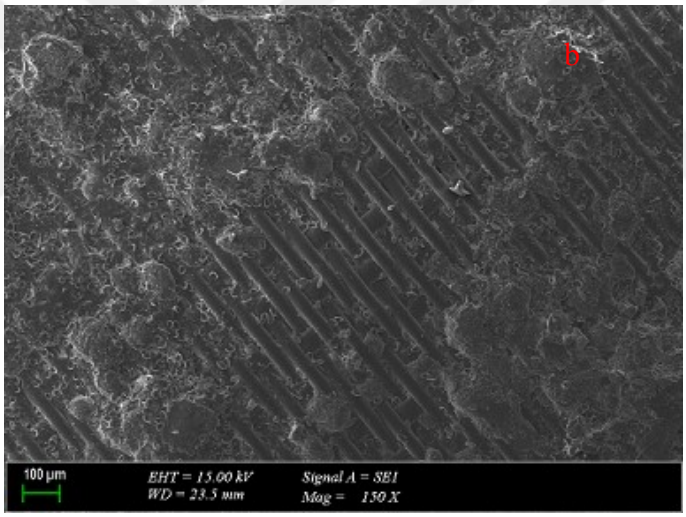


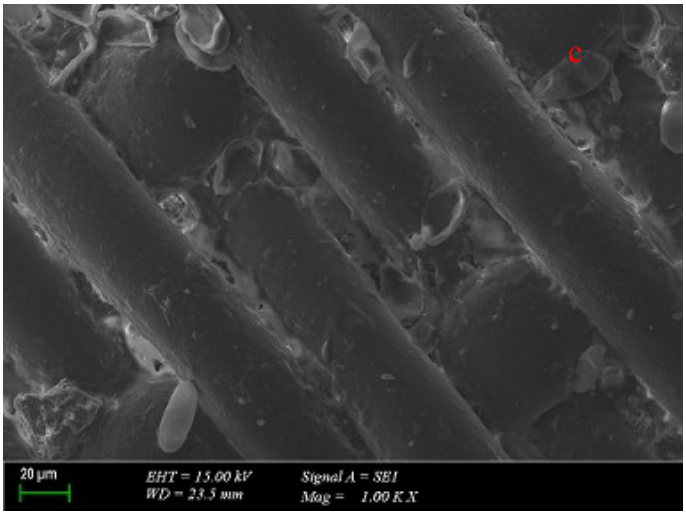


APPENDIX B

SEM Image of Gel layer (20µm) (Mag=100X (a), Mag=150KX(b), Mag=1.00KX(c))

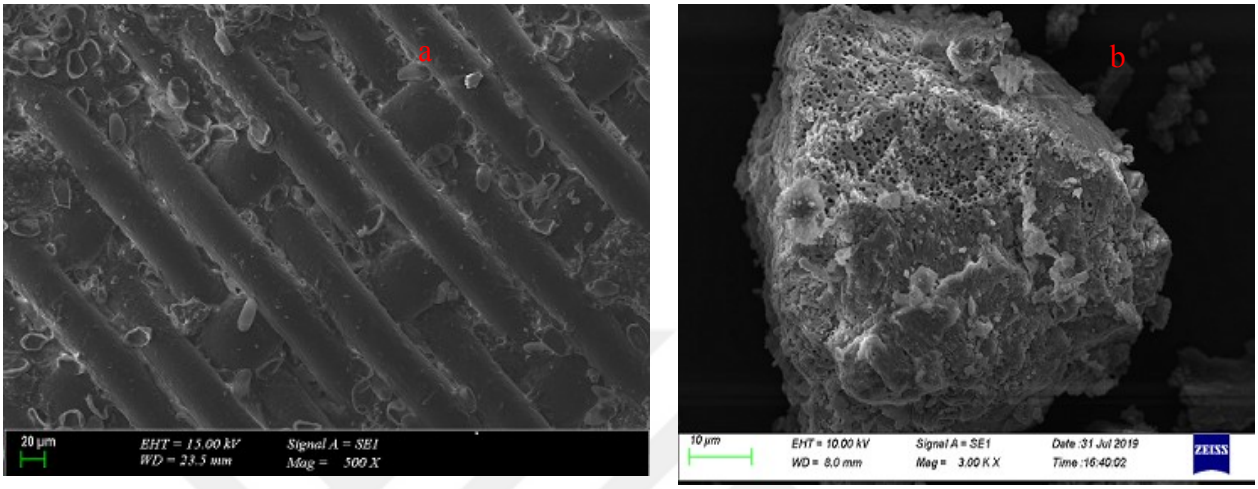






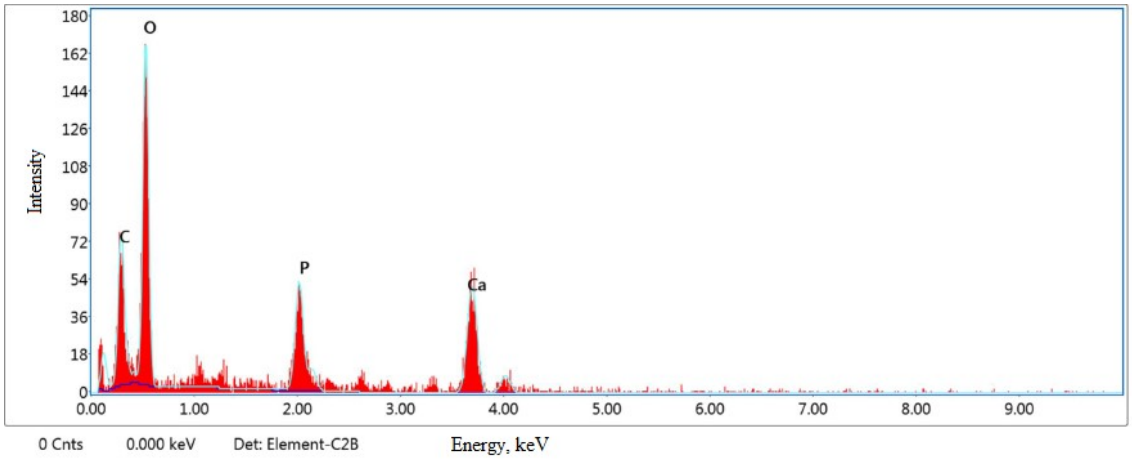
APPENDIX C

SEM Images: Gel layer (Mag=300X) (a) and Cake layer (Mag=3.00KX)(b) in DM (20 µm)



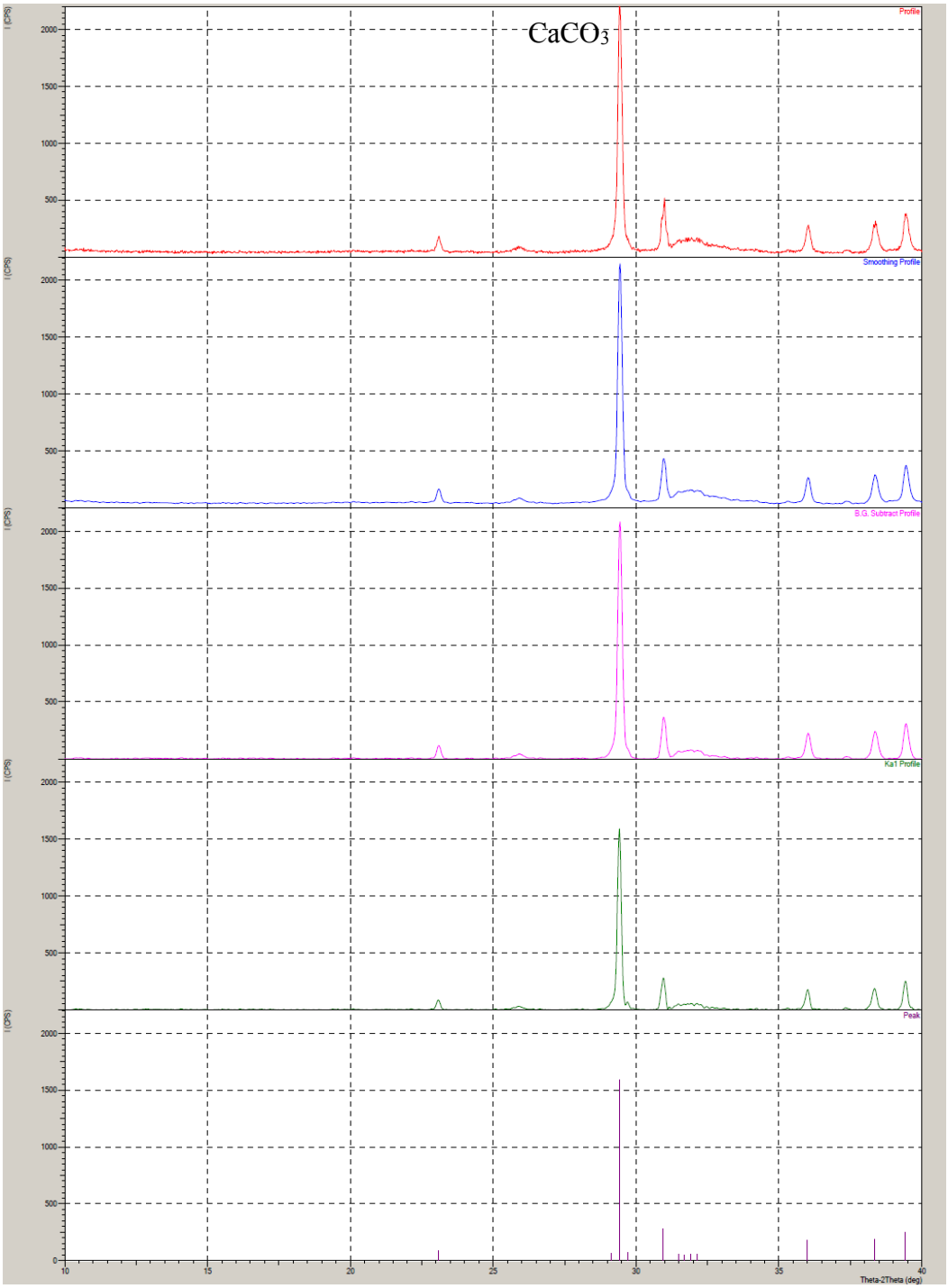
APPENDIX D

EDX analysis of gel layer (20 µm)



APPENDIX E

The X-ray powder diffraction pattern of DM layer



BACKGROUND

I graduated from Yıldız Technical University Faculty of Civil Engineering as Environmental Engineering in 2006. I completed my master's degree in Environmental Biotechnology at Boğaziçi University. I worked in a consultancy firm as an environmental officer. I was accepted to Marmara University Environmental Engineering Doctorate Program. During my doctoral study, I worked as a researcher in projects. Besides, I worked as an environmental officer in the consultancy firm.

Müge Paçal

Çevre Yüksek Mühendisi